FORMATION AND ELECTRICAL PROPERTIES OF POLYACRYLONITRILE THIN FILMS PREPARED BY PLASMA - POLYMERISATION

K. MOHANACHANDRAN

THESIS SUBMITTED IN PARTIAL FULFILMENT OF THE REQUIREMENTS FOR THE DEGREE OF DOCTOR OF PHILOSOPHY

DEPARTMENT OF PHYSICS
UNIVERSITY OF COCHIN
1983

CERTIFICATE

Certified that the work presented in this thesis is based on the original work done by Mr.K.Mohanachandran, D.S.T. Senior Research Fellow, under my guidance in the Department of Physics, University of Cochin, and has not been included in any other thesis submitted previously for the award of any degree.

Cochin 682 022

2 April 1983

K. Sathianandan

Professor K. Sathianandan
Supervising Teacher

DECLARATION

Certified that the work presented in this thesis is based on the original work done by me under the guidance of Professor K.Sathianandan, in the Department of Physics, University of Cochin and has not been included in any other thesis submitted previously for the award of any degree.

Cochin 682 022

2 April 1983

Mohanachandran

K. Mohanachandran

ACKNOWLEDGEMENTS

Finally, he extends his thanks to Mr.K.P.Sasidharan for neatly typing the manuscript.

CONTENTS

Page

INTRODUCTION

For the past few decades, the skills of thin film technologists have contributed a variety of techniques to prepare a large number of thin film materials with remarkable diversity of properties. The fast development of thin film technology has initiated the microminiaturisation of electronic hardware which has helped actively the progress of space physics and communication network. The development of thin film technology has created new diversions in areas of research in solid state physics and chemistry which are based on the phenomena uniquely characteristic of the thickness, geometry and structure of films.

Historically, metallic films are prepared from metal wires exploded by high electrical current density [1]. The deposition by thermal evaporation is relatively simple [2,3] and is widely used in academic and industrial fields. Clean ultra-high vacuum techniques and accurate measurement of thin film growth have initiated the preparation of single-crystal films of all types of material [4]. Though one may expect a metallic behaviour for Bi, Sb and As films, due to quantum size effect, a semiconductor-like behaviour is observed [5,6]. This type of peculiar phenomenon

explicitly shows the scope of investigation in thin films even if the data of bulk materials are known.

The electrical properties of all types of materials such as metals [7-9], semiconductors [10,11] and insulators [12,13] have been studied by a number of investigators. These information have led to the discovery of suitable materials for the preparation of solar cells [14,15], piezoelectric transducers [12,16], switching and memory circuits [17], magneto-optic records [18-20], microwave directional couplers [21] and photo-detectors [22,23] which are now in common use in satellites, computer hardware and communication purposes. Infra-red imaging tubes [24] are frequently used in defence for night observations. The modern trend in hetro-structure devices for optoelectronics such as injection lasers, light emitting diodes, solar cells and photo detectors are reviewed extensively [25]. The fast progress in vacuum technology and preparative methods of thin films have uplifted the electronic circuitory resulting in the development of integrated circuits.

Along with the development of systems with inorganic materials, different types of polymers (organic, inorganic and organometallic) are synthesised with a wide range of physical and electrical properties. Knowing the

electronic behaviour of polymers, their suitability in industrial applications can be established. These applications in turn would promote the development of new methods of preparation of polymers. The main advantage of a polymer thin film is that it can be obtained as a very thin film ($\sim 100\overset{\text{o}}{\text{A}}$) without pin-holes [26]. Most of them are very good dielectrics with temperature stability and high dielectric breakdown voltage. Hence plasma-polymerised dielectric polymers are used in the fabrication of microcapacitors [27].

Due to the great versatility of the properties of polymer thin films, special interest has been taken in recent years on their preparation and electrical properties. The present thesis is entirely devoted to the study of the formation, structure and electrical properties of plasma-polymerised polyacrylonitrile (PAN) thin films. Eventhough the studies are confined to a single polymer film, the results in general are applicable to similar polar polymer films.

The properties of polymer films prepared by different techniques are reviewed in the first chapter. This will highlight the present position of this subject in relation to the fast technological development. In the above review special emphasis is given to those outstanding

properties of polymers like semiconducting, piezoelectric, pyroelectric and electret which are significant in the development of devices in thin film technology. From the literature survey, it can be noticed that this field is relatively unexplored and wide scope exists for experimental and theoretical study.

In the second chapter, a detailed description of the preparation of plasma-polymerised PAN thin films sandwiched by aluminium electrodes is presented. The rate of growth of polymer film under different pressures and discharge currents are studied in detail. The design and fabrication of a vacuum coating unit and an evacuated chamber for the study of electrical properties of insulator thin films are discussed.

In the next chapter, the mechanism of plasma-polymerisation is studied by analysing the emission spectra of the plasma formed from acrylonitrile vapour and discussed in relation to the mechanism of chain formation in the polymer. From the infrared spectra of the monomer and the polymer, the probable structure of the polymer is suggested.

As -CN side group exists in the polymer chain, it is expected to show high dipole moment. Hence it is important to study the thermally stimulated depolarisation

current in PAN to obtain information regarding the dipolar
orientation and charge storage mechanism in the polymer.
As a part of such studies, the thermally stimulated current
of unpoled PAN film is studied and presented in chapter IV.
The results of thermally stimulated depolarisation current
in poled PAN is discussed in detail in the subsequent
chapter.

In chapter VI, the dielectric and electrical
properties of plasma-polymerised PAN are described. From
the current - voltage characteristics, the conduction
mechanism is analysed. The variation of dielectric constant
with temperature and frequency are studied to obtain inform-
ation on dielectric relaxation process and frequency response
of the capacitor.

All the observations are summarised in chapter VII.
On the whole, special interest is given to those properties
which point out the usefulness of PAN as a polar electret.
Part of the investigation presented in this thesis has been
communicated in the form of the following research papers:

1. Thermally stimulated short-circuited current
   from plasma-polymerised polyacrylonitrile thin
   films sandwiched between aluminium electrodes,
   J.Appl.Phys., 53(2), 1135 (1982).

2. Thermally stimulated depolarisation current
   in poled plasma-polymerised polyacrylonitrile
   thin films sandwiched by aluminium electrodes.
   (Communicated to Thin Solid Films)

3. Temperature change of dielectric constant in
   plasma-polymerised polyacrylonitrile thin films.
   (Presented at NP & SSP Symposium (DAE) 1982)

4. Thermally stimulated depolarisation current in
   poled plasma-polymerised polyacrylonitrile thin
   films.
   (Presented at NP & SSP Symposium (DAE) 1982)

REFERENCES

[1] M.Faraday, Phil. Trans. Roy. Soc. London, 147, 145 (1857).

[2] L.Holland, Vacuum Deposition of Thin Films, John Wiley and Sons, Inc. New York, Chapter VI (1956).

[3] L.Holland, Thin Film Microelectronics, L.Holland (Ed.), John Wiley and Sons, Inc., New York, Chapter IV (1956).

[4] K.L.Chopra, Thin Film Phenomena, Chapter I, Mc-Graw Hill Book Company, New York (1969).

[5] V.P.Duggal, R.Rup and P.Tripathi, Appl. Phys. Lett., 9, 293 (1966).

[6] Yu.F.Ogrin, V.N.Lutskii and M.I.Elinson, Soviet Phys. JETP Letters, 3, 71 (1966).

[7] J.Bardeen, J.Appl. Phys., 11, 88 (1939).

[8] C.A.Neugebauer, Physics of Thin Film, G.Hass and R.E.Thum (Ed.), Academic Press, Inc., New York, Vol.2, 1 (1964).

[9] Joy George, E.C.Joy and M.K.Radhakrishnan, Thin Solid Films, 68, 289 (1980).

[10] A.Many, Y.Goldstein and N.B.Grover, Semiconductor Surfaces, North Holland Publishing Company, Amsterdam, Chapter VIII (1965).

[11] B.J.Curtis, H.Kiess, H.R.Brunner and K.Frick, Society of Photographic Scientists and Engineers, 24, 5, 244 (1980).

[12] D.A.Payne and Jahar L.Mukherjee, Appl. Phys. Lett., 29, 11, 748 (1976).

[13] J.G.Simmons, Phys. Rev., 155, 657 (1967).

[14] M.Savelly and J.Bongnot, Solarcell Conversion, Academic Press, New York, B.O.Seraphin (Ed.), 213 (1979).

[15] A.G.Stanley, Cadmium Sulphide Solar Cells, Applied Solid State Science, R.Wolfe (Ed.), Academic Press, New York, Vol.5, 251-366 (1975).

[16] de Klerk, J. and E.F. Kelly, Appl. Phys. Lett., 5(1), 2 (1964).

[17] A.G.Abdullayev, A.M.Karnaukhov and N.M.Mamedov, Thin Solid Films, 78, 113 (1981).

[18] D.Chen, J.F. Ready and E.Bernal G., J.Appl. Phys., 39, 2916 (1968).

[19] R.S. Mezrich, Appl. Phys. Lett., 14, 132 (1969).

[20] Di Chen, Gary N. Otto and Francis M.Schmit, IEEE Trans. on Magnetics, MAG-9, 2, 66 (1973).

[21] Tanaka and M. Ohshita, IEEE Trans. On Microwave Theory and Technique, October (1976).

[22] P.Besomi, K. Christiansan and B.W. Wesels, Thin Solid Films, 87, 2, 113 (1982).

[23] S.V.Svechnikov and E.B. Kaganovich, Thin Solid Films, 66, 41 (1980).

[24] Jean-Jacques Brissot, Francois Desvigues, and Rene Martres, IEEE Trans. On Electron Devices, ED-20, 7, 613 (1973).

[25] Zh.I.Alferov, Czech. J. Phys. Sec.B (Czechoslovakia), B.30, 3, 249 (1980).

[26] Y.Segui and Bui Ai, Thin Solid Films, 50, 321 (1978).

[27] H.Carchano and M. Valentin, Thin Solid Films, 30, 351 (1975).

CHAPTER I

PREPARATION AND PROPERTIES OF POLYMER THIN FILMS

ABSTRACT

A brief review of the present understanding of electronic properties of polymer thin films is presented here. Different experimental techniques to prepare polymer films are also discussed. Special emphasis is given to those outstanding properties of polymers which are significant in the development of devices in thin film technology. Important applications of polymer thin films are also reviewed.

1

1.10 BASIC PICTURE OF POLYMERS

1.11 Polymerisation

The word polymer is derived from the Greek word 'polymeros' which means many parts. It is clear from the word itself that a single polymer consists of a number of units linked together by covalent bonds to form a large molecule or a macromolecule. The individual unit that repeats to constitute a polymer is called the monomer [1-3]. The monomers can link together linearly to form a linear polymer. Some polymers have branched chains, often as a result of side reactions during polymerisation. Cross-linked and network structures are formed in the case of monomers containing more than two reactive groups by step-wise polymerisation [2]. By co-polymerisation of a mixture, polymers with properties completely different from the individual polymers of mother monomers can be produced [3]. The degree of polymerisation is the number of monomers linked together to form a polymer and is a basic parameter used to characterise the material.

Organic [1-4], organo-metallic [3,5,6] and inorganic [5,7] materials may undergo polymerisation under suitable conditions. These materials have wide range of electronic behaviour [4] and their electronic transport

properties also vary widely. There are polymers whose electrical conductivity can be varied from insulator to metallic either by proper doping [8] or by changing the structure [9]. A summary of the mechanism of polymerisation, the electronic behaviour and related properties are given below as an introduction to the investigations presented on polyacrylonitrile in the subsequent chapters.

1.12 Mechanism of polymerisation

The process of polymerisation may be broadly divided into two: condensation polymerisation (step-reaction) and addition polymerisation (chain-reaction) [2]. The step-reaction polymerisation is the condensation of two polyfunctional molecules to produce one larger molecule with the possible elimination of a small molecule such as water. The chain-reaction polymerisation involves reactions in which the chain carrier may be an ion or a reactive substance with an unpaired electron called a free radical. The free radical is formed by the decomposition of a relatively unstable material called an initiator.

The fundamental kinetics of radical polymerisation is described elsewhere [3]. In high temperature polymerisation as well as plasma polymerisation the radical initiated process is more predominant [10]. In the case of the commonly

occurring monomers initiated by radicals, the forming temperature is that temperature at which the initiator splits itself readily into radicals, that is k_d the rate constant has reached a measurable value. At this stage, the initiator I is converted into an initiator radical Z^*, which again reacts to produce the monomer radical.

$$I \xrightarrow{k_d} Z^*$$ (1.01)

$$Z^* + M \xrightarrow{k_i} M_1^*$$ (1.02)

Here M is the monomer, k_i is the initiating rate and M_1^* is the monomer radical.

$$M_1^* + M \xrightarrow{k_p} M_2^*$$ (1.03)

k_p being the rate of polymerisation and M_2^* being dimer radical formed in the first process of polymerisation.

This propagation process proceeds as

$$M_2^* + M \xrightarrow{k_p} M_3^*$$ (1.04)

$$M_{x-1}^* + M \xrightarrow{k_p} M_x^*$$ (1.05)

There are mainly two termination reactions (a) combination
and (b) disproportionation. The combination can be repre-
sented as:

$$M_x^* + M_y^* \xrightarrow{k_t'} M_{x+y} \qquad (1.06)$$

The disproportionation can be represented as

$$M_x^* + M_y^* \xrightarrow{k_t''} M_x + M_y \qquad (1.07)$$
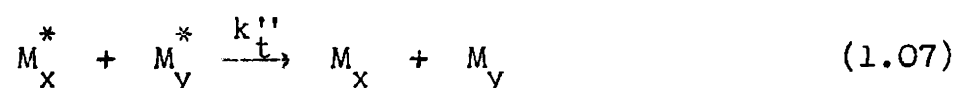
Here k_t' and k_t'' are the termination rates of polymerisation
process and these depend on the external conditions of the
process. In radical polymerisation, the termination is a
second order reaction in M^* and the radical can be terminated
by collision with the initiator radical. But this possibility
may be ignored due to the low concentration of the initiator.

The radical polymerisation is more predominant in
plasma-polymerisation process. Here the accelerated positive
ions and the electrons, formed by high electric field act as
initiators, which collide with monomer molecules producing
radicals. The initiator concentration in such a process is
very high resulting in fast polymerisation. Also due to the
high concentration of the initiator in the plasma-polymerisa-
tion process, the termination reaction can occur due to
collision.

1.13 Electronic states of polymers

The electronic properties of polymers have been characterised by utilising the skills of the chemists, material scientists and physicists and they have made sophisticated experimental and theoretical approaches to understand the basic phenomena and structure-property relationship [11]. In relation to the electronic states of polymers, they are classified into two: one class comprising of polymers with saturated or unsaturated backbones, but without pendant groups (eg., polyethylene and polyacetelene) and the other being made up of polymers with saturated back-bones and attached aromatic chromophores (eg., polystyrene and polyvinyl carbazole). In the former class the electronic properties are heavily controlled by the states associated with the strong intra-chain (back-bone covalent bond) so that one expects wide conduction band similar to the inorganic covalent solids. The latter has the electronic state similar to that of isolated aromatic molecules. Usually the experimental study of electronic states of polymers is confined to optical absorption. Since many of the polymers have their optical transition in the near and far ultra-violet regions, such studies are relatively routine and are carried out by commercial automatic instruments.

It has been recognised that the interaction between the pendant groups leads to small exchange energies and narrow bandwidths. Thus, these pendant groups, which have generally a much lower ionisation potential than saturated polymer back-bone, are expected to dominate the low energy transitions and play an integral role in the electrical properties.

Ionic excitation states such as ion-pair or charge transfer states have been discussed by many workers [12-14]. Ionisation energies of the highest occupied levels and binding energy of the lowest unoccupied levels for different polymers in gas phase and in crystalline state [15] are shown in Fig.1.01. From the figure it is seen that the energy required to separate a negative charge from a positive charge for an isolated molecule is I_g-A_g, where I_g is the gas phase ionisation energy and A_g is the energy gained by the binding of the ionised electron with a neighbouring homologue molecule. In a solid, the energy to produce these ionic states is reduced, as the molecules exist within a polarisable medium. Hence

$$E = I_g - A_g - 2P \qquad (1.08)$$

where P is the crystal polarisation energy of the free electrons. Thus in the case of solids one can think of the
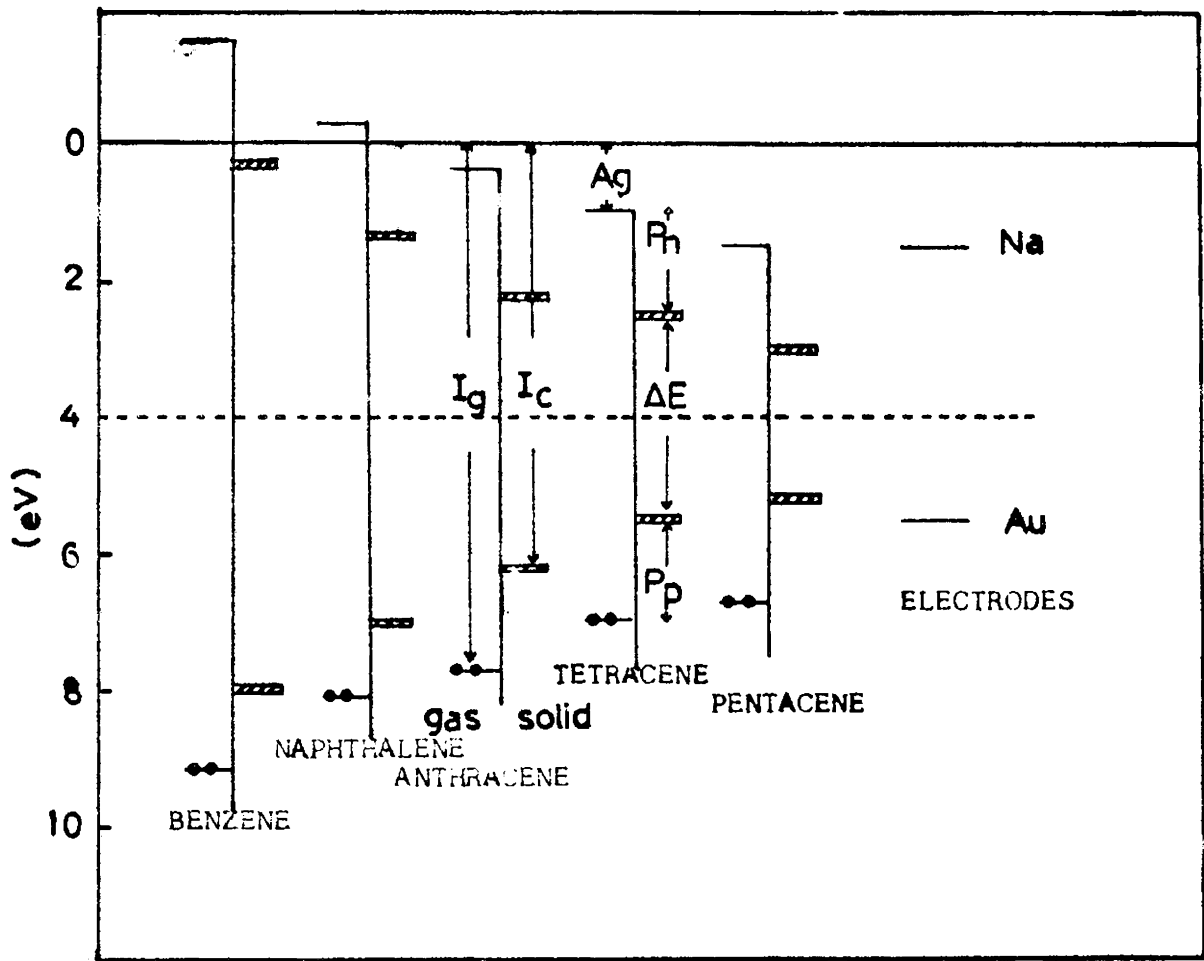
Fig.1.01. The ionisation energy of the highest occuoied
and binding energy of the lowest unoccupied
levels for different polyacenes in gas phase
in the crystalline state. The Fermi levels
of Na and Au are also noted. ΔE and Ag are
the band gap in solids and the energy gained
by binding of ionised electron with a molecule
in vapour phase [15].

excited energy levels as the conduction states for electron
and hole separated by a band-gap ΔE. For energies within
this gap non-conducting ion-pair states may exist [13].

The energy levels are first directly observed by
the carrier photo-emission from the metal electrodes in the
polymer poly N-Vinylcarbozole. The measured spectral
threshold for photo-emission of holes [16] together with
known values of I_g and P, form a self consistent picture
of probable energy levels of copper-polyvinylcarbozole as
shown in Fig.1.02. In the figure, the polarisation energy
of polyvinylcarbozole, P is taken as 1.5 eV and T and S_n
represent the triplet and singlet energy states.

The energy levels of different polymers are
discussed on the basis of the mechanism of conductivity by a
number of workers [17,18]. Analysis of thermally stimulated
depolarisation is a powerful tool for obtaining information
regarding the storage and transport of the charge carriers
in insulators and semiconductors [19-21]. It also gives
information about trap-levels as well as impurity levels.
Hence the energy levels of the polymers are discussed on the
basis of depolarisation current [22,23] which in turn gives
an insight into the nature of electronic states of the polymer
material. A detailed picture of the energy levels in
molecular solids is given elsewhere [24,25].
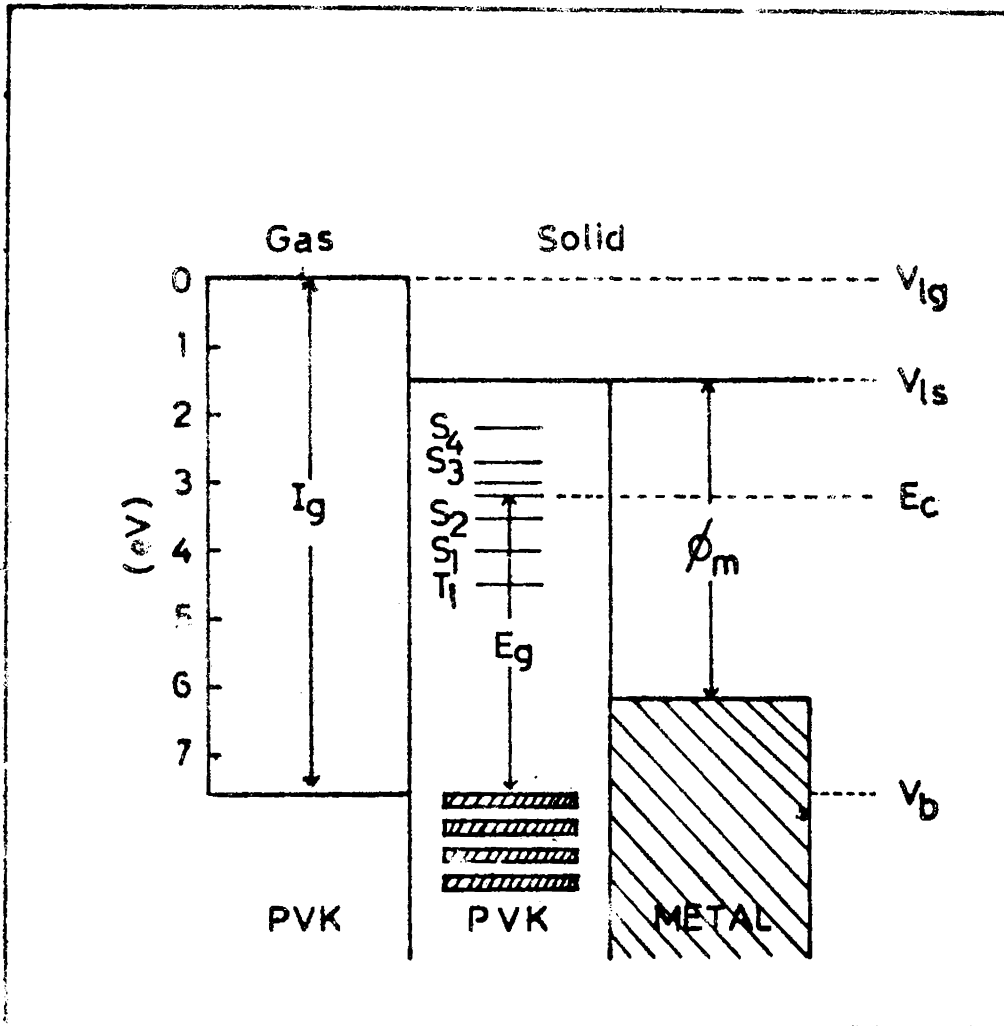
Fig.1.02. Energy band diagram for Cu - PVK interface.
I_g - ionisation potential, E_g - band gap,
$\emptyset_m$ - metal work function, V_{lg} - vacuum level
(gas), V_{ls} - vacuum level (solid),
E_c - conduction band, V_b - valence band,
S_n - singlet energy state and T - triplet
energy state [16].

In the class of polymers without pendant groups, the simplest polymer is the polyethylene, on which both theoretical and experimental studies have been reported [26,27] and many more studies are still being persued. Energy band calculations for a single polyethylene chain give a wide energy-gap between filled and vacant states. The strong covalent intra-chain binding broadens the electronic levels of polyethylene. Detailed calculations have conducted the existence of highly localised excitons with broad energy bands dictated by the periodic structure of polyethylene chain [28].

The introduction of semiconducting polymers with wide range of electrical conductivity when doped with controlled amounts of halogens is a breakthrough in the field of semiconductor physics as well as polymer technology. Usually conjugated linear polymers are considered to be semiconducting. The term conjugated is used to indicate the alternation in a series of single and double bonds and rarely tripple bonds. Polyacetylene is one of the simplest linear conjugated polymer with single chain structure which can exist in two different configurations: cis-and trans-, as shown in Fig.1.03. Each carbon is σ bonded to one of the hydrogens and two neighbouring carbon atoms consistent with sp^2 hybridisation [8]. The π electrons are therefore

CIS (CH)$_x$

TRANS (CH)$_x$
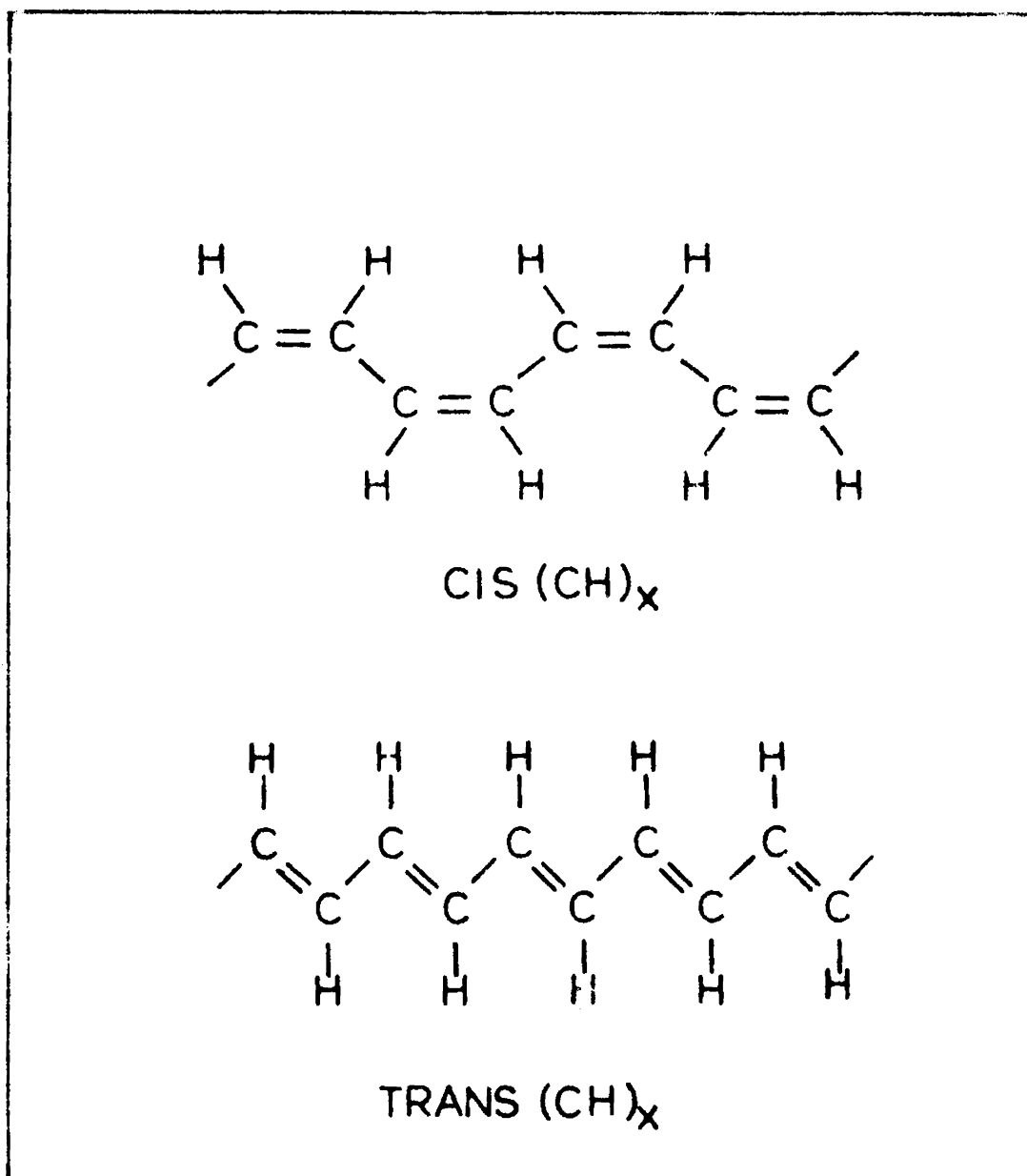
Fig.1.03. Structure of CIS- and TRANS-polyacetylene.

z
available to delocalise into a band. In the idealised

situation of uniform chain, the resulting conduction band

would give rise to metallic behaviour. However, such a

system is unstable with respect to bond alternation and a

characteristic gap opens up in the electronic energy

spectrum. The evolution of the molecular levels as a

function of the number of atom in a finite chain [29]

and the band structure and density of states for idealised

case and alternant polyacetylene are shown in Fig.1.04.

Studies of $\pi-\pi^*$ transitions in short-chain polyenes show

that frequencies do not fall as n^{-2} (where n is the number

of atoms in the molecule) as expected for free-electron

picture, but appear to saturate at $\Delta E_{(n \to large)}^{\pi-\pi^*} = 2.4eV$

[30]. Bond alternation is present in the polymer and would

be expected to lead to semiconducting behaviour.

In a long polyene chain limited or broken

sequences of electronic delocalisation are affected by

attached side groups. Depending upon the chain limitation

(even or odd) two types of conjugations are introduced,

(i) eka conjugation and (ii) rubi conjugation [31,32].

Theoretical as well as experimental evidences support the

existence of these two conjugated groups [24]. Still the

information regarding the electronic behaviour of conjugated

polymers is not complete.
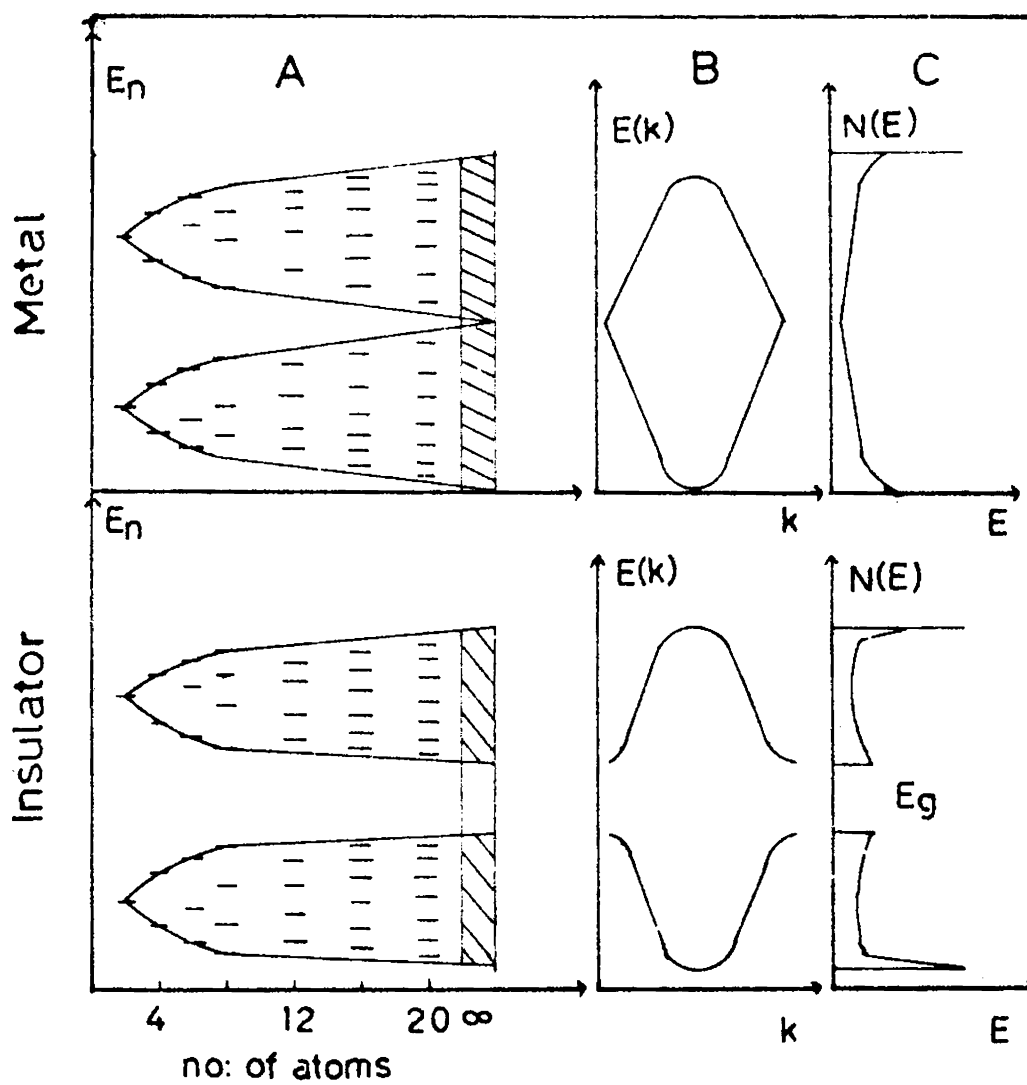
Fig.1.04. Molecular level (A), first brillouin
zone (B) and density of states (C)
for regular and alternate polyenes [29].

The useful electronic properties characteristic of amorphous and organic materials could both be manifested in polymers and the past few years have seen the beginning of coordinated programmes of study of electronic properties of polymers. A brief report of the electronic behaviour of polymers given above may lead to consider polymers as electronic materials and possible technological applications have to be thought of. As a part of that venture the properties of different polymeric materials have been studied by a number of scientists [5,24,33-38]. It was observed that the properties of polymers depend on the methods of synthesis and the structure [39,40]. It was also noted that electrical, structural, mechanical, chemical and optical properties of polymer thin films are different from the properties of bulk material. Though the information on the properties of bulk polymers are not complete, it is high time to carry over the studies to thin polymer materials such that this will promote the development of thin film technology further.

1.20 PREPARATION OF POLYMER THIN FILM

The preparation of polymer thin films can be broadly classified into two groups: (a) preparation of thin films from polymer bulk material [41,42] (b) preparation of

thin films from the monomer itself [43-45]. In the first
method, the polymers are prepared chemically which are
commercially popular [46-48]. Many of the workers [49,50]
have chosen commercial polymer materials for the preparation
of thin films.

1.21 Preparation of thin films from polymer bulk material

(i) Solution casting method

The films of soluble polymers can be prepared by
the simple technique of direct isothermal immersion of a
substrate into a suitable solution of the polymer [51-53].
The growth kinetics and structural details of polyvinyl
chloride (PVC) was studied in detail by Rastogi and Chopra
[54]. In this method a homogeneous solution of the polymer
is prepared. The solution is then maintained under constant
temperature and the substrates were held inside the constant
temperature bath vertically above the solution. After
bringing the solution and the substrates down to the required
temperature, the substrates were immersed isothermally in the
solution for a period varying from 1 min. to 60 min. Polymer
films are formed on the surface of the substrate with
sufficient thickness ($<1000\overset{o}{A}$). Epitaxial films of homo-
polymers have been prepared by this method [55].

(ii) Evaporation

Polymer materials can be prepared by conventional evaporation techniques [56,57]. Hogarth and Iqbal [58] have reported that the evaporated polypropylene has the same properties as the chemically processed polymer. In the process of heating, decomposition may occur and hence the degree of polymerisation may be different from the mother polymer. To reduce this, the temperature of the source should be less than decomposition temperature. Localised heating by electron beam source is successfully used for the evaporation of polymer materials [59]. In thermal evaporation process, the decomposed impurity concentration is much higher.

(iii) Sputtering method

The process used in sputtering of polymers are very similar to those used for inorganic materials [60,61]. The detailed process of sputtering and the various limitations are discussed by Holland and Prestland [61]. In this method also degradation of polymer occurs and contaminated polymers are formed. In the sputtering process, due to the high energy bombardment of ions, high degree of cross-linking occurs in the formed thin films. However, the formed films are often observed to be superior to the specimen prepared by evaporation method.

1.22 Preparation of polymer thin film from the monomer

Due to the optimum use of monomers, this is regarded as an economical method for the preparation of polymer thin films. Among different experimental methods, plasma-polymerisation is much more superior because of its simplicity and industrial importance.

(i) Radiation induced polymerisation

Here the polymerisation is achieved by the bombardment of electrons on the surface of the monomer [43] or by the irradiation of ^{11}V [62] or γ-rays [63,64]. Several workers have used electron beam bombardment to produce and study the properties of polymer films obtained from DC - 704 pump fluid [43], siloxanes [65], styrene [66] and butadiene [67]. It is well known that polystyrene is polymerised when exposed to UV light. The polymerisation takes place by conventional free radical polymerisation process [68]. By this method, the polymers can be made from solid, liquid and gaseous phases. The irradiation process is also known as photolitic process. Polymers like butadiene, styrene, acrylonitrile etc. can be produced by photolitic process [64]. Photolithography is one of the most important application of this process which is unavoidable in the preparation of micro-miniature patterns for I.C. fabrication [47]. The polymers having photolitic properties are called photoresists [63,69].

(ii) Pyrolytic method

In this process the polymerisation and deposition of thin film takes place simultaneously [45]. Here monomer vapour is leaked into a vacuum and passed through a catalyst. When the vapour is quenched on the cold substrate, polymerisation occurs and a thin film gets deposited on the substrate [70]. This method has been used extensively for preparing poly-p-xylene from p-xylene at $600^\circ C$ [45,71,72].

(iii) Plasma-polymerisation

Methods of preparing polymer films, previously described, cannot be applied to all monomers and also the conditions for preparation of good films are very critical. But plasma-polymerisation method [72-74] is superior to all the other methods because most of the organic, organometallic and certain inorganic materials can be polymerised by this method. The efficiency of this method is very high and the formed films are pin-hole-free. These good qualities attracted the researchers to pay more attention to study the properties of plasma-polymerised polymers. Also the properties of plasma-polymerised films are different and to a certain extent superior to those of polymers prepared by other methods [75]. For example glow-discharged polystyrene thin film has many different electrical and physical

properties like dielectric loss, flexibility and solubility
as compared to ordinary polystyrene [76]. Bradley and
Hammes [74] have studied the electrical properties and
deposition efficiency of about 40 polymers prepared by
plasma-polymerisation. For the preparation of polymers,
the plasma of the monomer vapour can be generated by
different ways [77]. They are silent discharge, direct
current discharge, low frequency glow-discharge (usually
50 Hz AC), high frequency discharge and microwave discharge.

Silent discharge:- The silent discharge tube is usually
made of glass or quartz. Normally it consists of a co-axial
section and the inner and outer surfaces of the co-axial
section are connected to high alternating voltage of the
order of 10KV by means of conducting liquids or steel
electrodes. Hirai and Nakada [9] have reported on the
formation of polyacrylonitrile (PAN) thin film by silent
discharge. They have modified the discharge cell as shown
in Fig.1.05. To avoid the concentration of discharge, the
metal electrodes are not exposed directly to the gas phase
by covering them with glass and epoxy resin. A vacuum
vessel attached to the top of the discharge tube is used
for preventing the inward leakage of air through the
interface between the tube and the cover. First the dis-
charge tube and top protecting vessel are pumped to 10^{-5} torr
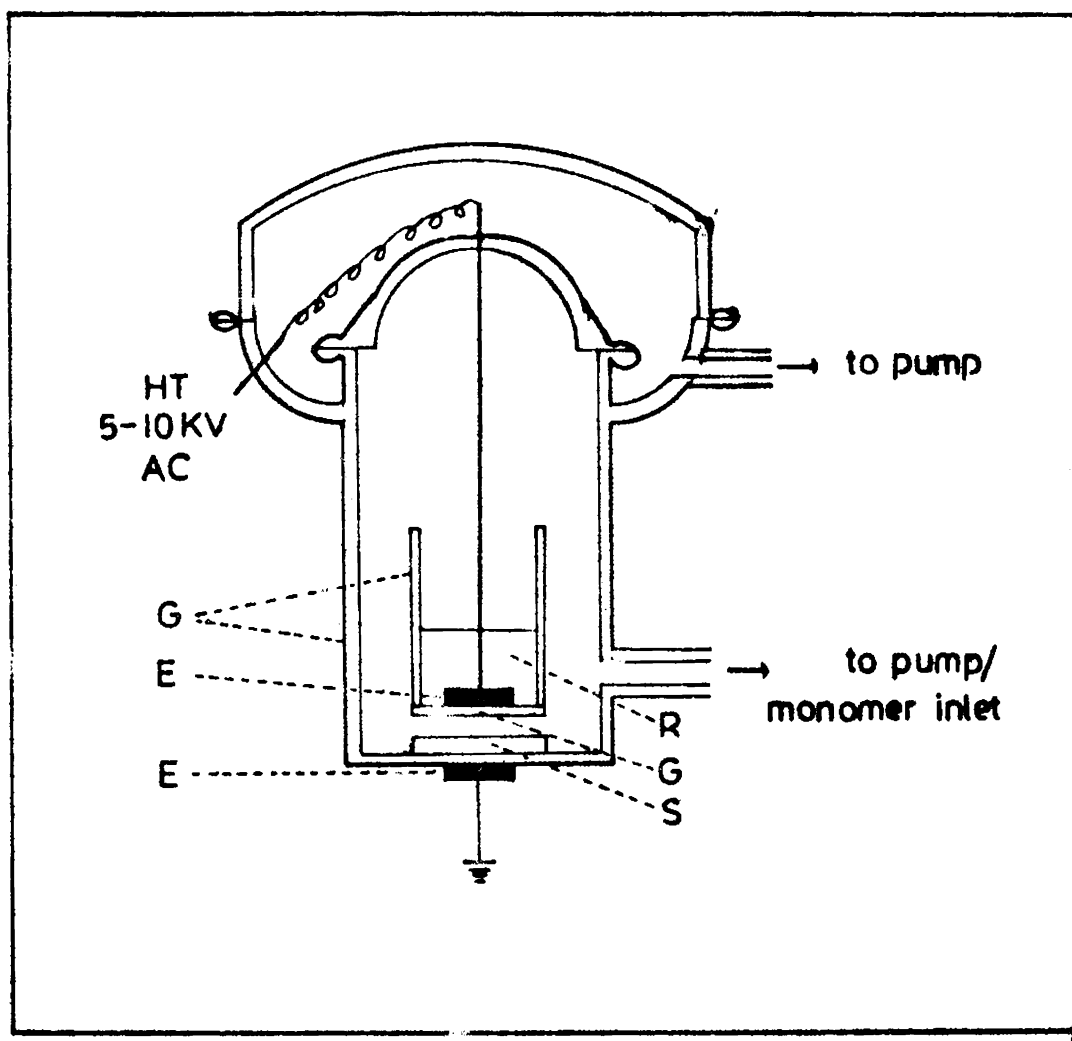
Fig.1.0. Silent discharge reactor for polymerisation
E - electrode, G - glass, R - epoxy resin
and S - substrate.

and the discharge tube is filled with monomer vapour at sufficient pressure. An A.C. voltage of 5 to 10KV (50Hz) is applied to the electrodes through a Neon transformer for causing a uniform and stable silent discharge which produces uniform PAN films. As electrodes are fully covered, there will be no interaction between the monomer vapour and the electrodes minimising the impurity effect.

Microwave discharge:- For plasma generation, microwave generators of a few KW can be used. The microwave power is led by a co-axial cable or a wave-guide from magnetorn or klystron to the resonant cavity enclosing the reactor. Microwave discharge have been found to be successful with inorganic compounds [78]. One of the advantages of this reactor is that it can be used at higher pressures but at low pressures ($\leq$ 1 torr) it is difficult to initiate and sustain discharge.

Direct current discharge:- In the direct current discharge, two metal electrodes are placed inside the plasma reactor and a high voltage is applied to produce plasma [79,80]. A reactor for DC discharge plasma-polymerisation is shown in Fig.1.06. First the reactor cell is evacuated to 10^{-5} torr and pure monomer vapour is fed into the cell raising the pressure ranging from 10^{-1} torr to 1 torr. When DC
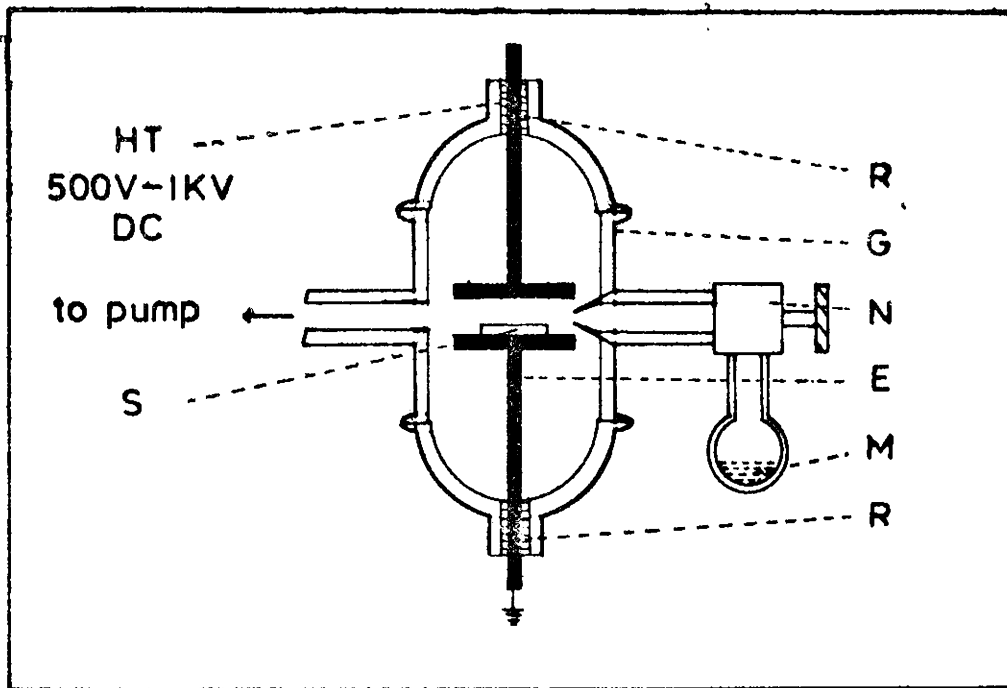
Fig.1.06 DC discharge plasma-polymerisation reactor
       E - electrode, N - needle valve, M - monomer,
       G - glass, R - epoxy resin and S - substrate.
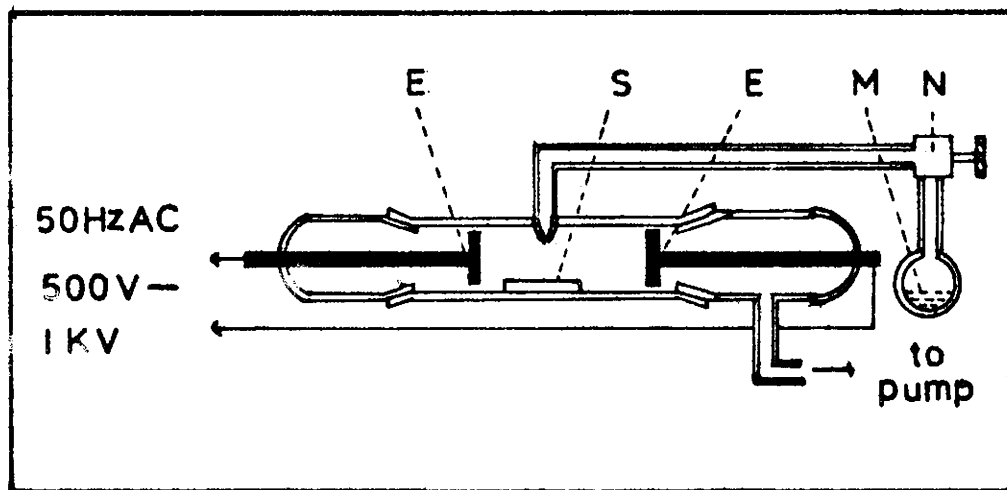
Fig.1.07. 50 Hz AC plasma-polymerisation reactor
       E - electrode, S - substrate, M - monomer
       and N - needle valve.

field is applied to the electrodes, the monomer molecules are polymerised and deposited mostly on the cathode. A smaller amount of polymer is deposited on the anode also [81]. It is observed that if the formed polymer is an insulator, after forming a few layers of the film, the glow discharge ceases. It is found that when the applied voltage is increased, arcing is developed which disturbs the film. Hence this method cannot be effectively used for the preparation of insulator polymer films of sufficient thickness.

Low frequency discharge:- Using this method, much work on polymer films from monomers has been reported [18,74,82]. Here 50Hz AC is sufficient for successful preparation of polymers. A detailed description of the reactor chamber is given elsewhere [18,74]. One such reactor is shown in Fig.1.07. The discharge chamber, with the substrate set at the central part, is evacuated to $10^{-4} - 10^{-5}$ torr. Then the monomer gas is introduced into the chamber from the monomer reservoir. When the pressure of the monomer gas rises to 10^{-1} to 1.5 x 10^{-1} torr, AC voltage of about 500-1000V (50Hz) is applied between the two electrodes for the generation of the glow discharge. Both the electrodes and the sides of the reactor tube are found to be coated with polymer.

This type of polymerisation is of interest in the present work and the detailed parametric studies are discussed in the next chapter. In this method the efficiency of polymerisation is good and there is no need of any special power supply. The output of a step-up transformer can directly be used as the electrical power source.

High frequency discharges:- An AC power supply working at a frequency of the order of a few MHz can be utilised for high frequency plasma-polymerisation. For AC discharge with electrodes, the same reactor shown in Fig.1.07 can be used. One of the important advantages of high frequency discharge is that it can work without electrodes (electrodeless discharge). The electrical power can be transferred to the plasma tube either by inductive method or capacitive method. In the inductive method, the discharge tube is located at the axis of a coupling coil and radio frequency power is fed to the discharge tube through this coil. In some cases, polymerisation as well as deposition take place in the tail of the glow-discharge [83]. An arrangement for inductive coupling to the plasma tube is shown in Fig.1.08(a). In the capacitive coupling, the power is fed to the discharge tube by means of two copper rings situated at about 5 cms apart as shown in Fig.1.08(b). The deposition will be mainly limited to the region of glow-discharge. Here the substrate is placed in
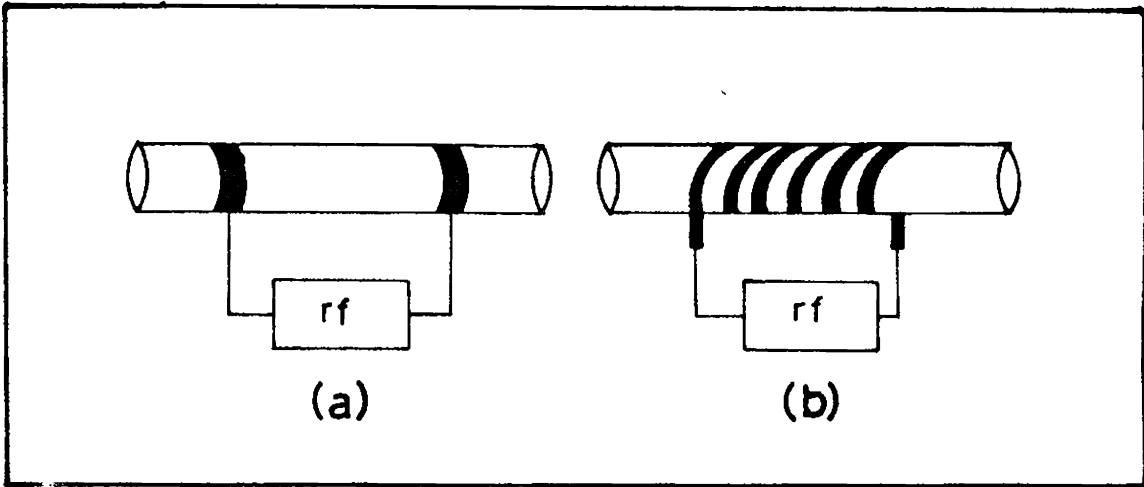
Fig.1.08 (a) Capacitive coupled and (b) inductive coupled
rf plasma tube.
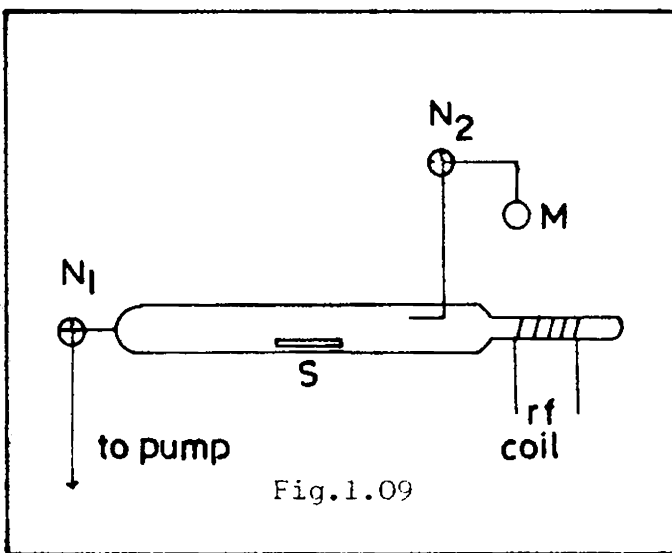
Fig.1.09
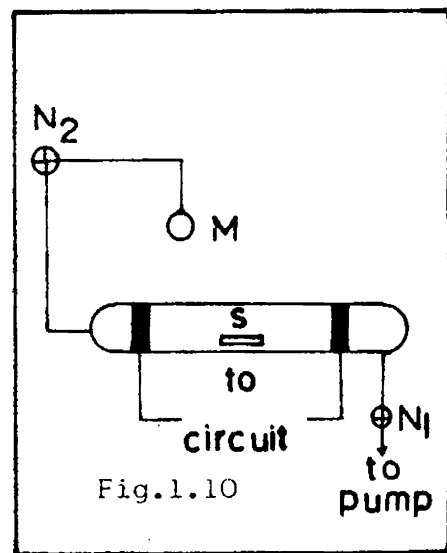
Fig.1.10

Fig.1.09 Schematic representation of inductive coupled plasma-
polymerisation reactor [83] N_1 - stop-cock,
N_2 - needle valve, M - monomer and S - substrate.

Fig.1.10 Schematic representation of capacitive coupled plasma-
polymerisation reactor [25] N_1 - stop-cock,
N_2 - needle valve, M - monomer, S - substrate.

between the copper rings so that the thickness of the film is uniform [84].

For RF discharge plasma-polymerisation, different types of reactors are in use. Fig.1.09 is one such type wherein inductive coupling method is used [83]. A capacitive coupled system is also commonly used in polymerisation process [25,85] and is shown in Fig.1.10.

The basic principle, involved in all the plasma-polymerisation processes, is that the free radicals are formed in the system and that they recombine among themselves to form polymeric chain. Under glow-discharge conditions, ionised radicals are formed and these radicals, when passed through the monomer, transfer their energy to the monomer molecules. The energy dissipation produces chemical changes which give rise to polymerisation [86]. Many investigators [9,74,87,88] have carried out extensive work on plasma-polymerisation and have suggested a mechanism in which free radicals are formed by the breaking up of covalent bonds. It is argued that the free radicals are formed by the processes such as opening of the double or tripple bonds, hydrogen abstraction, opening of ring and cleavage of C-C bonds. To identify the possible mechanism of plasma-polymerisation, the emission spectra of the plasma have been recorded by a number of scientists [89-94]. Also

discharges are known to be excellent sources of producing

simple free radicals from a number of aliphatic hydrocarbons

[95-97]. Hence the reaction mechanism of plasma-polymerisation

can be studied by a proper analysis of the glow-discharge

spectrum. A review of the techniques and mechanism of

plasma-polymerisation is given by Millard [75].

Usually the polymerisation method is more economic

and easy to prepare polymers. The general conclusions to be

derived from the plasma-polymerisation techniques are that

independent of the monomers being aromatic, olefinic, conjuga-

ted, unconjugated or fully saturated, the solid product is a

dense, highly branched and cross-linked polymer containing

considerable unsaturation in the form of both olifinic bonds

and free valence [75].

1.30 PROPERTIES OF POLYMER FILMS

The demand for polymers are increasing fast due

to its outstanding properties. The importance of the polymers

and their technological interest are well described [98,99].

In this context it is apt to review the present status of

our understanding of polymers as an electronic material and

the actual and possible technological applications.

1.31   Electrical behaviour of polymer thin films

The synthetic organic polymers that we ordinarily associate with fibers, films or moldings are generally insulators. Their electrical resistivity lie in the range of 10^9 to 10^{29} ohm-cm [100]. The common polymers may be differentiated from the semiconducting polymers on the basis of the chain structure, the semiconducting polymers being usually conjugated. The electrical conductivities of a number of amorphous polymers have been studied thoroughly for their dependence of temperature and pressure [101]. Similar experimantation and reasoning suggest ionic conductivity in polypropylene [102], polyalkylmethacrylate [103] and polyethylene terephthalate [104]. A hyperbolic sine relation between current and voltage in polyethylene terepthalate [105] and polyethylene [106] thin films has been taken as an evidence for electronic conduction. Protonic conduction has also been suggested for the mechanism of charge transport for polymeric films [107].

Different workers have taken special interest to study the process of conduction in polymers and suggested different mechanisms to satisfy their experimental results. Bradley and Hames [74] have studied a large number of insulating polymers formed by plasma-polymerisation and suggested that there is a characteristic magnitude and temperature

dependence of conductivity for organic polymer films basically due to the preponderance of carbon-carbon bonds in the structure. Ando and Kusabiraki [108] have suggested that electrical conduction of polystyrene film formed by glow-discharge is mainly due to Poole-Frenkel effect at higher applied fields. At low fields ohms law is satisfied. The conduction characteristics due to the Poole-Frenkel effect is given by the following equation [109,110].

$$\sigma = \sigma_0 \exp[-(\phi - \beta_{PF} V^{\frac{1}{2}})/kT] \qquad (1.09)$$

$$\beta_{PF} = (e^3/\pi \, \varepsilon_r \varepsilon_0 d)^{\frac{1}{2}} \qquad (1.10)$$

Here ϕ is the impurity level, β_{PF} the Poole-Frenkel coefficient, e the electron charge, ε_0 the permitivity of vacuum, ε_r the relative dielectric constant of the insulator at high frequency, d the thickness of the insulator, k the Boltzmann constant and T the absolute temperature. From eqn.(1.09) it can be deduced that

$$\log \sigma = \log \sigma_0 - \frac{\phi - \beta_{PF} V^{\frac{1}{2}}}{kT} \qquad (1.11)$$

Thus a logarithmic plot of conductivity against the root of applied field will be a straight line supporting the Poole-Frenkel effect. The above mentioned effect is also observed

in polyacrylonitrile films prepared by silent electric
discharge [9].

Chutia and Barua [111] have studied in detail
the current conduction mechanism of M-I-M structures of
polyacrylonitrile film prepared by the solution growth
technique. They have reported that Schottky emission [112]
is the main mechanism of the electrical conduction. For
Schottky mechanism the equation for current density is
given by

$$J = AT^2 \exp[-\phi_0 - \beta_s V^{\frac{1}{2}})/kT] \qquad (1.12)$$

where A is the Richardsons constant, ϕ_0 is the metal-
insulator potential barrier height, β_s is the Schottky
coefficient and is given by

$$\beta_s = [\frac{e^3}{4\pi\epsilon_r\epsilon_0 d}]^{\frac{1}{2}} \qquad (1.13)$$

The symbols have their usual meaning. In this case also
same type of current characteristic as seen in Poole-Frenkel
effect is observed. The only difference is that Schottky
emission will depend on the material of the electrode
whereas Poole-Frenkel effect is not.

Out of a number of different mechanisms of
conduction in polymers, space charge limited current (SCLC)
mechanism [113,114] is very often observed. Lampert [115,116]
and Rose [117] have reported that the analysis of
SCLC - voltage characteristics may provide a convenient tool
to study the parameters that characterise the traps present
in the insulator. A new method of interpreting the SCLC -
voltage curves which allows one to extract precise results
from experimental data is given by Sworakowski and Nespurek
[118]. The process of the SCLC is well described by a
number of authors [6,119,120]. In this process, when
injection into the conduction band or tunnelling, is not
a rate-limiting process for conduction in insulator, a
space-charge build up of the electrons in the conduction
band or at the centres may occur which will oppose the
applied voltage and impede the electron flow. At low applied
biases, if the injected carrier density is lower than the
thermally generated free carrier density, Ohms law is obeyed.
When the injected carrier density is greater than the free
carrier density, the current becomes space-charge-limited.
Two requirements must be satisfied if SCLC flow is to be
observed: (1) at least one electrode must make ohmic contact
to the insulator (2) the insulator must be relatively free
from trapping effects. Phadke [6,17,121] studied the SCLC
in plasma-polymerised malononitrile films and ferrocene

films. In this case there are four regions in the

voltage - current characteristic as shown in Fig.1.11. In

the first region A-B, the current density varies with

voltage as

$$J_{ohm} = n_o e\mu \frac{V}{d}$$
(1.14)

where n_o - the initial concentration of charge carriers,

μ - the mobility, V - the applied voltage and d - the

thickness. When voltage increases, the number of injected

carriers become greater than the thermally generated charge

carriers and SCLC starts. The presence of traps will reduce

the SCLC, since empty traps will remove most of the injected

carriers. Hence only a fraction of the carriers injected

from the contacts will be free. In Fig.1.11, B-C shows

SCLC region with shallow traps which follows

$$J_{SCL} = \frac{9}{8} \epsilon\mu \frac{V^2}{d^3} \Theta$$
(1.15)

where ϵ is the dielectric constant.

$$\Theta = \frac{N_c}{N_t} \exp \frac{-E_t}{kT}$$
(1.16)

where N_c is the effective density of state in conduction

band, N_t the trap density, E_t the energy level of traps
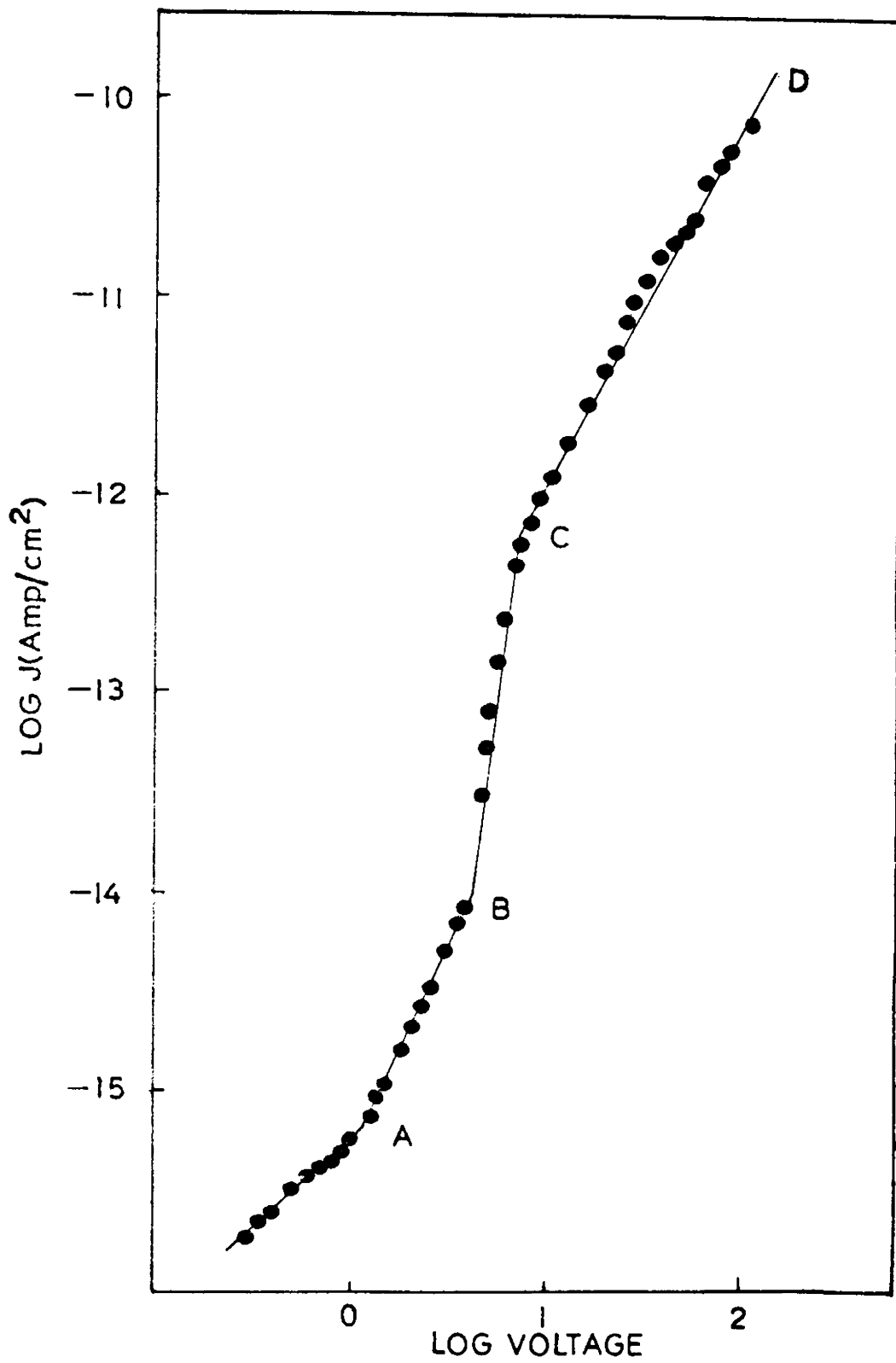
Fig.1.11. Current-voltage characteristic for polythiourea [6].

below the bottom of conduction band. For shallow trap SCLC and trap-free SCLC [122] θ is equal to unity. The transition voltage of ohmic region and SCLC (shallow trap) region is given by

$$V_{tr} = \frac{8}{9} \frac{n_o e d^2}{\varepsilon}$$ (1.17)

On further increasing the voltage, the Electron Steady State Fermi Level (ESSFL) moves up the energy gap towards the conduction band. When it moves through a trap level, the trap which is initially 'shallow' and effective in reducing the current, becomes 'deep' and loses its effectiveness. When the injection level is so high that the ESSFL lies above the trap levels, all traps are essentially full. Thus, all the injected carriers appear in the conduction band and the current increases rapidly back to the trap-free curve. The voltage at which this occurs is called trap-filled limit voltage (V_{TFL}) [123] and is given by

$$V_{TFL} = \frac{e N_t d^2}{2 \varepsilon}$$ (1.18)

Above this, any slight change in voltage will raise the current sharply as shown by C-D. On reaching the trap-free space charge limit given by D-E, the current - voltage relation becomes

$$J \propto V^n$$ (1.19)

where n is much greater than two. Phadke [6,17] has also studied the temperature variations of current density in polymalononitrile and polyferrocene thin films and the results are interpreted on the basis of appropriate energy level diagrams.

It was a break-through in polymer technology, when control on conductive properties of polymers is achieved analogous to that of covalent semiconductors. Most of the semiconducting polymers are conjugated polymers with alternate single and double bond configuration. The preparative methods and properties of a number of semiconducting polymers are described elsewhere [123,124]. Lupinski et al [125] gave one of the early reports on the controlled variable conductivity in a relatively stable system, viz., Tetracyanoquinodimethane (TCNQ) polymer salt. Recently various kinds of polymers are synthesised with wide ranges of conductivity from semiconductor to metallic. Tetrathiafulvalene - Tetracyanoquinodimethane (TTF-TCNQ) complexes have a conductivity of the order of $10^2 \, \Omega^{-1} cm^{-1}$ [126] which varies with the concentration of TTF. Recently, polymeric sulphur nitride $(SN)_x$ has attracted much attention because of its metallic [127-129] and even superconductive properties around $0.3^\circ K$ [130]. In room temperature the conductivity of $(SN)_x$ single crystal is $3.7 \times 10^3 \, \Omega^{-1} cm^{-1}$ and that of $(SN \, Br_{0.4})_x$ is $3.8 \times 10^4 \, \Omega^{-1} cm^{-1}$. Yoshino et al [7] have

studied the electrical properties of doped and undoped $(SN)_x$ thin film and explained the mechanism of charge transport.

In semiconductor technology, polyacetylene has an important place because of its unique semiconducting properties. By the successful synthesis of high quality flexible copper-coloured films of the CIS-isomer and silvery films of the trans-isomer [131-133] of conjugated polyene from acetylene in presence of a Ziegler catalyst and also by the successful control of the isomerism in the product [134,135], the attention of most of the polymer technologists has been turned to this material. The structures of CIS-$(CH)_x$ and trans-$(CH)_x$ are shown as Fig.1.03.

The electrical conductivity of CIS- and trans-$(CH)_x$ at room temperature and $1.7 \times 10^{-9} \Omega^{-1} cm^{-1}$ and $4.4 \times 10^{-5} \Omega^{-1} cm^{-1}$ respectively. The conductivity increases sharply when controlled amount of impurities like Cl, Br, I, AsF_5 and Na are doped. The method of doping and the change in the conductivities are already reported by Chiang et al [126]. The electronic properties are similar to those of a simple classical semiconductor with thermally activated conductivity at low dopant levels and transition to metallic properties at high dopant levels. The dopant can be either an acceptor (Br, I or AsF_5) or a donor (Li, Na or K) [136]. A typical behaviour for the electrical conductivity as a function of
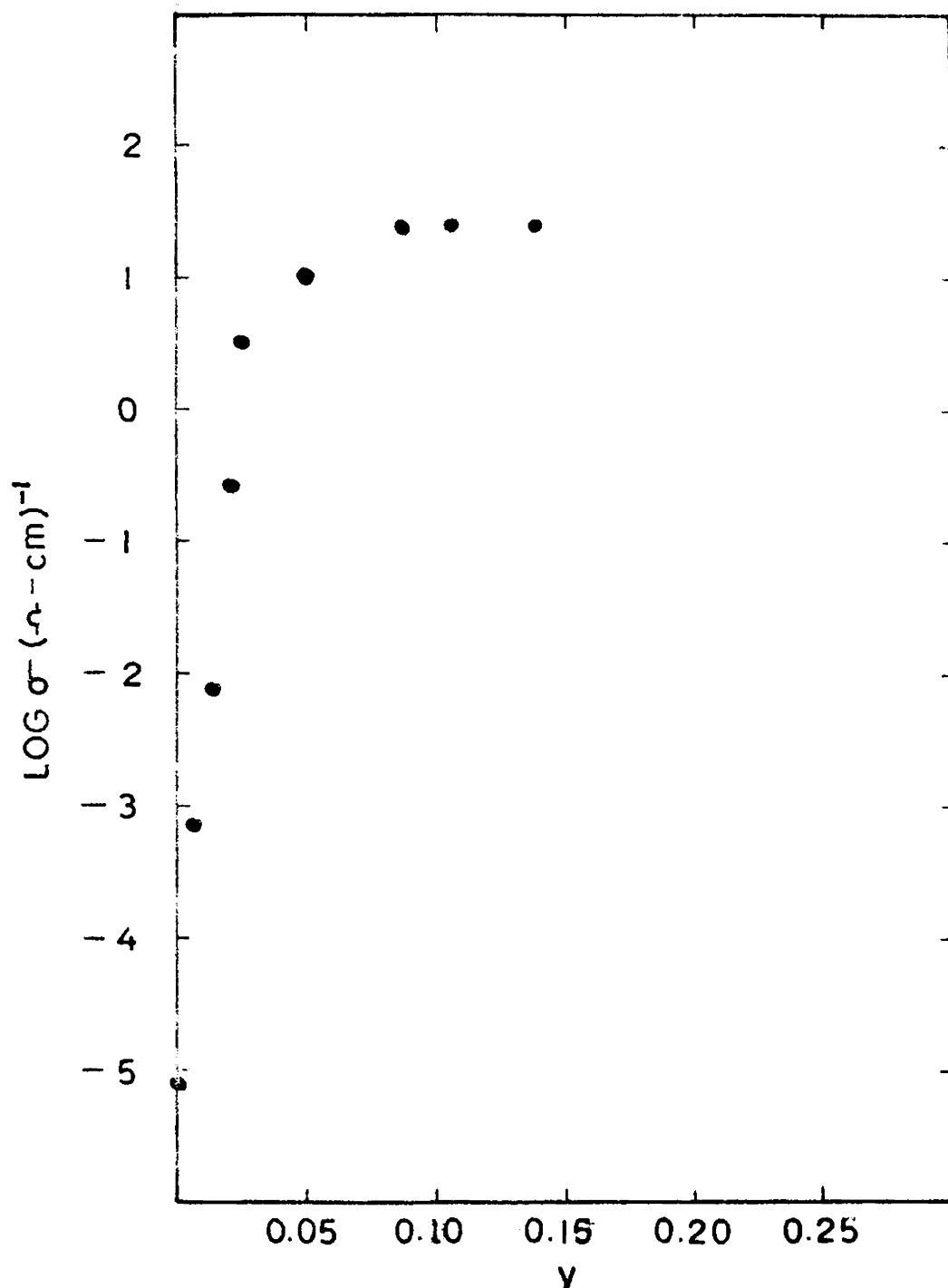
Fig.1.12. Electrical conductivity of trans-
$[CH(AsF_5)_y]_x$ as a function of
dopant concentration y [8].

the dopant concentration is shown in Fig.1.12. From the
above studies, polyacetylene exhibit many attractive features
for potential device applications. As an initial step,
Chiang et al [136] have fabricated p-n junction diodes
and their experiments are encouraging. The undoped
trans-$(CH)_x$ is confirmed to be p-type. The p-(CH_x): n-ZnS
hetrojunction has been demonstrated by Ozaki et al [137]
to give an open circuit voltage of 0.8V. These results point
to the potential of $(CH)_x$ as a photosensitive material for
use in solar-cell applications. If the polymer semiconductor
technology progresses at the present rate, then most of the
inorganic materials used in electronic circuitary will be
replaced by polymer materials thereby making these components
cheaper.

1.32 Dielectric behaviour of polymer thin films

Although most of the development efforts on thin
films have been concentrated around inorganic materials,
organic polymers offer highly desirable electrical and
mechanical properties which make them suitable as capacitor
dielectrics. The polymers show high dielectric strength and
low dissipation factor. The electrical properties and
mechanical properties of a number of polymers which are
commercially used as capacitor dielectrics are available
[138,139]. Exhaustive studies of the dielectric properties

of the polymers and appropriate theories to explain these

properties are well discussed in the literature [6,140,141].

Depending on the dielectric behaviour, the polymers are

broadly divided into two groups: (a) Non-polar polymers

and (b) Polar polymers. The first group of polymers are

characterised by the absence of a permanent dipole moment

and they show very low dielectric constant, practically

no dielectric loss and very little frequency dependence of

either of these quantities. In this case, the electrical

polarisation is principally due to the distortion of the

electronic and atomic structures. However, majority of

polymers belong to the polar group. They have permanent

dipole moment and hence exhibit dielectric dispersion. The

polar polymers usually show very high dielectric constant.

Good examples of such polymers are polyacrylonitrile (PAN)

[142] and polyvinylidene fluoride [143]. The side group in

PAN is a nitrile moiety, which by itself has a permanent

dipole moment of 3.4D. But there is evidence [144,145]

that the nitrile group in PAN may have dipole moment lesser

than the normal value. Bradley and Hammes [74] have given

the capacitance of a number of plasma-polymerised polymer

films sandwiched by two aluminium electrodes. Phadke [82]

has given information regarding the variation of loss factor

(tan δ) with temperature and frequency upto 6.5MHz and

variation of dielectric constant with frequency for a few

polymer films. Dielectric properties of a number of polymer films are thus available in the literature [146-148].

In recent years, the dielectric studies are extended to solid solutions like polyethylene oxide and polyvinyl alcohol at high frequencies (upto 40GHz) to obtain information on the adsorbed water vapour and oxygen [149-151]. To get the information on the origin of the dielectric properties, the spectra of loss peaks with temperature are analysed by different scientists [152,153].

Glow discharged polystyrene thin films have many different electrical and physical properties [eg. relative dielectric constant (ε_r) dielectric loss (tan δ), solubility etc.] in comparison with ordinary styrene [154]. Takeda [155,156] has reported that the temperature coefficient of the dielectric constant of glow-discharged polystyrene is different from the normal polystyrene. The temperature coefficient of the dielectric constant of a normal polystyrene film is negative, while it is positive for the polystyrene thin film formed by electrodeless excitation. The negative coefficient seems to be due to thermal expansion of volume while the other is due to the permanent dipoles with widely distributed relaxation times [157].

From most of the dielectric studies in the past
few decades, it is well established that polymers are very
good dielectric materials with comparatively high breakdown
voltage. Hence polymers have been identified, for their
application as capacitors for high voltage supplies.
Currently, the polymer scientists have switched over their
investigations to other allied properties such as thermally
stimulated depolarisation current, piezoelectric and
pyroelectric behaviour.

1.33 Thermally stimulated current in unpoled and poled polymer thin films

Extensive studies have been reported on the short-
circuited current of poled [158-160] and unpoled [161-163]
polymers to obtain information about the behaviour of trapped
charges and dipole relaxation process. Thermo-electric and
electro-chemical effects have also been studied in detail
on a variety of polymers [162,163]. Pillai et al [164]
have observed a spontaneous short-circuited current in
unpoled polyvinylacetate due to the dissociation of adsorbed
water into H^+ and OH^-. Pillai and Mollah [165] have also
studied the effect of electrodes in the polymer sandwich
system on heating. Carr et al [166,167] have worked on the
spontaneous current release from polyacrylonitrile. They
have suggested that this current is due to the chemical

degradation. There are investigations on thermally stimulated currents due to compositional inhomogeneity in plasma-polymerised Al-PAN-Al.

Thermally stimulated depolarisation (TSD) current analyses give detailed information on the mechanism of charge storage in electrets. In poled polymer electrets, usually two peaks are observed, one below (β-transition) and other above (α-transition) the glass transition temperature [168,169]. The α-transition is due to the relaxation of trapped charges while the β-transition is associated with movement of sidegroups around the equilibrium position where large scale confirmational rearrangement on the main chain are frozen. More detailed theoretical and experimental results on the mechanism of charge storage in electret polymers are given by Sessler and Van Turnhout [170].

Consider an ideal dielectric containing only one type of non-interacting dipoles of moment p and relaxation frequency α. In the absence of an electric field the dipoles are oriented randomly. If one applies a poling field E_p at a poling temperature T_p for an interval of time $t_p \gg \tau(T_p)$ (where $\tau(T_p)$ is the relaxation time at T_p) the dipoles will be polarised to saturation and in the meantime an exponential current decay will be observed. At this time the dielectric is cooled down to room temperature T_o, where the

relaxation time is of the order of hours. At $T = T_o$, the electric field E_p is turned off and a poled dielectric is obtained. When the specimen is short-circuited through an electrometer and the temperature is raised, depolarisation peaks are observed and these peaks are properly analysed to get the detailed information about the dipole moment and charge storage in dielectrics.

If a polar material contains N dipoles per unit volume, with a dipole moment p, the final polarisation after poling with a field E_p is

$$P_o = \frac{N p^2 E_p}{3kT_p} \tag{1.20}$$

During the subsequent TSD, the aligned dipoles will randomly disorient and the depolarisation current is given by the following expression [171].

$$J(T) = -\alpha(T)P_o \exp[-\frac{1}{\beta}\int_{T_o}^{T}\alpha(T)dT] \tag{1.21}$$

where β is the rate of heating $\frac{dT}{dt}$. Different depolarisation kinetic parameters like $\alpha(T_{max})$ and activation energy A can be derived from this expression. The total polarisation P_o can be

calculated from the area taken by the peak and is given by

$$P_o = \frac{1}{\beta} \int_{T_o}^{\infty} J(T)d(T)$$
(1.22)

Hence from eqn.(1.20) the dipole moment can be calculated. It is strange to see that the P_o calculated from the dipole moment of PAN by Stupp and Carr [172] is less than the polarisation observed experimentally from the depolarisation peaks. They have reported that the total polarisation calculated from eqn.(1.20) is only 0.05 $\mu C/cm^2$. The Onsager equation [173] has also been used to predict polarisation.

$$P_{ons} = \frac{Np^2 E_p}{kT_p} \frac{\epsilon_o (2\epsilon_o + 1)(n^2 + 2)^2}{9(2\epsilon_o + n^2)^2}$$
(1.23)

where ϵ_o is the dielectric constant at zero frequency and n is the index of refraction of the medium. Making no presupposition about the orientational aspects of the nitrile side-groups, one predicts $P_{ons} = 0.15\mu C/cm^2$. On the other hand, if one assumes that dipoles are constrained to orientational motions by rotation about axes perpendicular to the electrical field, this value can be increased to $P_{ons} = 0.23\mu C/cm^2$. The Frolich equation [172]

$$P_{fro} = \frac{Np^2 E_p}{kT_p} \frac{\epsilon_o (n^2 + 2)^2}{9(2\epsilon_o + n^2)} \cdot g$$
(1.24)

is capable of taking into account not only how the local environment of a dipoles modifies the impressed electrical field but also how the local environment imposes a force field upon the dipoles. In the case of numbers reported in the previous paragraph, 'g' would need to have values in the range 3 in order to reconcile with the experiments.

Charge storage properties in solution grown polyvinyl butral thin films have been studied by TSD technique by Jain et al [174]. Of the observed two peaks, one is associated with the deorientation of the aligned dipoles whereas the other is associated with trapped charges. Such types of studies are frequently reported for other polymers also [175,176]. Wintle and Sapieha [177] have reported a method namely optical detrapping (photon stimulated currents) to study the trap depth in polymer films.

The outcome of such TSD studies is that the scientists could contribute very good dielectric materials like polyvinylidene fluoride (PVF_2) which has very high dipole moment. TSD studies of PVF_2 reveal that the dipole orientation in thin polymer is reversible [178-180]. Even-though PAN has very high dipole moment (3.4D), from the results of TSD it is suggested that the nitrile side group has only a slight preferred orientation in the direction

of polarisation. Hence this material is neither piezo-
electric nor pyroelectric. Thus it will be of special
interest to understand the poling mechanism of PAN and the
limitation of dipolar orientation in an electric field.
In this direction extensive work has been carried out and
reported by Stupp et al [142,160,172].

1.34 Piezoelectric and pyroelectric polymer thin films

During the past few years, there is an increasing
interest in the phenomena of piezoelectricity and pyro-
electricity in polymers. The pyroelectricity is associated
with the temperature dependence of remnant polarisation.
When a pyroelectric material is heated, a voltage is
developed across the specimen which is proportional to the
rate of change in temperature. In the case of piezoelectric
material the voltage across the surfaces are associated with
the stress. Although a number of polymers have been studied,
none has matched in magnitude the effects found in PVF_2.
The fact that substantial piezoelectricity can be permanently
induced by suitable treatment in PVF_2 was first reported by
Kawai [181]. Shortly thereafter, Bergman et al [182]
treated PVF_2 in the same manner and demonstrated pyroelectric
behaviour also. Three crystal phases (α, β, γ) have been
reported for PVF_2 of which α and β phases are commonly used
as piezoelectric polymer.

Kepler [183] has reported that the origin of pyroelectricity in PVF_2 is the orientation of dipoles and pyroelectric coefficients are found to be -1.25×10^{-5} and -2.74×10^{-5} $Cn/m^2 K$ for biaxially oriented films and piezo-films respectively. Based on the observations of Glass, Oshiki and Fukada [184,185] it has been concluded that the origin of the spontaneous polarisation in PVF_2 is due to dipole orientation and the orientation can be in part reversed by an electric field. PVF_2, thus shows ferro-electric behaviour also. It is perhaps wise to highlight the fact that the particular piezoelectric and pyroelectric properties can be quite sample-dependant in terms of both purity, morphology and detailed processing procedure. Thus it has become difficult to identify a specific mechanism to explain the piezoelectric behaviour when several inter-related parameters are involved.

Pyroelectric studies of the copolymer of PAN and $PVCl_2$ reveal that the property is due to space charge mechanism [186]. The depolarisation of polyethylene tere-phthalate films under short-circuited conditions was well studied using white light as a probe [187]. A representative value for the pyroelectric coefficient is $4nC\ m^{-2}K^{-1}$. The pyroelectric current in PAN was also studied by Likhovidov et al [188] and suggested that the production of electrets films

with high pyroelectric coefficient like PAN enables the direct transformation of solar to electrical energy.

In summary, a detailed understanding of the origin of piezoelectric and pyroelectric properties of polymers are still lacking. Currently, work is in progress to understand the phenomenon, to improve the performance and processing of PVF_2 and if possible to identify or even design new materials. Recent reports indicate that efficient poling of PVF_2 can take place at room temperature by the use of Corona-charging [189].

1.35 Applications of polymer thin films

The polymer films are widely used for various industrial purposes. The main advantages of polymer thin films are that they can be prepared easily and cheaply, that they are stable and flexible and can be moulded into any form. Polymer films are very well in use in electronics as capacitors. Polystyrene capacitors are very popular in electronic industry. After the development of n-type and p-type polyacetylene, diodes and transistors are fabricated with this polymer [136,137]. Due to its very good photosensitivity, it can be used for solar cell applications. The electret properties of polymer are utilised to develop different types of devices. The applications of electrets are based on the piezoelectric and pyroelectric effects in polarised material.

Among them, special importance is given to electro-acoustic
transducers utilising piezoelectric films operating in
transverse or longitudinal modes [190,191]. The recent
discovery of strong piezoelectric effect in PVF_2 has led
a number of significant applications of this material in
electro-acoustic and electro-chemical transducers. Such
transducers are very well used for underwater communications
[192]. Composite resonators using PVF_2 piezoelectric films
have been applied in acoustic transducers for generating and
detecting VHF ultrasonic waves in water. The flexibility of
PVF_2 enables one to fabricate concave transducers for
focussing radiation [193,194]. The electret mocrophones are
generally used in loud-speakers and its advantage is that they
do not require bias voltage. Their frequency response is
superior to all other microphones. Among the research appli-
cations, such microphones are used in opto-acoustic spectro-
scopy especially in connection with the detection of air
pollution [195,196]. The variety of applications of electret
thin films may be listed under photo-conductive image
formation [197], Xerographic reproduction [198] and electret
motors [199]. Similarly pyroelectric polymers are used as
optical detectors [200], and vidicon tubes [201]. A detailed
review on the applications of polymer films is given by
Sessler and West [202].

L.40   AIM AND SCOPE OF PRESENT WORK

From the above survey it is clear that a lot of interest is paid to PVF_2 because of its appreciably good piezoelectric and pyroelectric properties. The dipole moment of PVF_2 is 2.27D and it is reported that a better dipole moment (3.4D) is observed in PAN. So it is natural to expect very high pyroelectric and piezoelectric coefficients for PAN. From the literature it can be seen that a number of investigations are made on PAN prepared by solution growth technique and it is found that even with such a large dipole moment, the charge storage capability is very small and piezoelectric and pyroelectric coefficients are very low. They have suggested that for such samples, the nitrile side-group has only a slight preferred orientation. From the above review, it can be seen that the dielectric properties may be different for polymer films prepared by different techniques. It is also important to note that the mechanism of conduction in PAN is varied with different preparative techniques. Hence it was thought to carry out a more detailed investigation in PAN prepared by a completely different method. PAN was prepared directly from monomer by plasma-polymerisation. The specimens were subjected to TSC studies for unpoled and poled specimens. The dielectric properties and conduction mechanism were also investigated. The dipole

moment is found to be very close to 3.4D. The structural information was attempted by infrared technique and the reaction mechanism was studied by observing the band spectra. The results were compared with PAN prepared by other methods. An appreciable amount of short-circuited current shown in Al-PAN-Al is an important observation of the present investigations of the plasma-polymerised PAN.

REFERENCES

[1] A.Tager, ' Physical Chemistry of Polymers ', Mir (Pub),
(1978).

[2] F.W.Billmayer Jr., 'Text Book of Polymer Science' ,
John Wiley and Sons, New York (1970).

[3] D.B.V.Parker, 'Polymer Chemistry', Applied Science
Publishers Ltd., London (1974).

[4] J.Mort, Advances in Physics, 29, 2, 367 (1980).

[5] B.A.Bolto, 'Organic Semiconducting Polymers' , J.E.Katon
(Ed.), Marcel Dekker, Inc., New York, p.200 (1968).

[6] S.D.Phadke, Ph.D. Thesis, Department of Physics,
University of Poona, India (1978).

[7] K.Yoshino, K.Tanimura, Y.Yamamoto, K.Kaneto and Y.Insuishi,
Technology Reports of the Osaka Univ. 28, 1430 (1978).

[8] C.K.Chiang, C.R.Fincher Jr., Y.W.Park, A.J.Heeger,
H.Shrakawa, E.J.Louis, S.C.Gav and A.G.Mac Diarmid,
Phys. Rev. Lett. 39, 17, 1098 (1977).

[9] Tadaaki Hirai and Osamu Nakada, Jap. J. Appl. Phys.,
7, 2, 112 (1968).

[10] H.Yasuda, 'Plasma Chemistry of Polymers', M.Shen (Ed.),
Marcel Dekker, New York (1976).

[11] M.Stolka, D.M.Pai, 'Advances in Polymer Science',
Heidelberg: Springer-Verlag, 29 (1978).

[12] M.M.Fox De Labes, 'Physics and Chemistry of Organic Solid
State', A.Weissberger (Ed.), Inter Science, New York, Vol.I
(1963).

[13] L.E. Lyons, Aust. J. Chem., 8, 507 (1971).

[14] D.M.Harison, 'C.R.C. Critical Reviews in Solid State Science', 267 (1973).

[15] N.Karl, Festkorper Problems, H.J.Queisser (Ed.), Pergamon Press, New York, XIV (1974).

[16] J.Mort and A.I.Lakatos, J. Noncrystalline Solids, 4, 117 (1970).

[17] S.D.Phadke, Thin Solid Films,55, 391 (1978).

[18] Keuchi Ando and Minoru Kusabiraki, Memoirs of Faculty of Engineering, Osaka City Univ. 19, (1978).

[19] M.M.Perlman, J. Electrochem. Soc., 119, 892 (1972).

[20] J.Van Turnhout, 'Thermally Stimulated Discharge of Polymer Electrets', Elsevier, Amsterdam (1975).

[21] P.C.Mehendru, K.Jain and Praveen Mehendru, J. Phys. D. Appl. Phys., 11, 1431 (1978).

[22] J.Van Turnhout, 'Thermally Stimulated Discharge of Electrets', Electrets, G.M.Sessler (Ed.), Springer-Verlag, Berlin, Heidelberg, New York, 93 (1980).

[23] G.M.Sessler, ' Physical Principles of Electrets', Electrets, G.M.Sessler (Ed.), Springer-Verlag, Berlin, Heidelberg, New York, 55 (1980).

[24] H.A.Pohl, 'Organic Semiconducting Polymers', J.E.Katon (Ed.), Marcel Dekker, New York (1968).

[25] Nirmala Paul, Ph.D. Thesis, Dept. of Phys., Univ. of Cochin, India (1981).

[26] R.H.Partridge, J. Chem. Phys., 49, 3656 (1968).

[27] J.Ritsko, J. Chem. Phys., 70, 5343 (1979).

[28] W.L.McCubbin, Chem. Phys. Lett., 10, 365 (1971).

[29] J.M.Andre, 'Electronic Structure of Polymers and
    Molecular Crystals', J.M.Andre and J.Ladik (Ed.),
    Plenum (1975).

[30] A.A.Ovchinnikov, Sov. Phys. Usp., 15, 575 (1973).

[31] H.A.Pohl, 'Modern Aspects of the Vitreous State',
    J.D.Mac Kenzic (Ed.), Butterworths, London, Vol.II (1962).

[32] A.Rembaum, J. Moacanin and H.A.Pohl, 'Progress in
    Dielectrics', J.B.Birks and J.A.Hart (Ed.), Academic
    Press, New York (1965).

[33] Handbook of Plastics, American Soc. of Plastics.

[34] B.J.Brophy and J.W.Buttrey, Organic Semiconductor Proc.,
    Mac Millan, N.Y. (1962).

[35] D.D.Fley, Nature (London), 162, 819 (1943), Trans
    Faraday Soc., 51, 152 (1955).

[36] H.Ino Kuchi, Bull. Chem. Soc. Jap., 24, 222 (1951).

[37] A.Rembaum and J. Moucanin, 'Polymeric Semiconductors',
    Jet Propulsion Laboratory, California (1964).

[38] K.Neki and P.H.Geil, The Solid State Physics (Report of
    the U.S.-Japan Joint Seminar), P.H.Geil, E.Baer and
    Y.Wada (Ed.), Marcel Dekker, INC., New York, 295 (1974).

[39] H.A.Pohl, J.A.Bormmann and W.Itoch, 'Semiconducting
    Polymers', Plastic Laboratory, Technical Report 60C,
    Princeton Univ.

[40] G.A.Edwards and Goldfinger, J. Poly. Sci., 16, 589 (1955).

[41] J.A. Koustsky, A.G.Walton and E.Bear, J.Polymer Sci., A-2, 4, 611 (1966).

[42] J.A.Koustsky, A.G.Walton and E. Bear, J. Polymer Sci., Part B, 5, 177 (1967).

[43] R.W.Christy, J. Appl. Phys., 31, 1680 (1980).

[44] J.Goodman, J. Poly. Sci., 44, 552 (1960).

[45] D.J.Valley and J.S.Wagener, IEEE Trans. Component PTS., CP-11, 205 (1964).

[46] Fred W.Billimeyer Jr., 'Textbook of Polymer Science', John Wiley and Sons, Inc., Chapter III, 253 (1971).

[47] G.A.Delzenne, 'Recent Advances in Photo-cross-linkable Polymers', Reviews in Polymer Technology, Irving Skeist (Ed.), Marcel Dekker, INC, New York, 185 (1972).

[48] David J. William, 'Polymer Science and Engineering', Prentice-Hall, INC., New Jersey, Part II, 43 (1971).

[49] Kamlesh Jain, Naresh Kumar and P.C.Mehendru, J. Electrochem. Soc., Solid-State Science and Technology, 126, 11, 1958 (1979).

[50] E.Sacher, IEEE Trans. Electr. Insul., EI-13, 2, 94 (1978).

[51] K.L.Chopra, J. Appl. Phys., 40, 906 (1969).

[52] A.C.Rastogi and K.L.Chopra, Thin Solid Films, 26, 61 (1975).

[53] K.L.Chopra, A.C.Rastogi and G.L.Malhotra, Thin Solid Films, 24, 125 (1974).

[54] A.C.Rastogi and K.L.Chopra, Thin Solid Films, 18, 187 (1973).

[55] P.W.Palmberg, T.N.Rhodin and C.J.Todd, Appl. Phys.
Letters, 11, 33, (1967).

[56] A.C.Cooper, A.Kellar and J.R.Waring, J. Polymer Sci.,
11, 512 (1953).

[57] M.White, Vacuum, 15, 449 (1965).

[58] C.A.Hogarth and I.Iqbal, Thin Solid Films, 51, 3,
L45 (1978).

[59] W.De Wilde, Thin Solid Films, 24, 101 (1974).

[60] G.N.Jackson, Thin Solid Films, 5, 209 (1970).

[61] L.Holland and C.R.D.Prestland, Vacuum, 22, 133 (1972).

[62] L.V.Gregor and H.L.Mc Gee, Proc. 5th Electron Beam
Symp., Boston, (1963), Alloyed Corp·,Cambridge,
Mass, 211 (1963).

[63] David S. Campbell, 'Handbook of Thin Film Technology',
Leon I. Maissel and Reinhard Glang (Ed.), McGraw-Hill
Book Company, New York, Chapter 5, 13 (1970).

[64] P.White, J. Phys. Chem., 67, 2493 (1963).

[65] R.W.Christy, J. Appl. Phys., 35, 2179 (1964).

[66] M.Stuart, Nature, 199, 59 (1963).

[67] I.Hellax and P.White, J. Phys. Chem., 67, 1784 (1963).

[68] A.Raave, 'Organic Chemistry of Macromolecules', Marcel
Dekker, Inc., New York (1967).

[69] R.Glang and L.V.Gregor, 'Handbook of Thin Film
Technology', Leon I. Maisel and Reinhard Glang (Ed.),
McGraw-Hill Book Company, New York, Chapter 7, 23 (1970).

[70] L.V.Gregor, 'Physics of Thin Film', G.Hass and
R.E.Thum (Ed.), Academic Press, New York, Vol.3 (1966).

[71] F.E.Garion, D.J.Valley and W.E.Loeb, IEEE Trans.,
PMP-1, 554 (1965).

[72] H.Pagnia, Phys. Stata Solidi, 1, 90 (1961).

[73] M.Yesuda, M.O.Bugarner and J.J.Hillman, J.Polym.Sci.,
17, 1519 (1973).

[74] Arthur Bradley and John P. Hammes, J. Electrochem. Soc.,
110, 1, 15 (1963).

[75] M.Millard, 'Techniques and Applications of Plasma
Chemistry', J.R. Hollahan and A.T.Bell (Ed.), Wiley,
New York (1974).

[76] M.Stuart, Proc. IEEE, 112, 1614 (1965).

[77] Suhr, 'Techniques and Applications of Plasma Chemistry',
J.R.Hollahan and A.T.Bell (Ed.), Wiley, New York (1974).

[78] R.L.Mc Carthey, J. Chem. Phys., 22, 1360 (1954).

[79] T.Williams and M.W.Hayes, Nature, 209, 769 (1966).

[80] A.R.Westwood, Eur. Polym. J., 77, 377 (1971).

[81] J.Stachura and S.Veis, Acta Phys. Solv., 29, 91 (1979).

[82] Shireesh D. Phadke, Thin Solid Films, 48, 319 (1978).

[83] H.Yasuda and C.E.Lamaze, J. Appl. Polym. Sci., 15,
2277 (1971).

[84] M.Millard, J.J. Windle and A.E.Pavlvath, J.Polym. Sci.,
17, 2501 (1973).

[85] Nirmala Paul, Thin Solid Film, 76, 201 (1981).

[86] H.Yasuda, Appl. Polym. Symp., 22, 2411 (1973).

[87] H.Yasuda, M.O.Bugarner and J.J. Hillman, J. Polymer
Sci., 19, 531 (1975).

[88] A.Beri, H.Carchano and J.Guastavina, Thin Solid Films,
21, 313 (1974).

[89] J.K.Stille, R.L.Sung, and J.Vander Kooi, J. Org. Chem.,
30, 3116 (1965).

[90] J.K.Stille and C.E.Rix, J. Org. Chem., 31, 1591 (1966).

[91] S.Walker and T.F.Bindley, Trans. Faraday Soc., 58, 217
(1962).

[92] H.Sculer and M.Stockburger, Spectrachem. Acta, 13,
841 (1959).

[93] S.Walker and R.F.Barrow, Trans. Faraday Soc., 50,
541 (1954).

[94] S.Walker, T.F.Bindley, and A.T.Watts, Trans. Faraday
Soc., 58, 849 (1962).

[95] B.D.Blaustein and Y.C.Fu, 'Organic Reactions in Physical
Methods of Chemistry', A.Weissberger (Ed.), Wiley,
Part IIB, 1 (1971).

[96] F.K.Me Taggart, 'Plasma Chemistry in Electrical Discharges',
Elsevier, New York (1967).

[97] A.S.Kana'an and J.L.Margrave,' Advances in Inorganic
Chemistry and Radiochemistry', H.J.Eneleus, and
A.G.Sharpe (Ed.), Vol.6, Academic Press, New York (1964).

[98] Raymond B.Seymour, 'Introduction to Polymer Chemistry',

McGraw-Hill, Kogakusha Ltd., Tokyo, Chapter 16,

370 (1971).

[99] Jerold Schultz, 'Polymer Materials Science', Prentice Hall,

INC., New Jersey (1974).

[100] A.Vou Roggen, Phys. Rev., Letters, 9, 368 (1962).

[101] S.Saito, H.Sasabe, T.Nakajima and K.Yada, J. Polym. Sci.,

6A2, 1297 (1965).

[102] A.Foss and W.Dannhauser, J. Appl. Polym. Sci., 7,

1015 (1963).

[103] H.Sasabe and S.Saito, J. Polym. Sci., 6A2, 1401 (1968).

[104] F.S.Smith and Clare Scott, Brit. J. Appl. Phys.,

17, 1149 (1966).

[105] L.E.Amborskii, J. Polym. Sci., 62, 331 (1963).

[106] W.G.Lawson, Brit. J. Appl. Phys., 16, 1805 (1965).

[107] L.F.Babcock and R.W.Christy, J. Appl. Phys., 43,

1423 (1974).

[108] Keiichi Ando and Minoru Kusabiraki, Memoirs of the

Faculty of Engineering Osaka 'City Univ., 19 (1978)

(The same ref.19).

[109] J.Frenken, Phys. Rev., 54, 647 (1938).

[110] D.R.Lamb, 'Electrical Conduction Mechanism in Thin

Insulating Films ', Mathiuen and Co. Ltd., London (1967).

[111] J.Chutia and K.Barua, Phys. Stat. Sol., A(a)55,

K13 (1979).

[112] J.G.Simmons, J. Appl. Phys., 35, 2472 (1964).

[113] P.J.Reucroft and S.K.Ghosh, Thin Solid Films, 20, 363 (1974).

[114] J.Gazso, Thin Solid Films, 21, 43 (1974).

[115] M.A.Lampert, A.Rose, A.W.Smith, Phys. Rev., 103, 1648 (1956).

[116] M.A.Lampert and P.Mark, 'Current Injection in Solids', Academic Press, New York (1970).

[117] A.Rose, Phys. Rev., 97, 1538 (1955).

[118] Juliusz Sworakowski and Scanislaw Nespurek, J. Electrostatics, 8, 97 (1979).

[119] K.L.Chopra, 'Thin Film Phenomena', McGraw-Hill Book Company, New York, 499 (1969).

[120] John G.Simmons, 'Electronic Conduction Through Thin Insulating Films', Handbook of Thin Film Technology, Leon I. Maissel and Reinhard Glang (Ed.), McGraw-Hill Book Company, New York, 14 (1970).

[121] Shireesh D.Phadeke, K.Sathianandan and R.N.Karekar, Thin Solid Films, 51, L-9 (1978).

[122] D.F. Barbe and C.R.Westgate, J. Chem. Phys., 52, 4046 (1970).

[123] Ya.M.Paushkin, T.P.Vrshnyakova, A.F.Lamin and S.A.Nizova, Organic Polymeric Semiconductors, D.Slutzkin (Ed.), John Wiley and Sons, New York (1974).

[124] B.A.Bolto, Organic Semiconducting Polymers, J.E.Katon

(Ed.), Marcel Dekker, INC., New York, 199 (1968).

[125] J.M.Lupinski, K.D.Kopple and J.J.Hertz, J. Polym. Sci.,

16, 1561 (1967).

[126] C.K.Chiang, M.A.Druy, S.C.Gau, A.J.Heeger, E.J.Louis,

A.G. Mac Diarmid, Y.W.Park and H.Shirakawa, J. Am. Chem.

Soc., 100, 3, 1013 (1978).

[127] V.V.Walatka Jr. and M.M.Labes, Phys. Rev. Lett., 31,

1139 (1973).

[128] H.Kamimura, A.M.Glazer, A.G.Grant, Y.Natsume, M.Schreiber

and A.D.Yoffe, Appl. Phys. C, Solid State Phys.,

9, 1451 (1976).

[129] C.K.Chiang, M.J.Cohen, A.F.Garito, A.G.Heeger,

C.M.Mikulski and A.C.Mac Diarmid, Solid State Comm.,

18, 145 (1976).

[130] R.L.Greene, G.B.Suter, Phys. Rev. Lett., 34, 577 (1975).

[131] Hideki Shirakawa, E.J.Louis, A.G.Mac Diarmid, C.K.Chiang

and A.J.Heeger, JCS. Chem. Comm., 578 (1977).

[132] H.Shirakawa and S.Ikeda, Polym. J., 2, 231 (1971).

[133] H.Shirakawa, T.Ito and S.Ikeda, Polym. J., 4, 460 (1973).

[134] T.Ito, H.Shirakawa and S.Ikeda, J. Polym. Sci., Part A-1,

Polym. Chem., 12, 11 (1974).

[135] T.Ito, H.Shirakawa and S.Ikeda, J. Polym. Sci., Part A-1,

Polym. Chem., 13, 1943 (1975).

[136] C.K.Chiang, S.C.Gau, C.R.Fincher Jr., Y.W.Park, A.G. Mac

Diarmid and A.J.Heeger, Appl. Phys. Lett., 33, 1, 18 (1978).

[137] M.Ozaki, D.L.Peebles, B.R.Weinberger, C.K.Chiang, S.C.Gau, n.J.Heeger and A.G.Mac Diarmid, Appl. Phys. Lett., 35, 1, 83 (1979).

[138] W.Mc Mahon, Plastics in Insulation, P.Brains (Ed.), John Wiley and Sons, Inc., New York, 141 (1968).

[139] Dieter Gerstenberg, Thin Film Capacitors, Handbook of Thin Film Technology, Lean I. Massel and Reinhard Glang (Ed.), McGraw-Hill Book Company, New York, 19 (1970).

[140] R.M.Higgin and J.Hirsh, IEEE (London), 210 (1970).

[141] A.K.Jonscher and Cell, Polym. Sci., 253, 231 (1975).

[142] R.J.Comstock, S.I.Stupp and S.H.Carr, J. Macromol. Sci. Phys. B 13(1), 101 (1977).

[143] M.Oshiki and E.Fukada, Jap. J. Appl. Phys., 15, 43 (1976).

[144] H.G.Olf, Appl. Polym. Symp., 25, 103 (1974).

[145] W.R.Krigbaum and N.Tolsta, J. Polym. Sci., 43, 467 (1960).

[146] R.Christy, J. Appl. Phys., 31, 1680 (1960).

[147] P.R.Emtage and W.Tantraparm, Phys. Rev. Lett. 8, 267 (1962).

[148] D.Sanchez, M.Cardiano and A.Bui, J. Appl. Phys., 45, 1233 (1974).

[149] V.Kaatze, 'Advances in Molecular Relaxation Processes', 7, 71 (1975).

[150] V.Kaatze, Progr. Colloid and Polymer Sci., 65, 214 (1978).

[151] U.Kaatze, O.Gottmann, R.Podbieiski, R.Pottel and
U.Terveer, J. of Phy. Chem., 82, 1 (1978).

[152] E.Sacher, IEEE, Electr. Insu., EI-13, 2 (1978).

[153] W.Wrasidlo, J. Macromol. Sci., B6, 559 (1972).

[154] M.Stuart, Proc. IEEE, 112, 1614 (1965).

[155] Shinichi Takeda, J. Appl. Phys., 47, 12 (1976).

[156] S.Takeda and Y.Saito, Jap. J. Appl. Phys., 12, 749 (1973).

[157] S.Takeda and M.Naito, Proc. 7th Inter. Vac. Congr.
3rd Inter. Conf. Solid Surface (1977).

[158] R.G.Kepler and R.A.Anderson, J. Appl. Phys., 49,
4490 (1978).

[159] D.K.Das Gupta and J.S. Duffy, J. Appl. Phys., 50,
561 (1979).

[160] S.I.Stupp and S.K.Carr, J. Appl. Phys. 46, 4120 (1975).

[161] Gorosawa, Shuhei Nakamura, Yoji Nishid and Masayuki Ieda,
Jap. J. Appl. Phys., 17, 1507 (1978).

[162] Gorosawa, Duck Chool Lee and Masayaki Ieda, Jap. J. Appl.
Phys., 16, 359 (1977).

[163] Gorosawa, Duck Chool Lee and Masayaki Ieda, Jap. J. Appl.
Phys., 16, 359 (1977).

[164] P.K.C.Pillai, S.F.Xavier and M.Mollah, Thermo Clinica
Acta, 35, 385 (1980).

[165] P.K.C.Pillai and M.Mollah, J. Macromol. Sci. Phys.,
B1,6, 3, 327 (1979).

[166] S.I.Stupp, S.H.Carr, J. Polym. Sci. Polym. Phys.,
15, 485 (1977).

[167] S.I.Stupp, S.H.Carr, J. Appl. Phys., 46, 4170 (1975).

[168] P.C.Mahendru, K.Jain and N.Kumar, Thin Solid Films,
70, 7 (1980).

[169] S.K.Shrivastava, J.D. Ranade and A.P.Shrivastava,
Thin Solid Films, 67, 201 (1980).

[170] G.M.Sessler, Electrets, Topics in Applied Physics,
33, G.M.Sessler (Ed.), Springer-Verlag, New York,
13 (1980); J.Van Turnhout, Electrets, Topics in Appl.
Phys. 33, G.M.Sessler (Ed.), Springer-Verlag, New York,
106 (1980).

[171] C.Bucci and R.Fiechi, Phys. Rev., 148, 816 (1966).

[172] S.I.Stupp and S.H.Carr, ' Charge Storage, Charge
Transport and Electrostatics with Their Applications,'
Studies in Electrical and Electronic Engineering 2,
Y.Wada, M.M.Pertmann and H.Kokado (Ed.), Elsevier, 123.

[173] N.E.Hill et al, ' Dielectric Properties and Molecular
Behaviour,' Van Nostrand-Reinhold, London (1969).

[174] Kamalesh Jain, Naresh Kumar and P.C.Mehendru,
J. Electrochem. Soc., Solid-State Science and Technology,
126, 11, 1958 (1979).

[175] P.C.Mehendru, K.Jain and Praveen Mehendru, J. Phys. D
Appl. Phys., 11, 1431 (1978).

[176] Shuhei Nakamura, Gorosawa and Hasayuki Ieda, Jap. J.
Appl. Phys.,18, 5, 917 (1979).

[177] H.J.Wintle and S.Sapieha, J. Electrostatics, 3, 195 (1977).

[178] H.Burkard and G.Pfister, J. Appl. Phys., 46, 3360 (1974).

[179] R.G.Kepler and R.A.Anderson, J. Appl. Phys., 49,
1232 (1978).

[180] R.G.Kepler, Ann. Rev. Phys. Chem., 29, 497 (1978).

[181] M.Kawai, Jap. J. Appl. Phys., 8, 975 (1969).

[182] Bergman, G.R.Grane, A.A.Ballman and H.O'Bryan, Appl.
Phys. Lett., 21, 497 (1972).

[183] R.G.Kepler and R.A.Anderson, J. Appl. Phys., 49, 8,
4490 (1978).

[184] A.M.Glass, J. Appl. Phys., 40, 4699 (1969).

[185] M.Oshiki and E.Fukada, Jap. J. Appl. Phys., 15, 622 (1975)

[186] H.Lee, R.E.Salomon and M.M.Labes, J. Appl. Phys.,
50, 5, 3773 (1979).

[187] H.J.Wintle and Jozefina Turlo, J. Appl. Phys.,
50, 11, 7128 (1979).

[188] V.S.Likhovidov, V.S.Golovanov and A.V.Vannikov,
Vysokomol. Soedin , Ser. ,A, (USSR) 20, 1, 71 (1978),
(In Russian). English translation in Polym. Sci.,
USSR (GB).

[189] P.D.Southgate, Appl. Phys. Lett., 28, 250 (1976).

[190] E.Fukada, Ultrason., 6, 229 (1968).

[191] M.Tamura, T.Yamaguchi, T.Oyaba and T.Yoshimi, J. Audio
Engg. Soc., 23, 21 (1975).

[192] T.D.Sullivan, J.M.Powers, J. Acoust. Soc. Ame., 63,
1396 (1978).

[193] N.Chubachi and T.Sannomiya, Ultrasonics Symposium

Proceedings, IEEE (1977).

[194] N.Chubachi, T.Sannomiya, Jap. J. Appl. Phys.,

16, 12, 2259 (1977).

[195] L.A.Farrow, R.E.Richtou, J. Appl. Phys., 48, 4962 (1977).

[196] C.K.N.Patel and R.J.Kerl, Appl. Phys. Lett., 30,

578 (1977).

[197] C.F.Carlson, U.S.Patent, 2, 221, 776 (1940).

[198] R.M.Schaffert, Electrophotography, Wiley, New York

(1975).

[199] O.D.Jefimenko, Electrostatic Motors, 'Electrostatics

and its Applications' , A.D.Moore (Ed.), Wiley, New York,

131 (1973).

[200] A.M.Glass and J.H.Mc Fee, J. Appl. Phys., 46, 3360 (1974).

[201] Jean-Jacques Brissot, Francois Desvignes, and Rene

Martres, IEEE Transactions on Electron Devices,

ED-20, 7, 613 (1973).

[202] G.M.Sessler and J.E.West, Electrets, Topics in Applied

Physics, V.33, G.M.Sessler (Ed.), Springer-Verlag,

New York, 347 (1980).

CHAPTER II

METHOD OF PREPARATION OF PLASMA-POLYMERISED POLYACRYLONITRILE
AND EXPERIMENTAL ARRANGEMENTS FOR ELECTRICAL MEASUREMENTS
AND THICKNESS DETERMINATION

ABSTRACT

The method of preparation of plasma-polymerised
polyacrylonitrile sandwiched by aluminium electrodes is
discussed in this chapter. Details regarding the design
of the plasma-polymerisation chamber, the vacuum coating
unit for the evaporation of aluminium electrodes and the
special chamber for electrical measurements are presented.
From the parametric studies of film growth, it is found
that the electrical energy is directly transferred to the
monomer molecules to form radicals. The methods of
thickness measurement of the polymer film and the aluminium
electrodes are also discussed.

59

2.10 INTRODUCTION

The properties of polymers play a significant role in the development of thin film devices due to their outstanding semiconductor, piezoelectric, pyroelectric and electret properties. It has been reported [1] that depending on the methods of preparation, the physical and electrical properties will vary in polymer thin films. Different methods have been suggested to prepare polymer films; among them plasma-polymerisation is one of the popular methods on account of the desirable qualities of thin films such as good adhesion to substrates, pin-hole-free nature and excellent electrical and mechanical properties [2]. Also this method is more economical due to the optimum use of monomer, high efficiency of polymerisation and absence of any type of catalyst. Polymer films of many organic and organo-metallic materials have been prepared by the glow discharge method [3]. Different techniques of preparing polymers by glow-discharge have been discussed in the first chapter.

In the present investigation, polyacrylonitrile (PAN) is prepared directly from its monomer vapour by low frequency plasma-polymerisation process. For electrical measurements, the polymer thus formed is sandwiched by aluminium electrodes prepared by thermal evaporation in a vacuum. A detailed description of the polymerisation chamber, the vacuum

evaporation unit and the vacuum cell designed for the study of the electrical properties of insulators is presented in the following sections.

2.20 PREPARATION OF ALUMINIUM-POLYACRYLONITRILE-ALUMINIUM (Al-PAN-Al) SANDWICH STRUCTURES

2.21 The plasma-polymerisation chamber

The plasma-polymerisation chamber is schematically shown in Fig.2.01. It consists of mainly three parts: (1) pumping module, (2) glow-discharge chamber and (3) monomer feeding system. The pumping module consists of a two inch diffusion pump D (IBP torr), liquid nitrogen trap LNT and a baffle valve B. The baffle valve separates the pumping module and the glow-discharge chamber. A 100 litres/min. rotary pump (Hind High Vacuum) is connected to the diffusion pump and the glow-discharge chamber through the diaphram valves V_2 and V_1 respectively. The upper flange of the baffle valve is coupled to the mild steel base plate P of fourteen inches diameter. A thermocouple gauge TG which is connected at the rotary pump side can sense the pressure of the system upto 10^{-3} torr and below this pressure a Penning gauge PG connected to the plasma-polymerisation chamber can be used. All the vacuum connections are made by conventional O-ring seals [4].
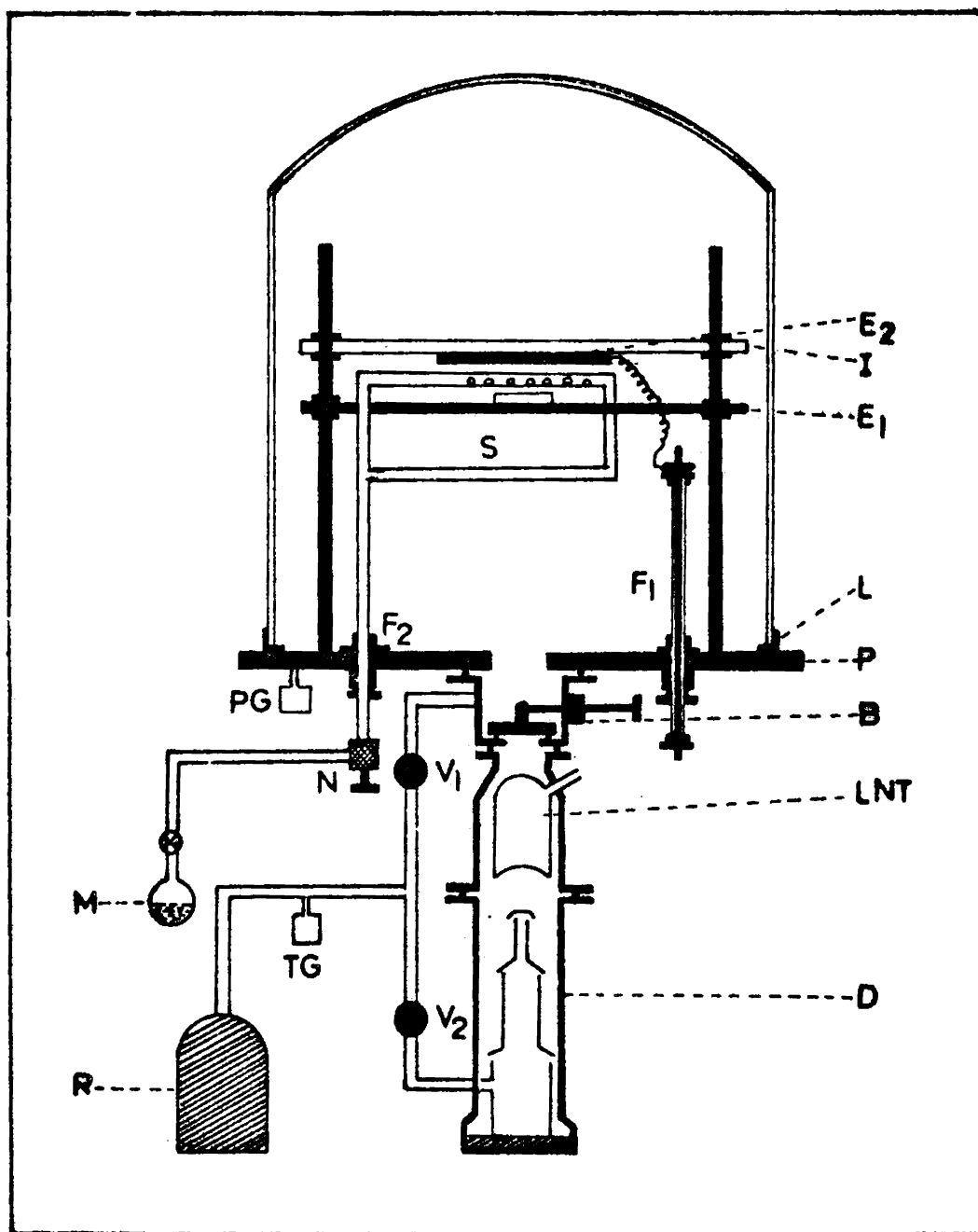
Fig.2.01. Schematic diagram of plasma-polymerisation chamber.

D - diffusion pump, LNT - liquid nitrogen trap, B - baffle valve, R - rotary pump, V_1 - diaphram valve for roughing, V_2 - diaphram valve for backing, P - base plate, TG - thermocouple gauge, PG - penning gauge, G - bell jar, L - neoperene L - gasket, E_1 and E_2 - electrodes for polymerisation, I - glass plate, F_1 - high voltage vacuum feed through, M - monomer reservoir, N - needle valve, F_2 - monomer feed through and S - sprayer.
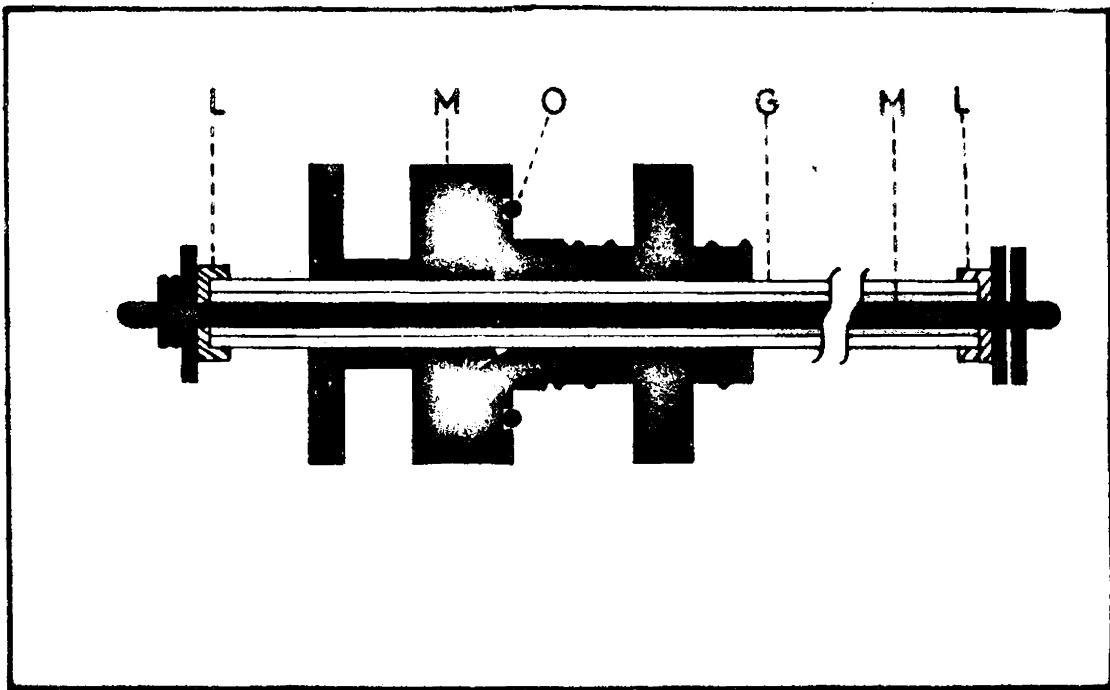
Fig.2.02(a) High voltage feed through F_1.
L - neoperene L-gasket, M - metal parts,
G - glass tube and O - neoperene O-ring.
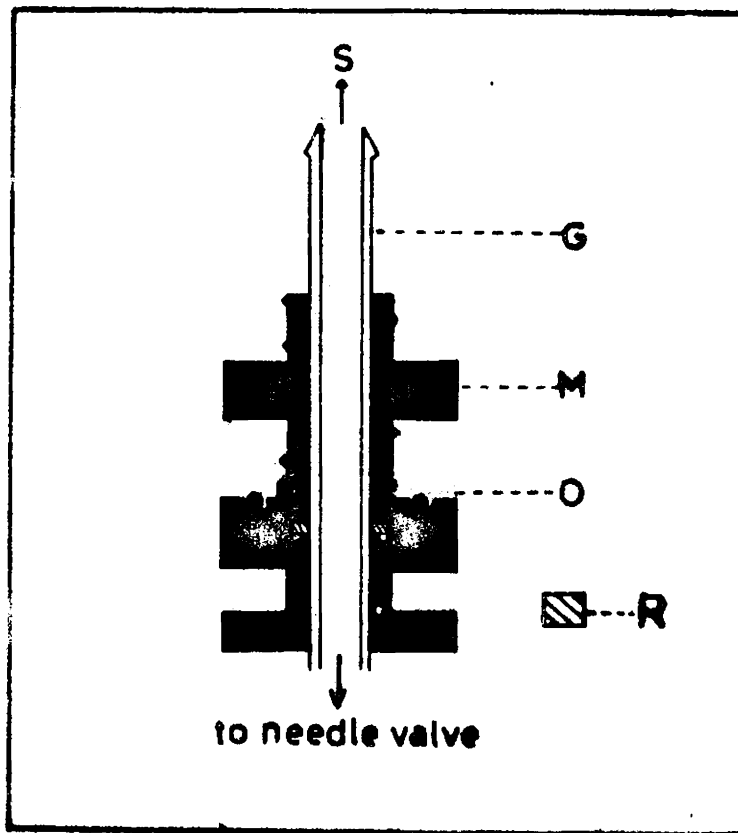
Fig.2.02(b) The monomer feed through F_2.
G - glass tube, M - metal parts, O - neoperene
O-ring and R - neoperene gasket.
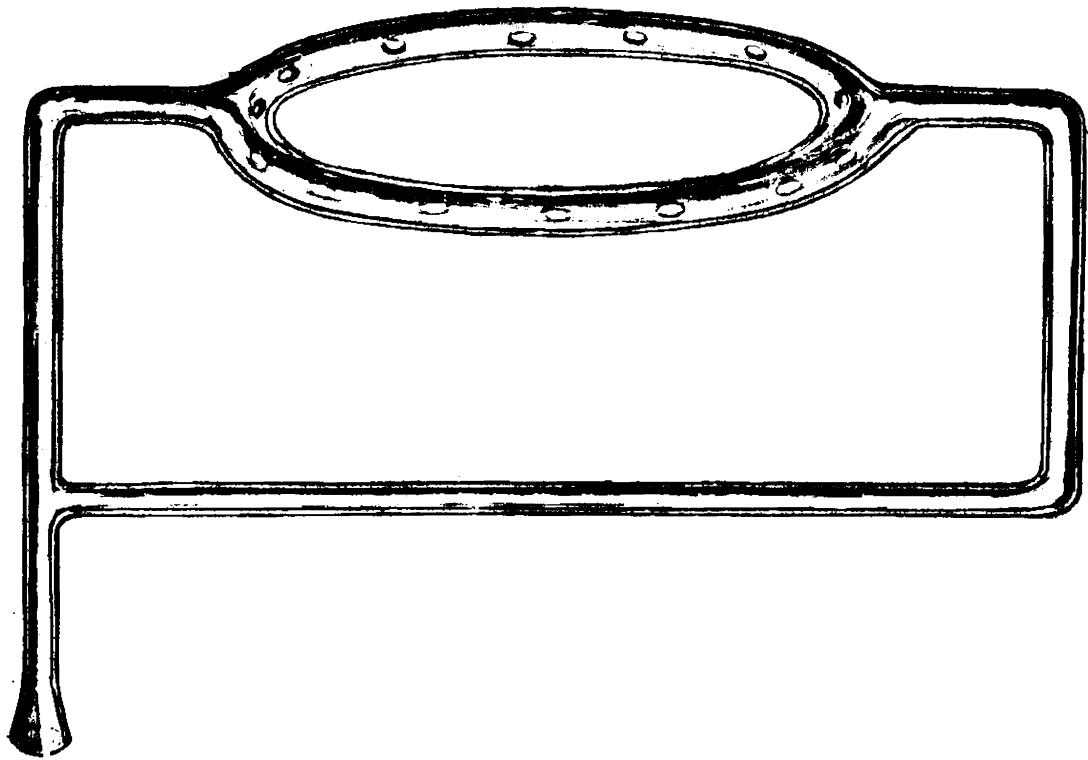
Fig.2.02(b) Circular monomer sprayer S.

The glow-discharge chamber mainly consists of a twelve inch bell jar G which is coupled to the base plate using Neoperene L-gasket. Inside the discharge chamber, two mild steel electrodes E_1 and E_2 are mounted on two vertical metal rods as shown in Fig.2.01. The electrode E_1 is of eighteen centimeters diameter and situated twenty centimeters above the base plate. It is directly connected to the vertical rods such that this electrode is always earthed. The other electrode E_2 is parallel to E_1 and mounted one to four centimeter above the former electrode. This electrode is of sixteen centimeters diameter and mounted on a glass plate I using adhesives. The glass plate is fixed on the vertical rods tightly, taking care to maintain E_2 electrically isolated. To E_2, a high voltage AC power supply is connected through a high voltage vacuum feed-through F_1. One such vacuum feed-through designed and fabricated for this purpose is shown in Fig.2.02(a).

As presented in Fig.2.03, the high voltage power supply consists of a 3KV step-up transformer with 150 mA current rating. The primary voltage is controlled by a variac which is connected to mains (50Hz AC). Hence a voltage upto 230V can be given to the primary of the transformer. One of the secondary leads is earthed and other is connected to the isolated electrode E_2 through a resistance (1 K$\sim$,10W) and a milliammeter (0-300 mA). By adjusting
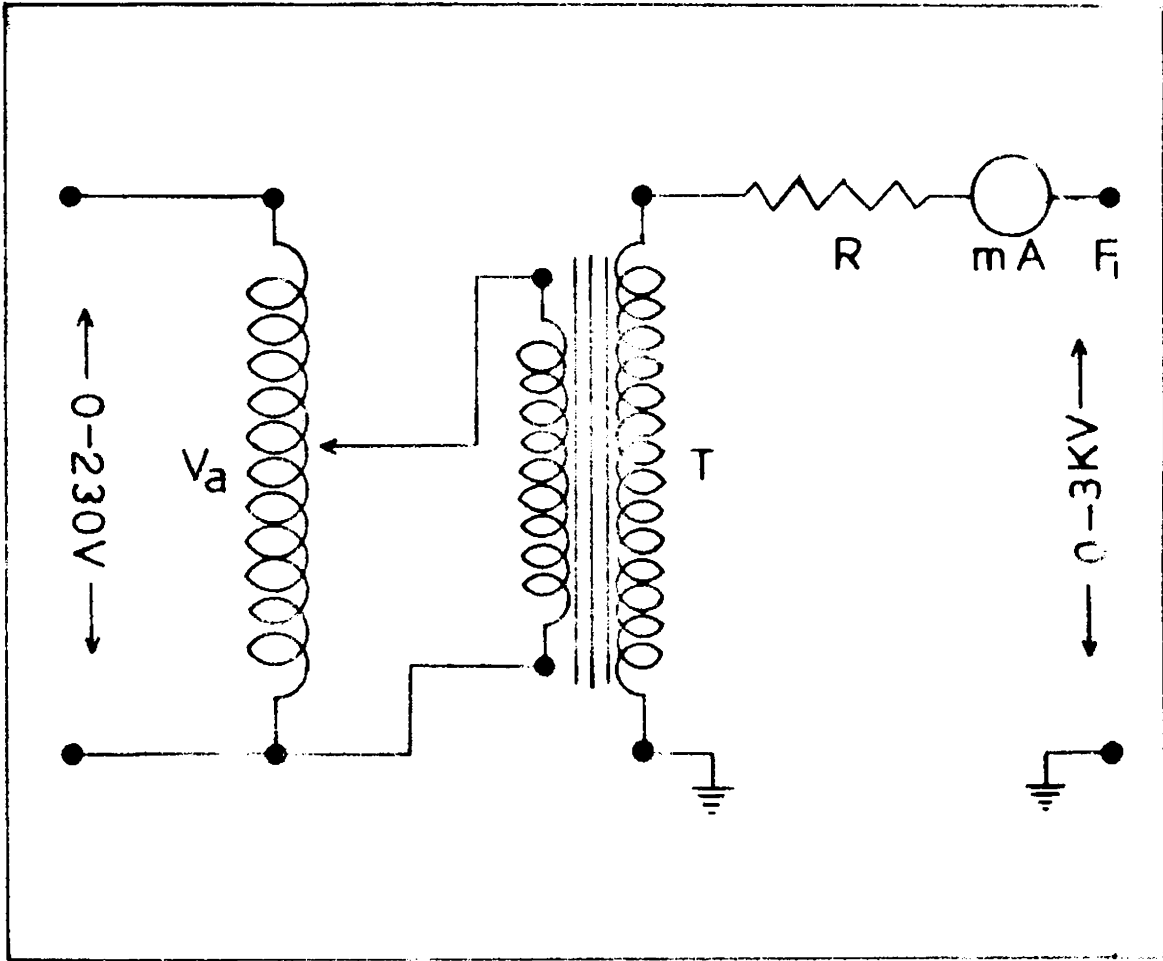
Fig.⠀.03. High voltage p⠀⠀⠀⠀⠀⠀⠀⠀⠀⠀⠀⠀⠀⠀⠀⠀⠀⠀⠀⠀⠀
V⠀—⠀⠀⠀⠀⠀, ⠀⠀⠀⠀⠀⠀⠀⠀⠀⠀⠀⠀⠀⠀⠀⠀⠀⠀⠀(⠀⠀⠀T),
—⠀⠀⠀⠀⠀⠀⠀⠀⠀⠀⠀⠀⠀⠀⠀⠀⠀⠀, R⠀),
A⠀—⠀⠀⠀⠀⠀⠀⠀⠀⠀⠀⠀⠀A).

63

the primary voltage, the discharge current flowing across the electrodes can be controlled.

The monomer feeding system consists of a reservoir in which liquid monomer is collected. On opening the stop-cock, the monomer vapour passes through the needle valve N (Hind High Vacuum), the vacuum feed-through F_2 and gets sprayed into the inter-electrode region. N is used for regulating the monomer vapour flow which will optimise the polymerisation process. The feed-through F_2 designed for the monomer feeding system is shown in Fig.2.02(b). For spraying the monomer to the inter-electrode region, a jet tube sprayer is used. In this case the monomer vapour density is uniform only at the centre of electrodes, but varies when it moves to the sides of the electrodes. Hence the sprayer S is modified to a circular configuration with equally spaced fourteen side holes as shown in Fig.2.02(b). This sprayer has a special advantage of giving equal amount of monomer throughout the circumference of the electrodes. As a result, polymer film of uniform thickness is formed in the whole area of the electrodes. A vacuum coating unit modified for the plasma-polymerisation process is shown in Fig.2.04.

Usually plasma-polymerisation occurs at medium vacuum. The substrates on which the polymer has to be prepared is placed at the centre of E_1. For initial

Fig.2.04 The plasma-polymerisation chamber

pumping, baffle is closed tightly and the chamber is pumped down to 10^{-2} torr through V_1 using rotary pump. Then the chamber is pumped down to 10^{-4} torr using the diffusion pump keeping baffle valve open. With the needle valve N open, the monomer feed-through upto the stop-cock is evacuated. Then the voltage is applied across the electrode and a glow discharge is formed in the inter-electrode region (Since the electrodes are of dissimilar diameter, arcing through the edges is minimised). The current is adjusted to 50 mA. Initially the pressure in the system increases due to disorption of gases from the electrodes, substrates and the sides of the chamber. After about ten minutes, the pressure decreases to 10^{-4} torr. At this stage the needle valve N, the baffle B and diaphram valve V_2 are closed and the chamber is pumped through V_1 using the rotary pump. The monomer stop-cock is opened completely and by controlling the needle valve, the chamber is fleshed with the monomer for about 10 minutes. Now N is closed and when a pressure of 10^{-2} is regained the voltage and the pressure are simultaneously adjusted to obtain a discharge condition suitable to the formation of a good polymer film.

2.22 Growth rate of the polymer

The rate of growth of the polymer depends on the amount of the monomer vapour present in the chamber and

on the current flowing across the electrodes. The amount of

monomer vapour present in the system is proportional to the

effective pressure in the polymerisation chamber. For a

constant voltage the current across the electrode depends

on the monomer vapour pressure. Hence the main parameter

for rate of growth of polymer film is the current across the

electrodes. It is also noted that a minimum voltage is

required to produce the glow-discharge and the threshold

voltage depends on the inter-electrode spacing.

To study the growth rate of the polyacrylonitrile

films, the polymer is prepared on ultrasonically cleaned

glass substrates. Initially the pressure of the monomer

vapour and duration of polymerisation are kept constant. The

thickness of polyacrylonitrile obtained by varying the

electrode current are measured by Fizeau fringes method.

In Fig.2.05, the film thicknesses of polyacrylonitrile grown

on the surface of the glass substrate are plotted against

the square of the electrode current for two different

pressures of 0.5 torr and 0.7 torr. For all the measurements,

the time duration of polymerisation is ten minutes and the

interelectrode distance is three centimeters. From the figure,

it is observed that for a constant pressure the thickness

is proportional to the square of the electrode current. As

reported earlier [5], it is also found that as the pressure
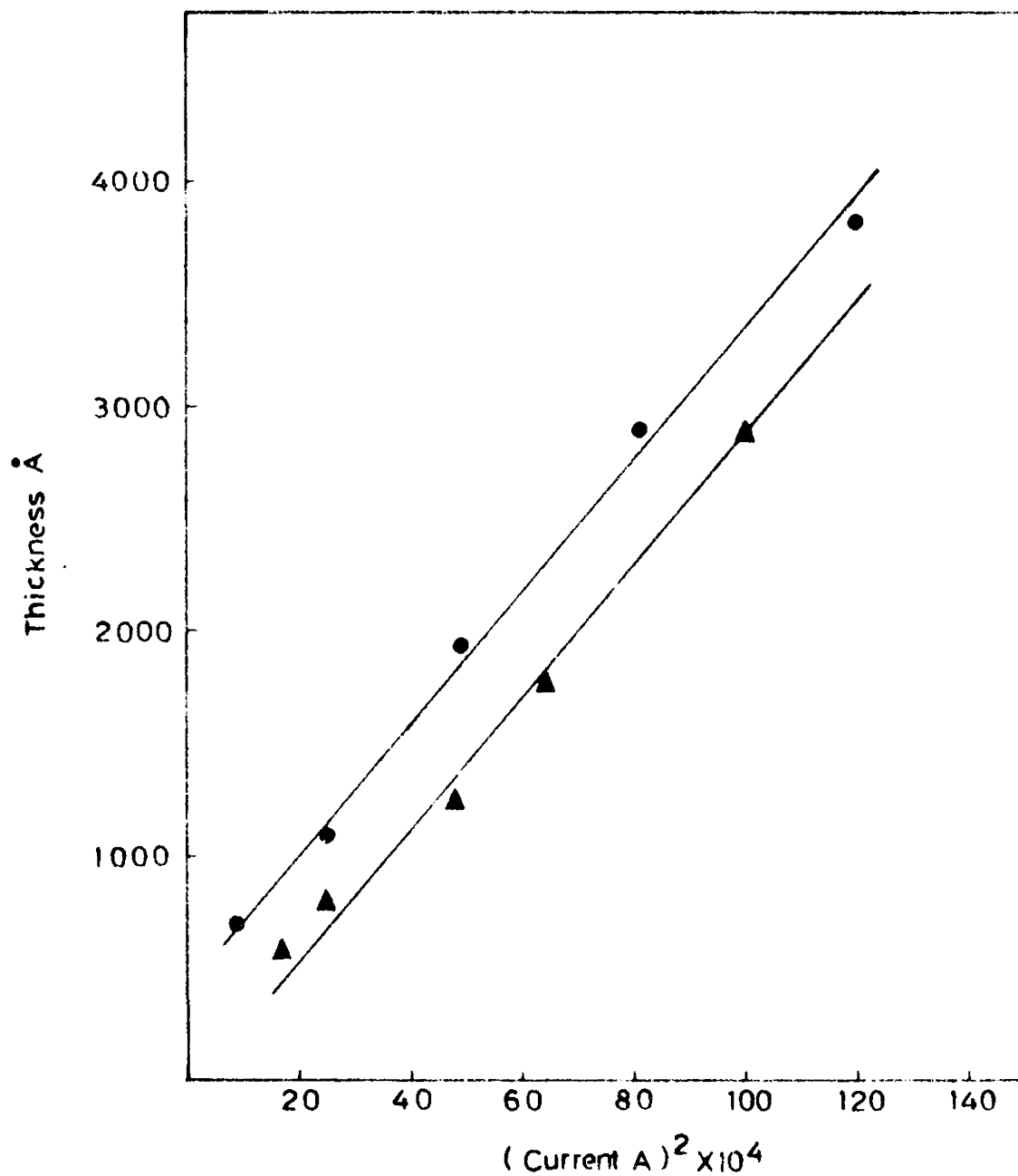
Fig.2.0... Thickness of the PA... ...lotted against (current)², (●) for ... torr and (▲) for ... torr.

in the system is increased, the growth rate is also increased.
Since the growth rate is proportional to the square of the
current it can be concluded that the growth rate is pro-
portional to the electrical power transferred to the system.
The electrical power is directly transferred to the monomer
molecules to break the bands which have minimum binding
energy. When a voltage is applied to the electrodes, the
ions and electrons are accelerated towards the electrodes.
The accelerated ions collide with monomer molecules and due
to the impact the energy is transferred to the monomer
molecule generating the radicals of the monomer. These
radicals combine together to form a polymer chain. Certain
accelerated ions will collide with the electrodes raising
the temperature of the electrodes, thereby dissipating a
part of the energy.

2.23 Preparation of metal electrodes

For the preparation of the metal electrodes
thermal evaporation under high vacuum is used in the present
investigation. For this purpose usual designs [6] of high
vacuum coating units are adopted. The vacuum coating unit
which has been designed and fabricated for this purpose
consists of a mild steel base-plate, 6 inch diffusion pump
and 550 litre/min. rotary pump. The design of vacuum coating
unit is presented in Fig.2.06.
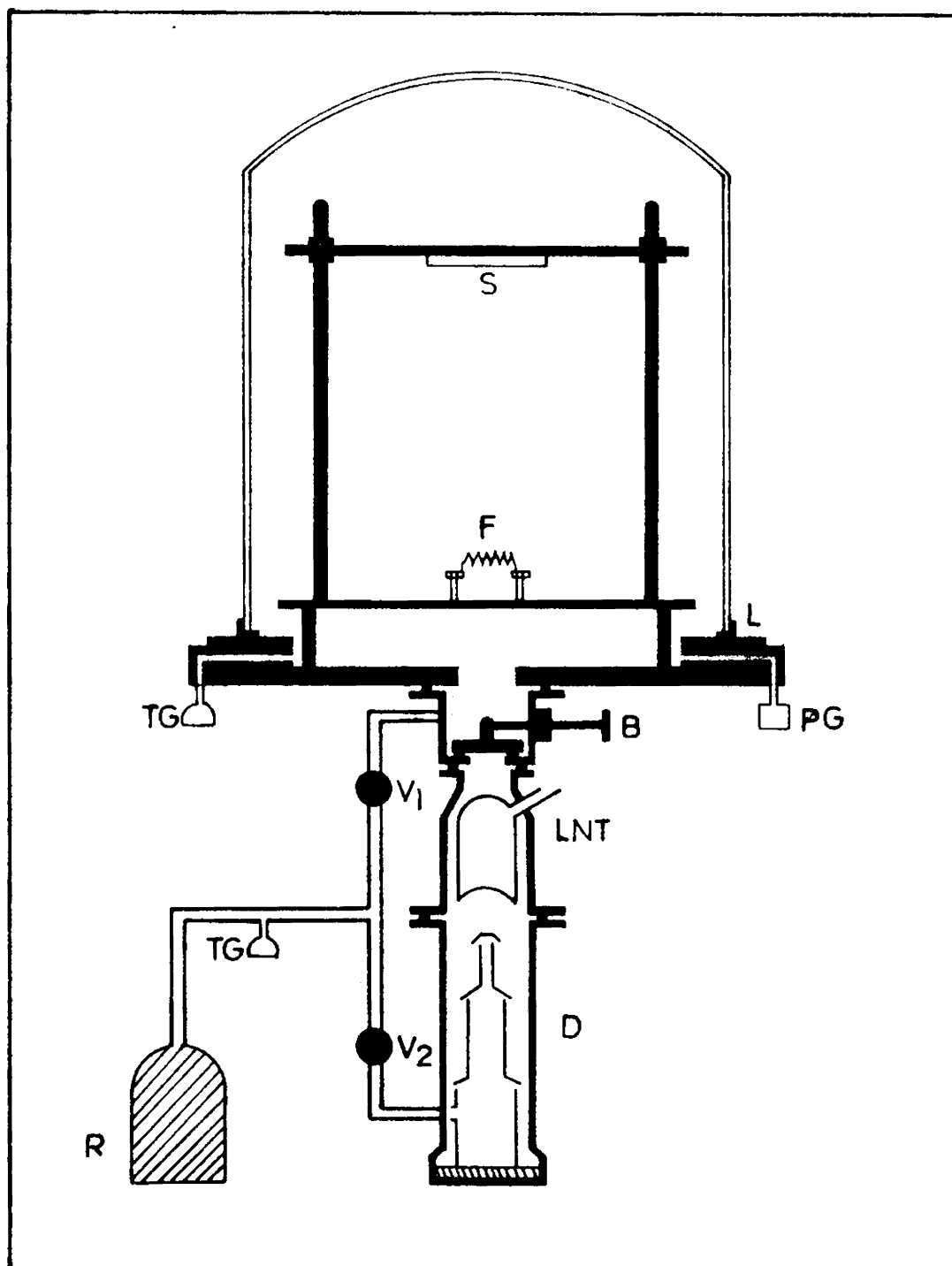
Fig.2.06. Schematic diagram of vacuum coating unit for the
evaporation of metal electrodes.
D - diffusion pump, LNT - liquid nitrogen trap,
B - baffle valve, PG - penning gauge, L - neoperene
L-gasket, S - substrate, F - filament, TG - thermo-
couple gauge, R - rotary pump, V_1 - diaphram valve
for roughing and V_2 - diaphram valve for backing.

The base-plate designed for this purpose is polished well and chromium plated. The thickness at the side of the base-plate is 3.5 cm. As shown in Fig.2.06 a step with 27.5 cm diameter and 2.5 cm depth is made on the base-plate. A bore of 19.5 cm diameter is made at the centre of the plate for connecting the diffusion pump. Fourteen feed-throughs, each of 1 cm diameter, are provided on the sides of the base-plate. High current and high voltage feed-throughs [7] are designed for the side ports. Two filament evaporators are also provided so that they could be operated one after the another. Two side-ports are used for the penning and pirani gauges. The remaining ports are closed by dummies. A 30 cm glass dome is pressure-sealed on the base-plate using an L-gasket.

The diffusion pump is connected to the base plate through the baffle valve and liquid nitrogen trap (LNT) as shown in Fig.2.06. 200 cc of silicon oil (DC 704) is used to charge the diffusion pump and the maximum pumping speed is 1000 litre/sec.

For efficient pumping, a 550 litre/min. rotary pump (Toshniwal Bros.) is used in series with the diffusion pump. This pump is also used for roughing the whole system to 10^{-2} torr. As shown in the figure, V_1 and V_2 are two valves used for roughing and backing the coating unit

respectively. Without using liquid nitrogen trap, a pressure of 5×10^{-6} torr is obtained in the vacuum coating unit. The photograph of the vacuum coating unit designed and fabricated in this laboratory is shown in Fig.2.07.

The aluminium electrodes are evaporated thermally using tungsten filaments. The tungsten helix is mounted tightly on the filament holders situated at the centre of the base plate. A high current transformer (10V, 100 amp.) is connected to the filament holders with high current leads (100 amp.). The substrates are mounted horizontally fifteen to twenty centimeters above the filament. Proper masks are used on the substrates to achieve the necessary configuration of aluminium films. The aluminium is evaporated at a pressure < 5×10^{-6} torr and the films are formed on cold substrates.

2.24 Preparation of aluminium-polyacrylonitrile-aluminium sandwich structures

Most of the investigations presented in the thesis are on aluminium-polyacrylonitrile-aluminium (Al-PAN-Al) sandwich structures. For making sandwich samples, proper patterns of individual films are prepared using masks to reduce inter-electrode shorting and surface arcing.

The samples are prepared on clean glass substrates of 75 mm x 25 mm x 1.5 mm size. These glass slides are
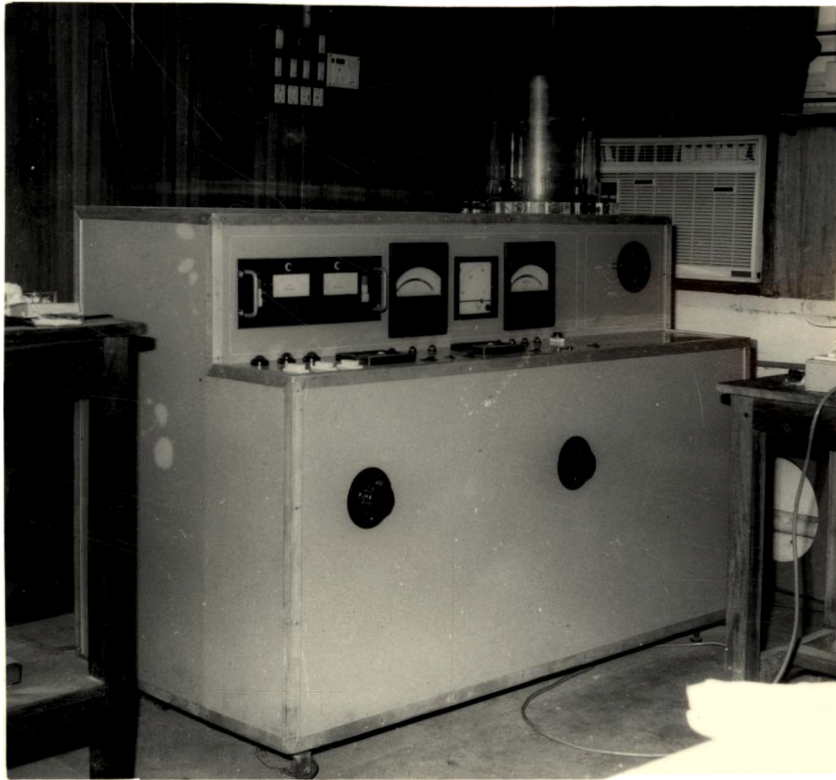
Fig.2.07 The vacuum coating unit fabricated for evaporation
of metal electrodes

thoroughly cleaned by different processes. At first the
substrates are cleaned under running water and soap solution
and then dipped in a freshly prepared chromic acid for five
hours to remove alkaline and other oxidising impurities.
The oxidation is promoted by warming the acid to 70°C.
After this process, the substrates are washed in running
water. The surfaces of each slide are rubbed with cotton
dipped in soap solution and cleaned thoroughly with ordinary
water. These slides are cleaned in distilled water and
transferred into an ultrasonic cleaner. The microscopic
impurities are stripped off by ultrasonic agitation in water
and the process is continued for 20 minutes. After removing
from this bath, the substrates are dried slowly in a dust-
free box and then transferred to vacuum coating unit.

For the preparation of aluminium electrode on
the specified area, proper mica masks are used. In Fig.2.08(a)
the masking of the substrates for the first electrode is
shown. By masking the substrate, an evaporated aluminium
electrode of thickness 1500Å and dimensions 42.5 mm x 15 mm
is prepared. The electrode coated glass slides are now
transferred to the polymerisation chamber. The substrates
are masked as shown in Fig.2.08(b). As discussed in the
section 2.21, the polymer is allowed to grow on aluminium
coated glass slides. The specimens are allowed to remain

in vacuum for slow cooling and after three hours, they are transferred to vacuum coating unit for making counter electrodes.

For the preparation of counter aluminium electrode, the masks are arranged as shown in Fig.2.08(c). The aluminium is coated on the PAN film with 10 mm width and 42.5 mm length. The Al-PAN-Al sandwich structure thus prepared are schematically shown in Fig.2.09(a). A cross-sectional view of Al-PAN-Al is also given in Fig.2.09(b). With proper arrangement of the masks, the effective area of the sandwich structure becomes 1 cm^2. After the preparation of Al-PAN-Al sandwich structures, the samples are stored in a vacuum desiccator. This is essential because PAN polymer is highly water absorbing.

During polymerisation the chamber is also coated with the polymer film. For cleaning the chamber, proper solvents of the polymer has to be identified. PAN is insoluble in organic acids and alkalies. But it is highly soluble in organic solvents like ethyl alcohol, dimethyl formamide (DMF) and acetone. Hence the polymerisation chamber is cleaned by acetone. The electrodes are usually cleaned by zero grade emery paper or steel wool.

(a)

(b)
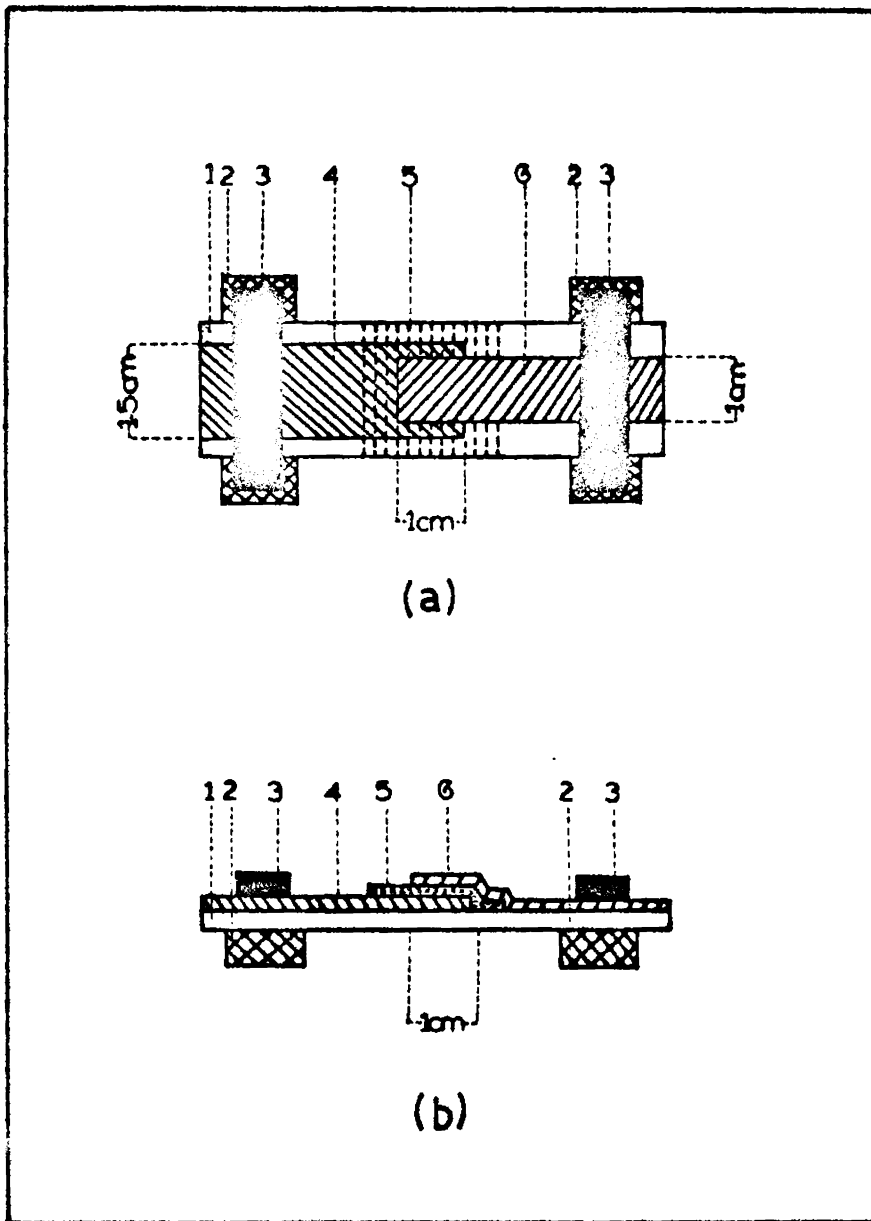
Fig.2.09. Schematic diagram of Al-PAN-Al.
(a) The top view and (b) the side view of the specimen. 1 - glass substrate, 2 - heating copper block, 3 - copper block for electrical connection, 4 - inner bound aluminium electrode, 5 - PAN thin film, and 6 - outer free aluminium electrode.

2.30 THICKNESS MEASUREMENT

2.31 Thickness measurement of aluminium electrodes

The thickness of aluminium electrode is measured from the mass of aluminium evaporated from the tungsten helix. For simplicity it is considered as a point source and hence equal amount of the material is evaporated to all directions. In such a case, for a substrate situated far away from the source, the thickness of the film [8] is given by

$$t = \frac{m}{4\pi \rho R^2} \tag{2.01}$$

where m the mass of the material, ρ the density (in the case of aluminium =2.7 gm/cc)and R the distance from the source to the substrate. Actually, the filament source is not a point source and hence the thickness measured by this method is only approximate. However in the present case better accuracy is not necessary. The mass of aluminium m is measured accurately by using a chemical balance.

2.32 Thickness measurement of PAN

The thickness of the polymer film is measured by a more accurate method. When a partially reflecting surface is placed on a fully reflecting surface forming an air wedge

and a monochromatic parallel beam falls on it, interference
fringes will be produced. The path difference of the beam from
one minimum point to other is λ where λ is the wavelength
of the monochromatic beam. Hence difference in height of the
air gap at adjacent minimum points is given by $\lambda/2$. If a
step is formed by the thin film whose thickness is to be
measured, the interference fringe pattern will be shifted
as shown in Fig.2.10(a). The thickness of the film can be
measured from the fringe shift x and fringe separation y as

$$t = \frac{x}{y} \times \frac{\lambda}{2} \tag{2.02}$$

Wiener [9] was the first person to measure the thickness
of thin films using this principle. The interference fringes
method has been developed to a remarkable degree by Tolansky
[10] and now it is accepted as an absolute standard method
for thickness measurement of thin films.

The experimental set up for the measurement of
thickness is presented in Fig.2.11. G is the glass substrate
on which the polymer thin film is prepared with a step as
shown in Fig.2.10(b). On this, thick aluminium coating is
made for complete reflection. A partially reflecting glass
plate is placed on the substrate to form an air wedge. A
mercury lamp with a green filter (5461Å) form a monochromatic
source S. Using a circular aperture A and a lens system L,
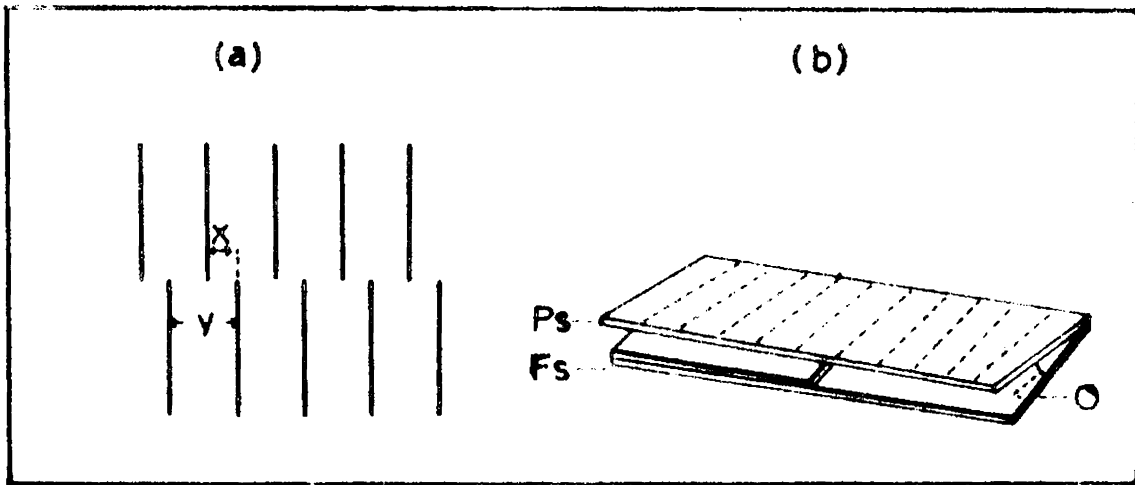
Fig.2.10(a) The illustration of fringe shift: x is the fringe shift and y is the fringe seperation. (b) The air wedge for thickness measurement: Ps - partial reflecting surface, Fs - fully reflecting surface and O - the wedge angle.
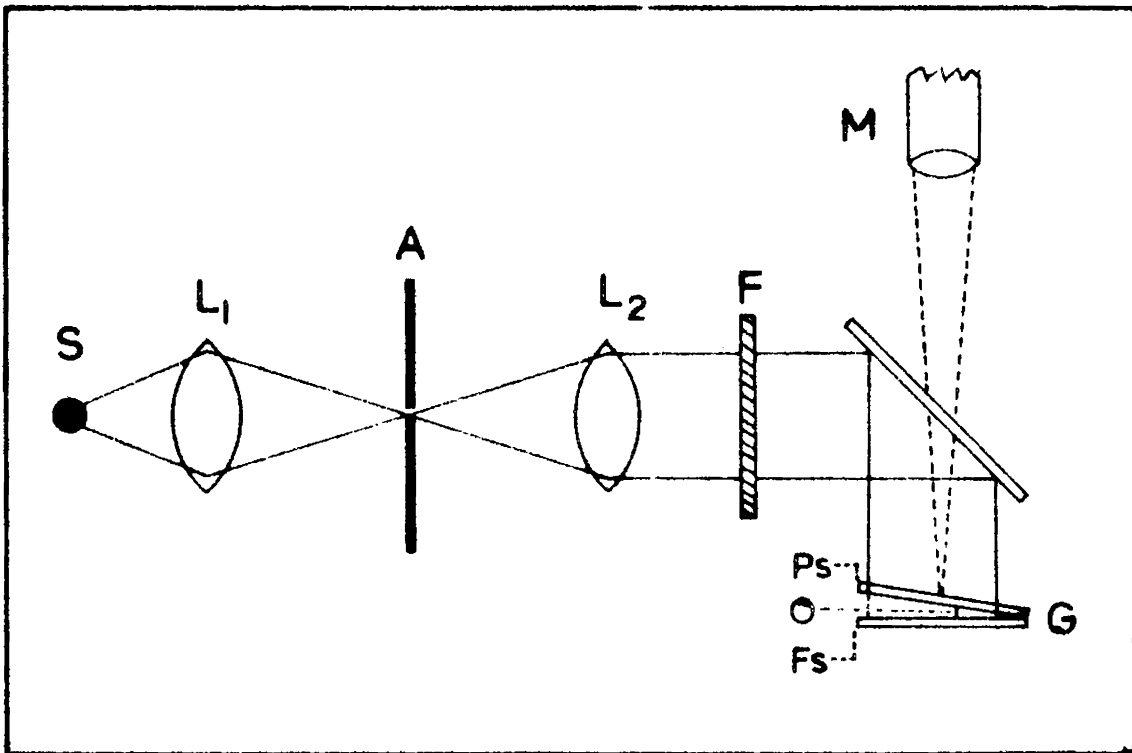
Fig.2.11. Experimental set-up for the thickness measurement: S - mercury source, L - lens system, F - filter ($5461\text{\AA}$), A - aperture, G - glass substrate and M - travelling microscope.

the beam is made parallel. This beam falls on the wedge

G producing a fringe system as shown in Fig.2.10(a). The

fringes can be clearly seen through a microscope. The

fringe separation and fringe shift can be accurately

measured with the help of a travelling microscope. On

substituting the values in eqn.(2.02) the thickness of the

film can be calculated. It is important to note that the

polymer film as well as the exposed glass surface should be

coated with the same reflecting layer in order that phase

change or reflection from the two sides of the step will be

the same.

2.40 VACUUM CHAMBER FOR ELECTRICAL MEASUREMENTS

In the case of electrical measurements of

insulator films, the current flowing through the sandwich

structure is of the order of $10^{-13} - 10^{-15}$ amps. In such

cases, the external electrical noises and surface currents

may disturb the measurements. A metallic chamber is designed

and fabricated to shield the external noises. Fig.2.12(a)

shows the schematic diagram of the chamber used for electrical

measurements. This chamber consists of a metallic outer

tube of diameter 16 cm and height 15.5 cm which is connected

to a diffusion pump backed by a rotary pump. The top flange

of the outer tube is vacuum sealed with a metal plate of

19.5 cm diameter and 1.5 cm thick having liquid nitrogen
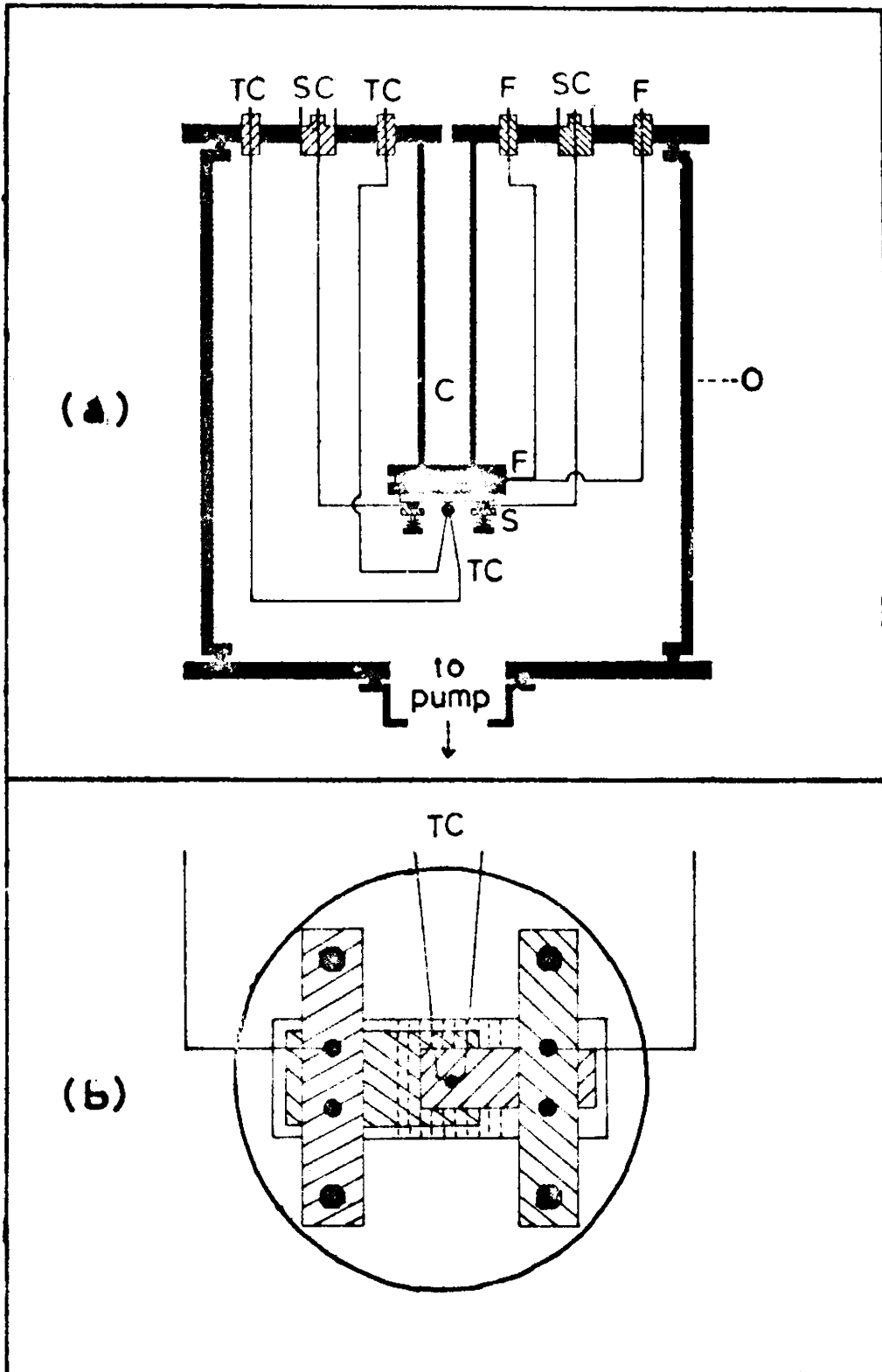
Fig.2.12(a) Schematic diagram of the chamber used for
electrical measurements: O - outer tube,
C - liquid nitrogen cold finger, S - specimen
connector, F - filament, IC - iron-constantan
thermocouple, SC - shielded cable.
(b) The top view of the specimen connector.

cold finger as shown in the figure. At the bottom of this cold finger a specimen connector S is fixed. In between the cold finger and specimen connector, a 60W electric heater F is mounted to heat the specimen, if required.

As shown in the Fig.2.12(b), the specimen connector S consists of two copper blocks mounted on two teflon sheets of 3 mm thickness. These teflon sheets are fixed on a spring loaded sliding arrangement so that proper pressure contacts can be made with specimen electrodes and copper connectors. An iron-constantan thermocouple is provided for the measurement of temperature of the specimen.

Four nylon feed-throughs are provided on the top metal plate for electrical connections of the heater and thermocouple. The teflon insulated leads from the copper blocks are connected to teflon insulated shielded-cable connectors which are mounted on the top plate. These connectors provide proper insulation from the metal chamber. The whole chamber is earthed properly.

(Using a diffusion pump backed by a rotary pump, the chamber is evacuated to 10^{-5} torr. The specimen can be kept at any desired temperature (-193°C to 250°C) by cooling it initially by liquid nitrogen and subsequently by controlled heating using a 60W heater. The thermocouple connected to microvolt meter will give the temperature of the substrate.
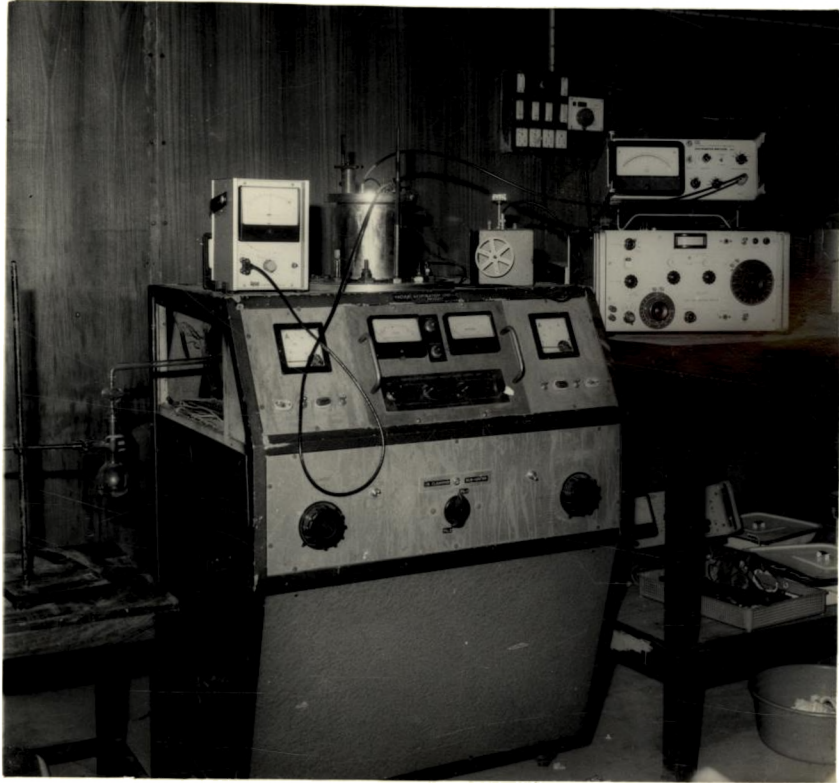
Fig.2.13 A set-up for electrical measurements

Using shielded cables, the specimens are electrically

connected to the measuring instruments. Provision is also

made to measure the pressure using a Penning gauge. With

all the precautions for electrical shielding and proper

insulation a current of the order of 10^{-15} amp. was success-

fully measured with an electrometer amplifier and a stabilised

power supply. The set-up is shown in Fig.2.13.)

REFERENCES

[1] Shinichi Takeda, J. Appl. Phys., 47, 12, 5480 (1976).

[2] S.Morita, G.Sawa, T.Mizutani and M.Ieda, J. IEEE,
Japan, 92-A, 65 (1972).

[3] Arthur Bradly and John P.Hammes, J. Elect. Chem. Soc.,
110, 1, 15 (1963).

[4] A.Roth, Vacuum Technology, North Holland Publishing
Company, New York, Chapter VII, 397 (1976).

[5] T.Hirai and O.Nakada, Jap. J. Appl. Phys., 7, 2, 112 (1968).

[6] K.L.Chopra, Thin Film Phenomena, McGraw-Hill Book Company,
New York, Chapter I, 57 (1969).

[7] A.Roth, Vacuum Technology, North-Holland Publishing
Company, New York, Chapter VII, 329 (1976).

[8] Robert W.Berry, Peter M.Hall and Murray T. Harris, Thin
Film Technology, Van Nostrand Rheinhold, New York,
Chapter III, 160 (1960).

[9] O.Wiener, Wied. Ann., 31, 629 (1887).

[10] S.Tolansky, Surface Microtopography, John Wiley and Sons,
Inc., New York (1960).

CHAPTER III

STRUCTURE AND POLYMERISATION MECHANISM OF PLASMA-POLYMERISED POLYACRYLONITRILE

ABSTRACT

The structure of plasma-polymerised poly-acrylonitrile thin film was studied by the infrared absorption spectra. A long chain planar zig-zag structure is proposed. The emission spectra of the monomer plasma is studied to investigate the reaction mechanism of plasma-polymerisation process. From the analysis, it is concluded that the radical polymerisation is the most suitable mechanism for plasma-polymerisation of acrylonitrile. An additional band present in all the cases is attributed to carbonyl impurity. The visible and ultraviolet spectra of the polymer is also presented.

77

3.10 INTRODUCTION

It is well known that molecular vapours form polymers in electrical discharges [1]. The properties of polymers formed by electrical discharge of organic materials have been studied extensively [2,3], but very little attention has been given even qualitatively to their structures. Some information is available from the analysis of the discharges of benzene [4] and certain other aromatic compounds [5]. It has been found that a majority of the studies involving benzene or its derivatives point to the formation of the products through a free radical mechanism rather than ionic mechanism. For studying the mechanism of polymerisation process, the molecular structure of the monomer and the polymer formed are analysed by conventional methods. The emission spectrum of monomer vapour glow-discharge is analysed and from the characteristic emission spectrum the intermediate state viz., the plasma state is studied. From these data, the mechanism of plasma-polymerisation can be interpreted.

In this chapter an attempt is made to study the reaction mechanism suitable to the formation of polyacrylo-nitrile (PAN) in a plasma-discharge. The probable structure is also proposed in comparison with the spectral studies reported earlier [6,7]. The visible and ultraviolet absorption

spectra of the polymer thin films are also studied for obtaining additional information on the characteristic chromophors in PAN.

3.20 MOLECULAR STRUCTURE OF PLASMA-POLYMERISED POLYACRYLONITRILE

3.21 Absorption spectra of the monomer and the polymer

The infrared spectra of monomer and polymer are recorded using Backman infrared spectrometer (I.R-20). Acrylonitrile (BDH, Laboratory reagent) is sandwiched by two well polished KBr crystals and introduced into the sample compartment. The absorption spectrum is recorded for the range 4000 cm^{-1} to 600 cm^{-1}.

The polyacrylonitrile thin films are prepared on well polished KBr crystals by plasma-polymerisation method. By repeated experiments, it is found that the optimum thickness of the specimen to get a good infrared absorption spectrum is $\sim$ 4000$\overset{o}{A}$. In Fig.3.01 (a and c) the infrared spectra of polymer and monomer are presented. Initially the different absorption peaks of the monomer are assigned in comparison with a standard spectrum [6] and the scheme of the assignment is given in Table 3.01. The standard spectrum used for comparing the assignment is also shown in Fig.3.01(b).
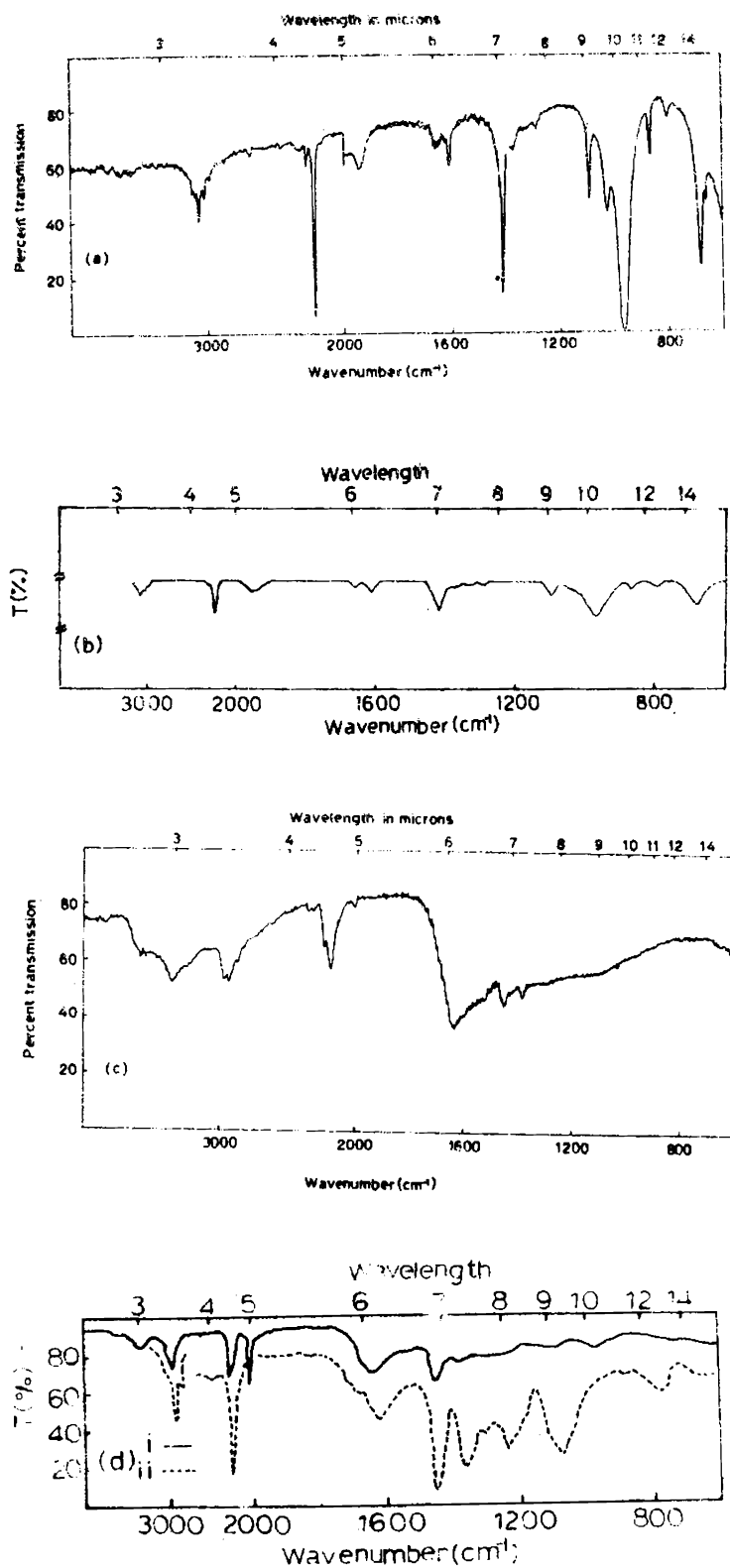
Fig.3.01(a) Infrared spectra of the acrylonitrile
      (b) Standard spectra of the acrylonitrile [6]
      (c) Infrared spectra of the polyacrylonitrile
      (d) Standard spectra of the polyacrylonitrile:
          (i) sample prepared by silent discharge [9]
          and (ii) sample prepared by solution
          growth [10]

Table 3.01   Band assignment for acrylonitrile

Present investigation wave number cm^{-1}	Reported earlier* wave number cm^{-1}	Assignment
3100	3080	$\nu_a\ (CH_2)$
3060	3030	$\nu\ (CH)$
3030	3010	$\nu_s(CH_2)$
2270 2220	2220	$\nu(CN)$
1610	1620	$\nu(C=C)$
1410	1415	$Def(CH_2)$
1290	1300	$Rk(CH)$
1090	1100	$Rk(CH_2)$
980	980	$Wag(CH$ and CH_2
870	870	$\nu\ (C-C)$
690	680	$H^+\quad H^+$ $C\ =\ C$ H^-

*Taken from references 6 and 8.

The infrared absorption spectrum of PAN is presented in Fig.3.01(c). In Fig.3.01(d), the infrared spectra of two samples (i) sample prepared by silent

discharge [9] and (ii) sample prepared by solution growth [10] reported earlier, are presented for comparison. The band assignments of the PAN are given in comparison with earlier studies [11] and presented in Table 3.02.

Table 3.02 Band assignments of PAN

Present investigation wave number cm^{-1}	Reported earlier* wave number cm^{-1}	Assignment
2960	2950	$\nu_a(CH_2)$
2920	2930	$\nu(CH)$
2860	2870	$\nu_s(CH_2)$
2240 2200	2237	$\nu(CN)$
1650	--	$\nu(CO)$
1450	1447	Def(CH_2)
1380	1362	Def(CH)
--	1355	Wag(CH_2) + $\nu_a(C-C)$
--	1310	Wag(CH_2)-Def(CH)
--	1247	Wag(CH)+Wag(CH_2)-$\nu_a(C-C)$
--	1115	$\nu_s (C-C)$-Def(CH)
--	1073	$\nu_s (C-C)$+ $\nu_a(C-C)$
--	1015	Wag(CH)
--	865	Rock(CH_2)
--	778	$\nu(C-CN)$+tor (CH_2)

*Taken from reference 11.

On comparing with the spectrum of the monomer it
is found that in the present spectrum of PAN the stretching
frequencies of CH_2 and CH have shifted to the lower energy
side. The two CN stretching frequencies have also shifted
by 20 cm^{-1}. A new strong band is observed at 1650 cm^{-1}.
This band is usually found in plasma-polymerised materials
and is reported to be associated with carbonyl group [12].
In the present spectrum no bands are observed in the region
1300 cm^{-1} to 600 cm^{-1}. A similar observation has been
reported by Hirai and Nakada [9] for PAN prepared by silent
discharge.

3.22 Structure of PAN

The structure of PAN has been studied in the
past [13] and two possibilities have been clearly indicated
viz., isotactic placement and syndiotactic placement as
shown in Fig.3.02. If an equal probability exists for the
isotactic and syndiotactic placements, the configuration is
called atactic placement. Many investigators have carried
out infrared, X-ray and Raman spectral studies for the steric
structural configuration of PAN [14,15]. All these investi-
gations are related to polymers having stereoregular
arrangement. In all the cases a C-C stretching band is
observed in the low frequency infrared spectrum. The
plasma-polymerised PAN has not shown any band below
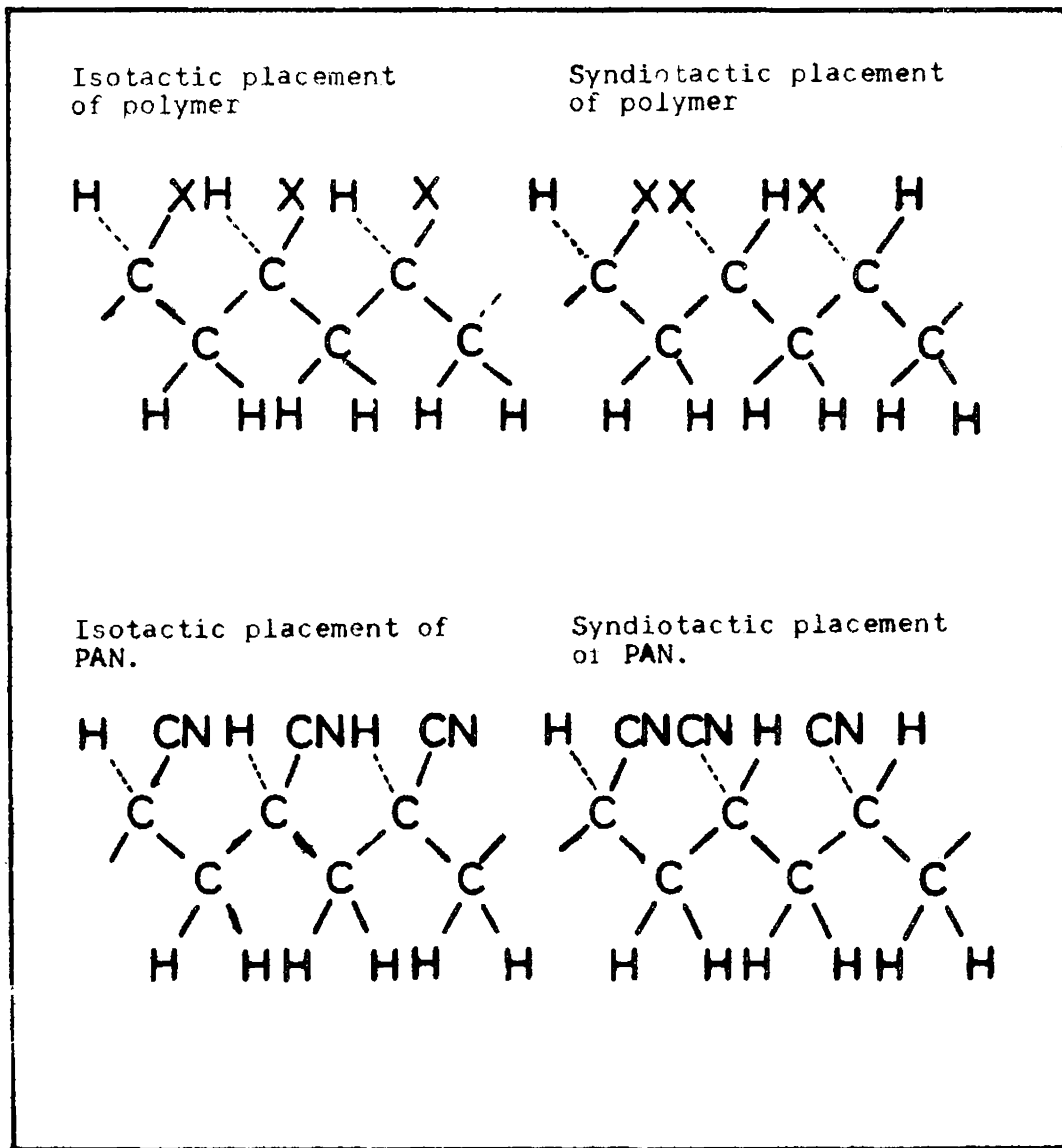
Fig.3.02. The probable structure of polyacrylonitrile.

1300 cm^{-1}. In all probability, the polymer formed due to the process is highly amorphous and the above structural configurations are not well oriented in the polymer. The absence of C-C backbone frequency can only be due to the lack of crystalline orientation. It may therefore be generally concluded that the forming process of plasma-polymerisation is not a controlled process as compared to solution growth resulting in the formation of amorphous polymer which cannot be strictly classified into any of the steric configurations. The splitting of the CN band observed by Hirai and Nakada [9] will indicate that there is interaction between CN groups with the same polymer unit. In the present case the interaction is comparatively weaker because it is between the side groups of the polymer units randomly oriented. The infrared spectrum reported for the silent discharge shows larger CN splitting possibly due to the combination of two CHCN groups together (Head to Head addition [13]). Hence, it is inferred that in the present polymerisation method, an amorphous PAN thin film is formed by the combination of CH$_2$ and CHCN radicals resulting in a long planar zig-zag chain molecule as shown in Fig.3.02 with random orientation. The additional band at 1650 cm^{-1} observed in this case and also reported by Koning and Brockes [16] for benzene polymer by plasma-discharge can be attributed to carbonyl impurity which is

perhaps the characteristic of the gas phase discharge
method of polymerisation.

3.30 THE POLYMERISATION MECHANISM OF ACRYLONITRILE IN GLOW-DISCHARGE

3.31 Emission spectrum of the glow-discharge plasma

The emission spectrum of plasma is photographed
using a high resolution three prism spectrograph (Carl zeiss,
Jana, Germany). The experimental arrangement is schemati-
cally shown in Fig.3.03. The plasma-polymerisation chamber
discussed in the section 2.22 is completely covered with
black paper. A small window (1 inch dia.) is made on the
side of the cover facing the spectrograph. At the opposite
side, an aluminium foil reflector is placed to reflect more
light towards the window. The emitted light is focussed on
the slit of the spectrograph. The collimator and the drum
of the spectrograph are adjusted to record the spectrum
in the visible and ultraviolet regions on a photographic
film.

When the monomer vapour is fed into the poly-
merisation chamber and discharged, the adsorbed gases get
released. These gases are usually atmospheric gases.
Hence, to get an idea of the residual gases, initially the
spectrum of glow-discharged adsorbed gases is taken at a
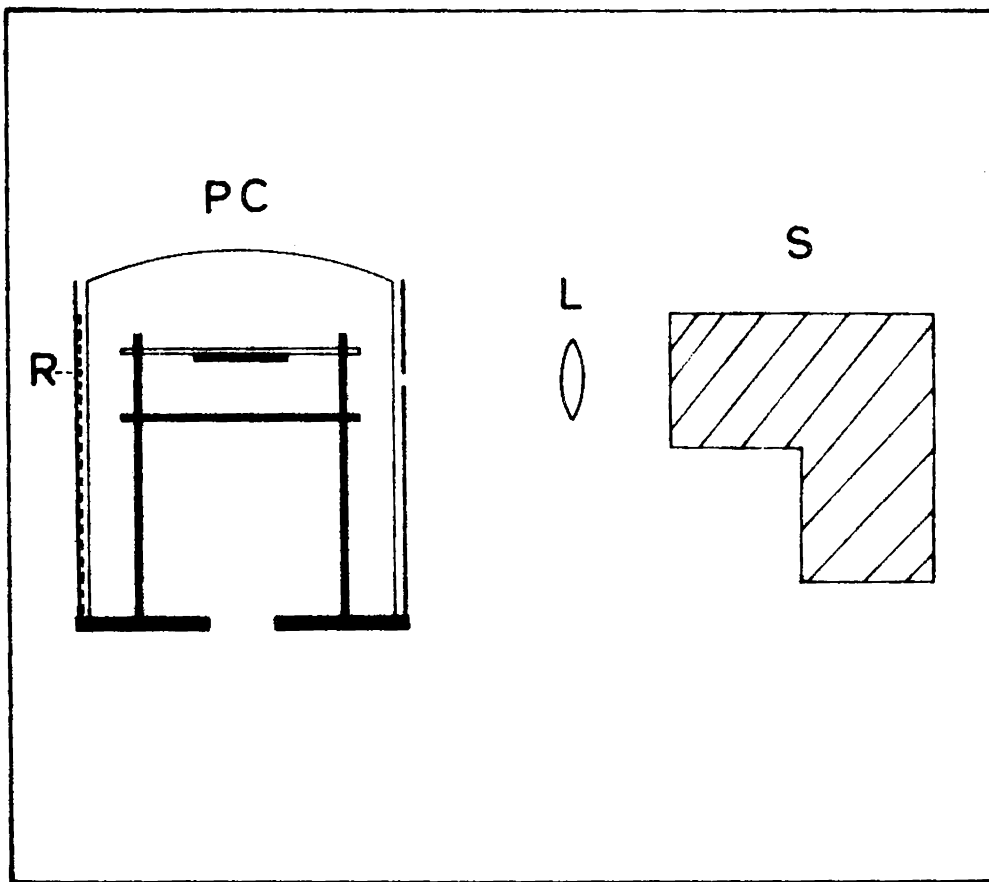
Fig.3.03. Schematic diagram of the experimental set-up
for the spectral study of the glow-discharge
plasma: S - spectrograph, PC - plasma-poly-
merisation chamber, L - lens and R - aluminium
foil reflector.

pressure of 10^{-1} torr. For the available experimental
conditions, an one hour exposure is required for obtaining
a satisfactory spectrum.

Subsequently the spectrum of the glow-discharged
monomer is taken at a pressure of 1 torr. The intensity of
this plasma spectrum is much higher than the previous one
and an exposure of ~30 minutes is sufficient to give a
good spectrum. For the calibration of the obtained spectra,
iron-arc spectrum is used as a standard. Thus the spectra
of the residual gases, iron-arc and the monomer plasma are
recorded on a single photographic film. One such spectrum
is presented in Fig.3.04. The spectrum thus recorded is
charted by using a photodensitometer (Carl zeiss, Jana,
Germany) and is given in Fig.3.05. All the bands in the
discharge spectrum are thus identified.

From Fig.3.04, the emission spectrum of acrylo-
nitrile vapour is identified after eliminating the bands
due to residual gases by comparing with the standard
band spectra of the radicals [17]. Accordingly, the bands
and the radicals associated with it are presented in
Table 3.03.
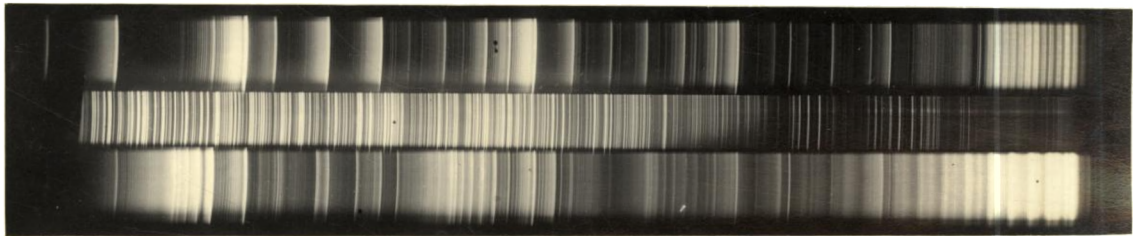
Fig.3.04   Spectra of glow-discharge plasma of (a) residual
           gas and (b) acrylonitrile

Table 3.03   Band assignment of plasma

Wave length $\overset{\circ}{A}$	Radical	Assignment v', v''
3855	CN	3,3
3860	CN	2,2
3870	CN CH	1,1 CN main system 0,0 CH 3900$\overset{\circ}{A}$ system
3880 3890 3895 3905 3920	CN	CN-violet system,tail bands
3960	CH^+	1,0
4050	CH_2	due to C_3?
4150 4158 4170 4180 4200 4215	CN	CN-violet
4310 to 4200	CH	Q-Head
4320	CH	2,2 Q-Head
4330 to 4400	CH	—
4500 to 4600	CN	5,7 to 0,2 Violet system
4830	CO	0,2
5190	CO	0,1
5260 to 6250	CN	Red system Active nitrogen

In the spectrum of plasma, there is no indication of the Swan band showing the absence of a carbon-carbon radical in the system. Even after prolonged discharge, there is no indication of the formation of carbon. Also there is no unusual increase in the pressure during discharge. These observations are sufficient to prove that the C-H bands are not broken during discharge. It has been reported [18] that a many line system in the region 9500 to 5500Å is the characteristic band of CH_2 radical. But these bands are unobserved possibly due to intense Red system of CN. Hence it is inferred that in the initial process of plasma-polymerisation, the monomer molecule is dissociated into CH_2, CH and CN radicals. Moreover in the polymerisation process, additional bands of CO radical is observed which is neither in the residual gas discharge nor in the monomer molecule.

3.32 Polymerisation mechanism

From the emission spectrum, the radicals CH_2, CH and CN are identified. These radicals will recombine in such a way that the resultant system will tend to possess minimum energy. For the formation of solid long chain polymer molecules, the favoured combination of CN radical is with CH radical because combination of CH_2 with CN is always a termination reaction. Hence CHCN is most probably

an intermediate radical. Subsequently CH_2 radicals and
CHCN radicals will combine either themselves or alternately
or randomly to form a linear polymer. But from the structure
of the resulting polymer, it is concluded that CH_2 radical
and CHCN radical will combine alternately as shown in
Fig.3.02. Hence the radical polymerisation of acrylonitrile
can be illustrated as follows:

$$n(CH_2 = CH-CN) \xrightarrow{g} n(CH_2^*) + n(CH^*) + n(CN^*) \qquad (3.01)$$
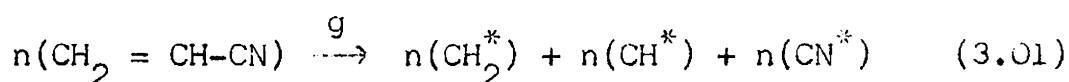
where g is the collision rate of gas ions with high energy.

$$n(CH^*) + n(CN^*) \xrightarrow{R_{co}} n(CHCN^*) \qquad (3.02)$$

where R_{co} is the recombination rate of CH radicals with
CN radicals.

$$n(CH_2^*) + n(CHCN^*) \xrightarrow{R'_{co}} (-CH_2-CHCN-)_n \qquad (3.03)$$
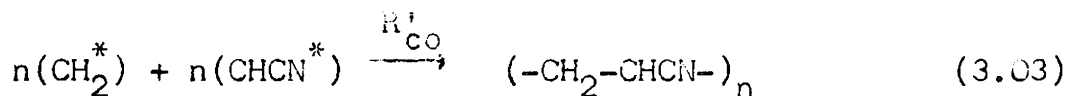
where R'_{co} is the recombination rate of CH_2^* and $CHCN^*$. The
chain molecules produced by polymerisation may be long but
are never infinite. Thus in the present case the growth of
the chain is brought to an end by a termination process
normally by any one of the three processes. In the first
process, the residual hydrogen atom in the system can combine
at the tail ends

$$(-CH_2-CHCN)_n \xrightarrow{T} CH_3-CHCN - (-CH_2-CHCN-)_{n-2} - CH_2-CH_2CN$$

$$(3.04)$$
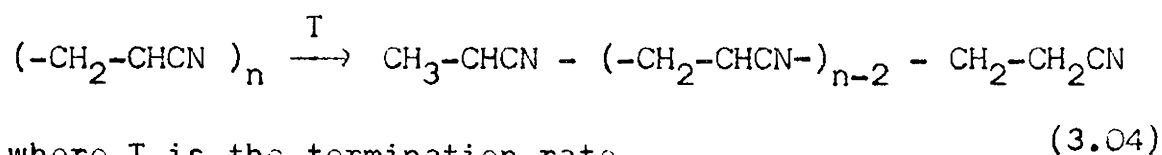
where T is the termination rate.

In the other case trapped charges can combine with the tails of the polymer. Usually this will be an unstable system. On heating the specimen thermal degeneration is possible. In the third case CN radical can combine at the tail ends of the polymer. But since such a reaction indicates structural change in the infrared spectrum, the possibility of such a termination is deleted on comparing with standard spectrum. Hence in most cases, for a stable system, the termination process is associated with the addition of hydrogen atoms. But the possibility to terminate with trapped charges cannot be ruled out because there are evidences of thermally stimulated short-circuited current in Al-PAN-Al due to trapped charges and degradation of the polymer [19] on heating the specimen. The end group analysis is the most reliable method to understand termination reaction. With the present experimental set up it is very difficult to confirm this process.

In plasma-polymerisation process, since the initiator concentration is very large, the polymer formation is fast. Also, as discussed in chapter II, the relation of the growth-rate with the square of the current density is a supporting observation for radical polymerisation. This gives an evidence for direct transfer of energy to the monomer vapour for polymerisation. From all the available data, it can be concluded that the formation of the polymer product

through radical mechanism is the most appropriate mechanism
for plasma-polymerisation. Moreover, it is noted that in
the formation process CO radical is formed as an impurity
(Table 3.03). Also from the infrared spectra of polymer
(Fig.3.01c), it is found that this CO impurity is combined
with the polymer to form an additional side group. This CO
impurity may originate from the decomposition of the monomer
molecule and is commonly found in plasma-polymerisation
process [12].

3.40 ULTRAVIOLET AND VISIBLE SPECTRA OF POLYACRYLONITRILE

The coloured substances owe their colour to the
presence of one or more unsaturated linkages. The linkages
or groups conferring colour to a substance are called
chromophors. Usually the effect of chromophors is studied
by the absorption spectra of the material. A preliminary
result of the absorption spectra of polyacrylonitrile in the
range of $2000\overset{o}{A}$ to $9000\overset{o}{A}$ is presented in this section.

3.41 Experimental method

The polyacrylonitrile thin films are first
prepared on glass slides and they are scraped out from the
substrates. This polymer powder is then dissolved in ethyl
alcohol and absorption spectrum of the solution is taken
in a visible and ultraviolet spectrograph (Hitachi 220).
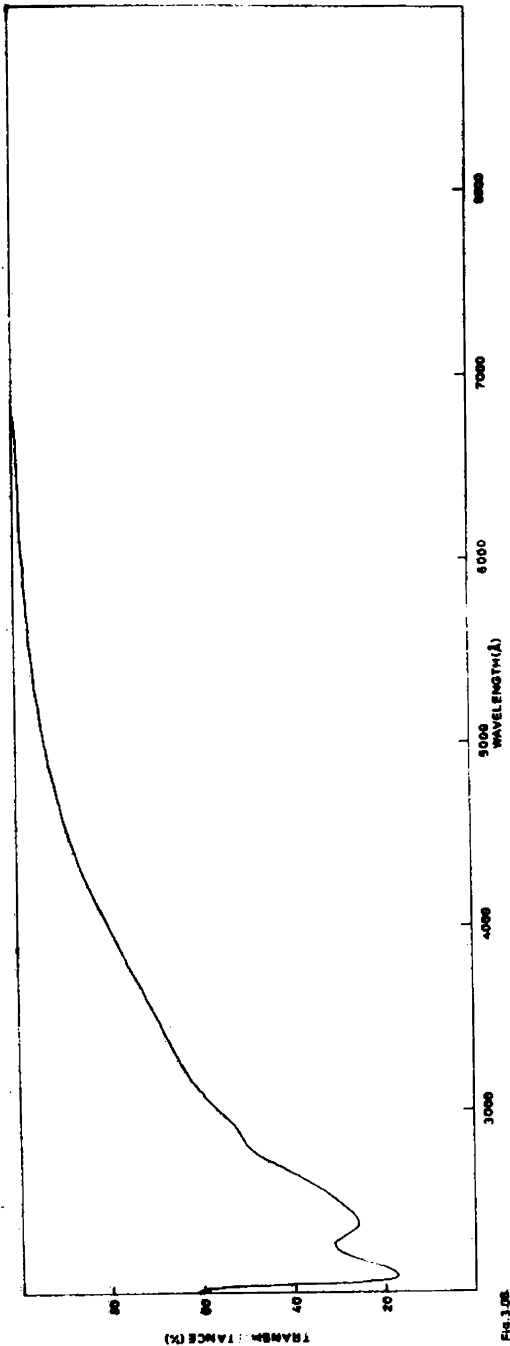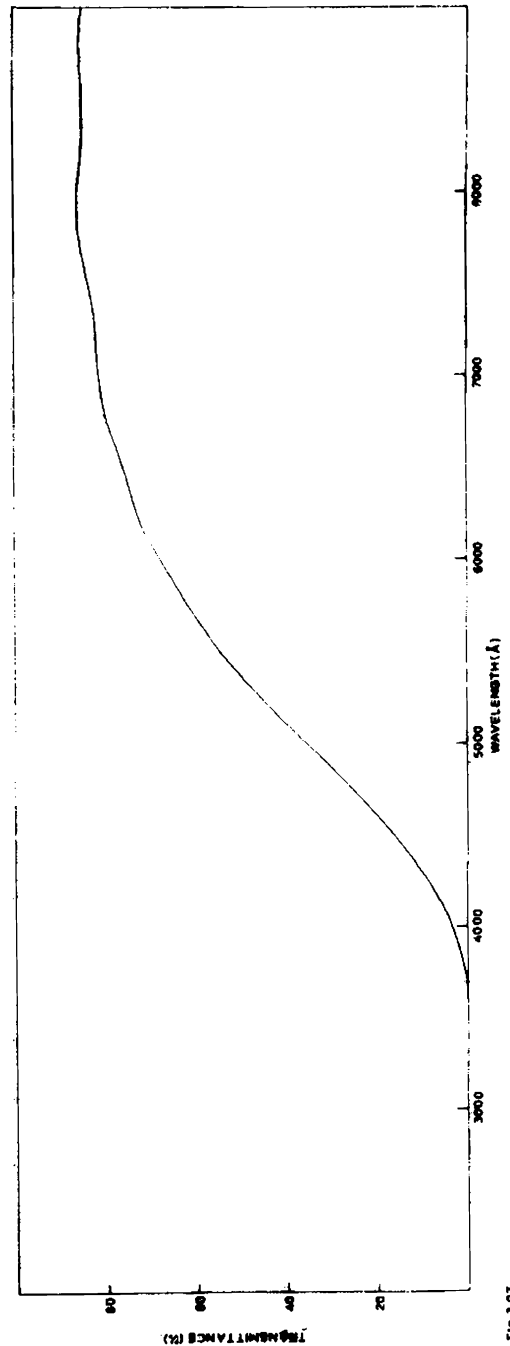
Fig.3.06 Visible and ultraviolet spectra of PAN dissolved
in ethyl alcohol

Fig.3.07 Visible and ultraviolet spectra of PAN thin
film prepared on quartz substrate

Another identical cell with solvent ethyl alcohol is put as
compensator. The absorption spectrum in the region $2000\overset{o}{A}$ to
$9000\overset{o}{A}$ for PAN dissolved in ethyl alcohol is shown in Fig.3.06.

The experiment is also conducted with PAN films.
PAN films are prepared on quartz substrates and visible and
ultraviolet absorption spectra are taken with similar
substrates as compensators. The thickness of the film is
adjusted so that very little change in absorption is observed
on further reducing the thickness. Such a spectrum is shown
in Fig.3.07 (Thickness of PAN is $\sim 1000\overset{o}{A}$).

3.42 Visible and ultraviolet spectrum of PAN

In Fig.3.06, the visible and ultraviolet spectrum
of a solution of PAN in ethyl alcohol is shown. In the
spectrum two strong and broad peaks are observed, one with
$\lambda_{max} = 2100\overset{o}{A}$ and the other with $\lambda_{max} = 2400\overset{o}{A}$. But in the
case of polymer film, the absorption band is more broad. As
shown in Fig.3.07, the absorption starts from the wavelength
$7600\overset{o}{A}$ and all the wavelengths below $3700\overset{o}{A}$ is completely
absorbed.

3.43 Absorption band in PAN

Usually solvent ethyl alcohol shows a sharp
absorption peak at $2100\overset{o}{A}$ [20]. Since sufficient compensation
is given to the system, and since the observed band is broad

the possibility of an absorption band at 21$\overset{\circ}{\text{JJA}}$ due to the solvent can be deleted. From the earlier data [21], the absorption spectra of acrylonitrile dissolved in ethyl alcohol is at $\lambda_{max} = 215\overset{\circ}{\text{JA}}$ and that of a carbonyl group is at $\lambda_{max} = 2140$ A. Due to the interaction of CN and the impurity CO a splitting of the absorption band may be possible. For macromolecules like polymers, the existence of highly localised excitons are possible which dominate the absorption threshold with the broad energy bands indicated by the periodic structure of the polymer [22]. Hence the broadening of absorption peak of acrylonitrile indicates that a long polymer chain is formed with a periodic structure of the monomer.

In the case of PAN thin films, all the molecules are closely packed and are amorphous in nature. Hence the broadening of the band is still larger. The formation of different types of exciton levels and trap levels develop a number of energy levels in the amorphous solid as illustrated by Pohl [22]. To get the complete information of the electronic transitions, further investigations are necessary. From the present results it is concluded that a polymer is formed in the process of glow-discharge with a broad absorptio band. A carbonyl group also exists with the polymer chain which may be the cause for the band splitting.

REFERENCES

[1] Harold Suhr, Techniques and Application of Plasma Chemistry, John R. Hollahan and Alexis T.Bell (Ed.), John Wiley and Sons, New York, Chapter II, 57 (1974).

[2] Keiichi Ando and Minorw Kusabiraki, Memoirs of the Faculty of Engineering, Osaka City University, 19, 95 (1978).

[3] T.Williams and M.W.Hayes, Nature, 216, 614 (1967).

[4] K.Jesch, J.E.Bloor and P.L.Kronick, J. Polym. Sci., A-1, 4, 1487 (1966).

[5] P.L.Kronick, K.F.Jesch and J.E.Bloor, J. Polym. Sci., A-1, 7, 767 (1969).

[6] Norman B. Colthup, Lawrence H.Daby and Stephen E.Wiberly, Introduction to Infrared and Raman Spectroscopy, Academic Press, New York, Chapter XIII, 366 (1964).

[7] H.W.Siesler and K.Holland-Moritz, Infrared and Raman Spectroscopy of Polymers, Marcel Dekker, INC., New York, Chapter IV, 253 (1980).

[8] Norman B.Colthup, Lawrence H.Daby and Stephen E.Wiberly, Introduction to Infrared and Raman Spectroscopy, Academic Press, New York, Chapter VII, 211 (1964).

[9] T.Hirai and O.Nakada, Jap. J. Appl. Phys., 7, 2, 112 (1968).

[10] C.Y.Liang and S.Krimm, J. Polym. Sci., 31, 513 (1958).

[11] R.Yamadera, H.Tadokoro and S.Murahashi, J. Chem. Phys., 41, 1233 (1964).

94

[12] M.Millard, Techniques and Applications of Plasma Chemistry John R.Hollahan and Alexis T.Bell (Ed.), John Wiley and Sons, New York, Chapter V, 177 (1974).

[13] D.B.V.Parker, Polymer Chemistry, Applied Science Publishers Ltd., London, Chapter IV, 119 (1974).

[14] J.K.Smith, W.J.Kitchen and D.B.Mutton, J. Polym. Sci.,C 2, 499 (1963).

[15] R.Stefani, M.Chevreton, M.Garnier and M.C.Eyrand, Compt. Rend., 251, 2174 (1960).

[16] H.Koning and Brockes, Z.Physik, 152, 75 (1958).

[17] R.W.B.Pearse and A.G.Gaydon, The Identification of Molecular Spectra, Chapman and Hall LTD, London, Chapter V 332 (1965).

[18] Gerhard Herzberg, Electronic Spectra and Electronic Structure of Polyatomic Molecules, Van Nostrand Reinhold Company, New York, Chapter II, 215 (1966).

[19] S.I.Stupp and S.H.Carr, J. Polym. Sci. Polym. Phys., 15, 485 (1977).

[20] C.N.R.Rao, Ultraviolet and Visible Spectroscopy, Butterworths, London, Chapter I, 11 (1967).

[21] J.Ritsko, J. Chem. Phys., 70, 5343 (1979).

[22] Herbert A. Polil, Organic Semiconducting Polymers, J.E.Katon (Ed.), Marcel Dekker, INC., New York, Chapter II 51 (1968).

CHAPTER IV

THERMALLY STIMULATED SHORT-CIRCUITED CURRENT IN PLASMA-POLYMERISED POLYACRYLONITRILE

ABSTRACT

An appreciable amount of thermally stimulated short-circuited current is observed during heating and cooling between $30^{\circ}C$ and $160^{\circ}C$ from unpoled plasma-polymerised polyacrylonitrile thin film sandwiched by aluminium electrodes. The observed current is attributed to the space charges accumulated at the vicinity of the outer electrode producing a charge gradient towards the inner. The disorientation of dipoles also contributes to the thermally stimulated current. The temperature activation energy of 1.4 eV indicates that charges are formed from the covalent bond of the carbon atoms. An additional current is also developed which is associated with the electrodes of dissimilar thicknesses. Observations are made by the application of low fields and the relative magnitudes of the various components are discussed.

4.10 INTRODUCTION

Extensive studies have been reported on the short-circuited current of poled [1-4] and unpoled [1,5-7] polymers to obtain information about the behaviour of trapped charges and dipole relaxation process. Thermoelectric and electromechanical effects have also been studied in detail on a variety of polymers [6,7]. It is understood from the thermally stimulated depolarisation current (TSD) studies of polyvinylidene fluoride that the dipole orientation in this polymer is reversible [8-10]. The existence of large piezoelectric and pyroelectric coefficients have extended its application to transducers [11] and thermal sensors [12]. All the interesting properties of polyvinylidene fluoride originate from the preferential orientation of the dipoles.

Polyacrylonitrile (PAN), which has been investigated here in detail, also possesses a permanent dipole moment and is expected to show similar electrical properties [1]. The TSD current spectrum of PAN shows three different peaks, centered around $90^{\circ}C$, $145^{\circ}C$ and $190^{\circ}C$ and these peaks are characterised by various physical techniques. They are due to loss of preferred orientation of dipoles, the onset of chain segmental mobility ionic diffusion, and solvent diffusion [4,13]. Trapped space charges and residual

solvent molecules also contribute to a broad and strong peak [1] at the vicinity of 195°C. These peaks are suppressed on repeated heating cycles. Persistent polarisation due to stretching has also been reported [14]. The structural and dipolar properties of the polymers are known to depend on the history of the material, namely, method of polymerisation, stretching details and poling parameters. Considering the increased application of polymers as electrets in recent years, it is felt important to undertake an extensive investigation on the short-circuited current in plasma-polymerised PAN thin films. As a part of the studies, the short-circuited current for the temperature range 30°C to 160°C on PAN films of different thicknesses using aluminium electrodes, is reported here.

4.20 EXPERIMENTAL

All the measurements are made on plasma-polymerised PAN films sandwiched by vacuum deposited aluminium electrodes. Initially, known amount of aluminium is evaporated in a vacuum and is deposited on ultrasonically cleaned glass slides. PAN thin film is now deposited on the electrode coated glass slide by plasma-polymerisation method. This substrate is transferred to the high vacuum unit and the thermally evaporated outer free electrode is prepared. The details of

preparation of Al-PAN-Al sandwich specimen have been discussed in section 2.24. The sandwich structure thus prepared for short-circuited current studies are schematically shown in Fig.2.09 (a and b). For the thickness measurement of the polymer film separate samples are prepared simultaneously with the specimen and Fizeau fringes method is adopted. The details of Fizeau fringes method are discussed in section 2.32. From the mass of the aluminium taken for evaporation, the thickness of electrodes are estimated.

4.21 Thermally stimulated short-circuited current measurement

The Al-PAN-Al sandwich specimen is transferred to a specially designed chamber which is kept at a pressure of 10^{-3} torr. The description of conductivity chamber has been given in section 2.40. Proper electrical connections are made using copper block pressure contacts. For the present investigations, one of the electrodes is connected to the Electrometer amplifier (ECIL-EA-815) while the other is earthed. The electrical connections for the measurement of short-circuited current is shown in Fig.4.01. Before making the thermally stimulated short-circuited current measurements, the short-circuited specimen is heated in vacuum to $160^{\circ}C$ at the rate of $1^{\circ}C/min.$ maintained for one
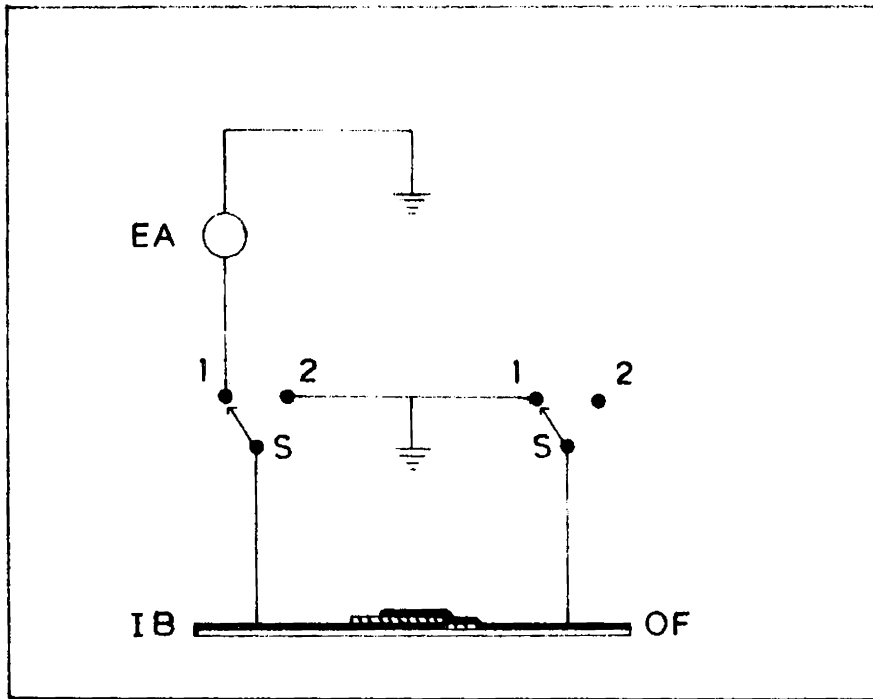
Fig.4.01. Electrical connections for short-circuited
current measurements: IB – inner bound
electrode, OF – outer free electrode,
S – double pole double throw switch,
EA – electrometer amplifier.
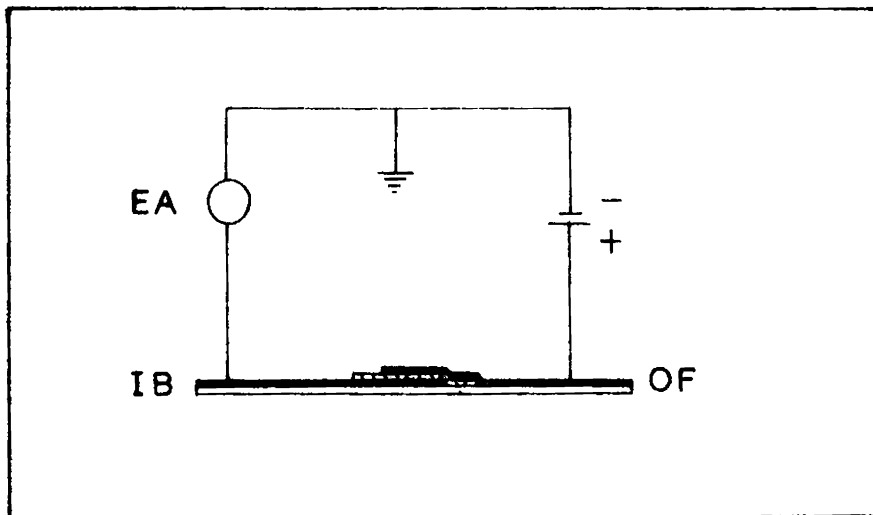
Fig.4.02. The electrical connection for ISC with
applied voltage: IB – inner bound
electrode, OF – outer free electrode,
EA – electrometer amplifier.

G3188

hour and then cooled to room temperature at the same rate
for removing condensed monomer vapours and charges, if any.
Each specimen is subjected to heating and cooling before
final readings are recorded. In general, it is observed
that logarithmic short-circuited current against temperature
curve during the first heating and cooling operation is
very much different from the subsequent curves. However
these subsequent readings show only very small changes
among themselves. The readings reported here are for the
second heating and cooling operation. The short-circuited
current for different specimens of Al-PAN-Al is recorded
for the temperature range $30^{\circ}C$ - $160^{\circ}C$.

4.22   Parameters controlling the short-circuited current

From the preliminary investigations, it is found
that the important parameters on which the short-circuited
current depends are the film thickness of the inner bound
and outer free electrodes and the range of temperature.
From the observations on the direction of the short-circuited
current, it is possible to classify the specimens into
two groups (1) specimens for which the outer free electrode
is thicker than the inner (2) specimen for which the inner
bound electrode is thicker than the outer. The investigations
presented here are mainly centered on the magnitude and
direction of short-circuited current as a function of electrode

thickness and temperature. In the present study, effort is
not given to correlate the thickness of PAN thin film with
short-circuited current. Different specimens with thicknesses
ranging from 700$\overset{\circ}{A}$ to 1500$\overset{\circ}{A}$ are presented to illustrate the
validity of the observed effect. Special effort is not
taken to study the specimens having thicknesses below 700$\overset{\circ}{A}$
because most of them are short-circuited on heating.

4.23   Thermally stimulated current in low applied fields

        In order to have a better insight into the
mechanism of short-circuited current, particularly to
illustrate the current reversibility when two exponentially
varying currents are added vectorially, the potential of
the outer free electrode is raised by an external voltage
and the resulting thermally stimulated current is studied.
For such studies, the positive terminal of the external
voltage source is given to the outer free electrode and the
negative terminal is earthed. The electrometer amplifier is
connected to the inner bound electrode (Fig.4.02). The
current flowing through the sandwich structure is recorded
for heating and cooling processes. The investigations are
also made by increasing the field across the specimen.

4.30   RESULTS OF THE EXPERIMENTS

        From the initial results, it is clearly understood
that two main mechanisms drive the process of short-circuited
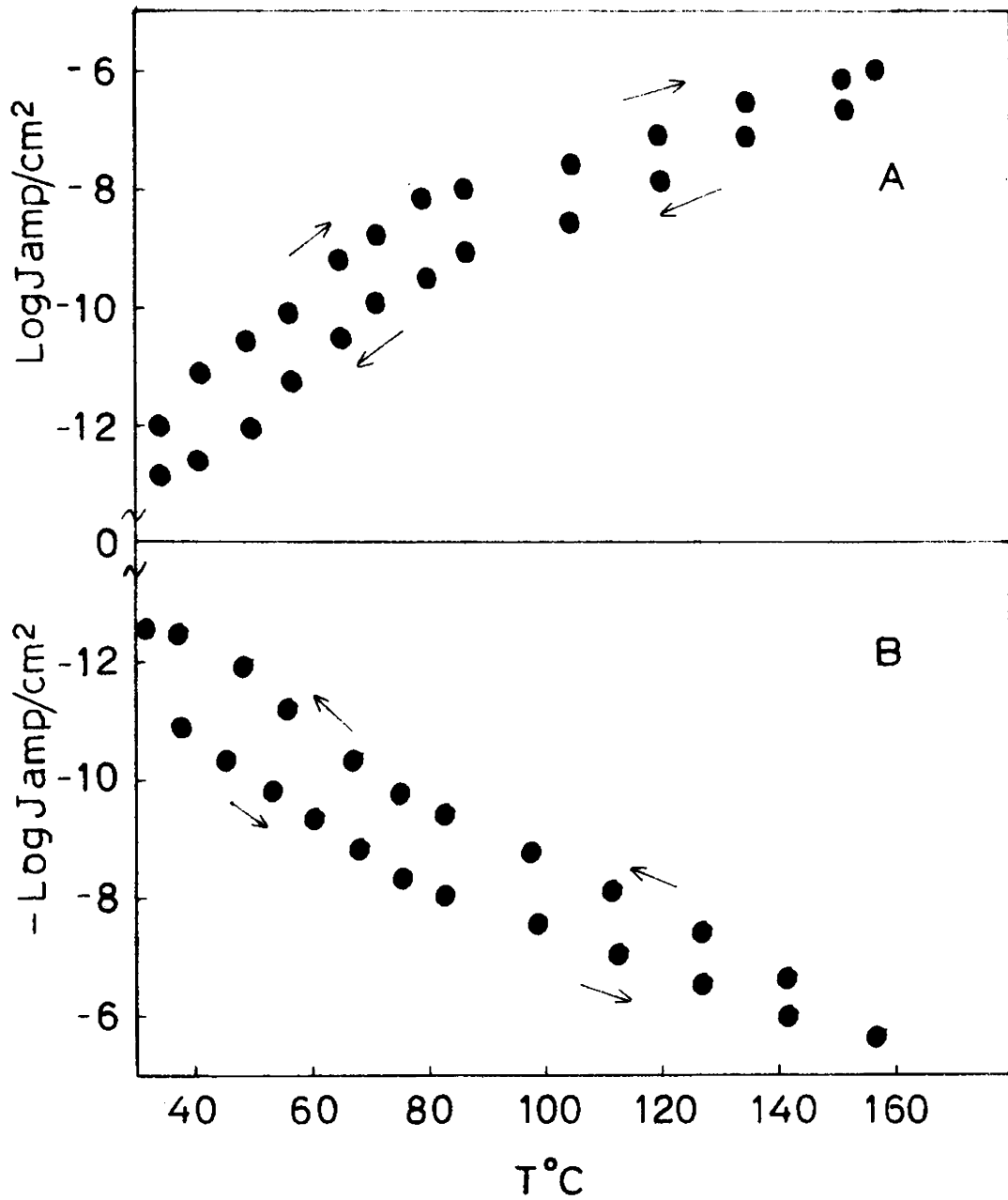
Fig.4.03. The logarithmic short-circuited current vs.
temperature for Al-PAN-Al when the inner bound
electrode is thicker. (A) is the current when
electrometer is connected to the outer free
electrode and (B) the current when electrometer
is connected to the inner bound electrode.

The thicknesses of inner electrode is 2500Å,
the outer electrode is 650Å and the PAN is
1200Å. (- log j implies that the current flows
from the outer electrode to the inner in the
short circuit).

current. Depending on the relative thicknesses of the inner

bound electrode or outer free electrode the direction of the

current generated due to one mechanism is reversed while

the direction of current due to other is maintained. These

processes are classified and explained to understand the

mechanism. For specimens with the inner bound electrode

thicker than the outer free electrode, it is found that the

current is flowing from the outer free electrode to the inner

bound one in the external circuit when inner bound electrode

is thicker. In Fig.4.03, the short-circuited current when

the electrometer is connected to the outer electrode (A)

and also when the electrometer is connected to inner

electrode (B) is recorded against temperature. The current

is recorded for every alternate intervals of temperature

on heating and cooling processes. The symmetric curves A

and B ensure that the short-circuited current is a bulk

process of the material rather than a surface process.

Unlike the reversible pyroelectric materials [8], on the

cooling cycle, the direction of the current is not reversed,

but log J vs. T curve retained the same form with a decrease

of one to two orders of magnitude forming a closed loop as

shown in Fig.4.03. In Fig.4.04, the short-circuited

current against temperature for Al-PAN-Al films when the

inner bound electrode is thicker, is presented for various
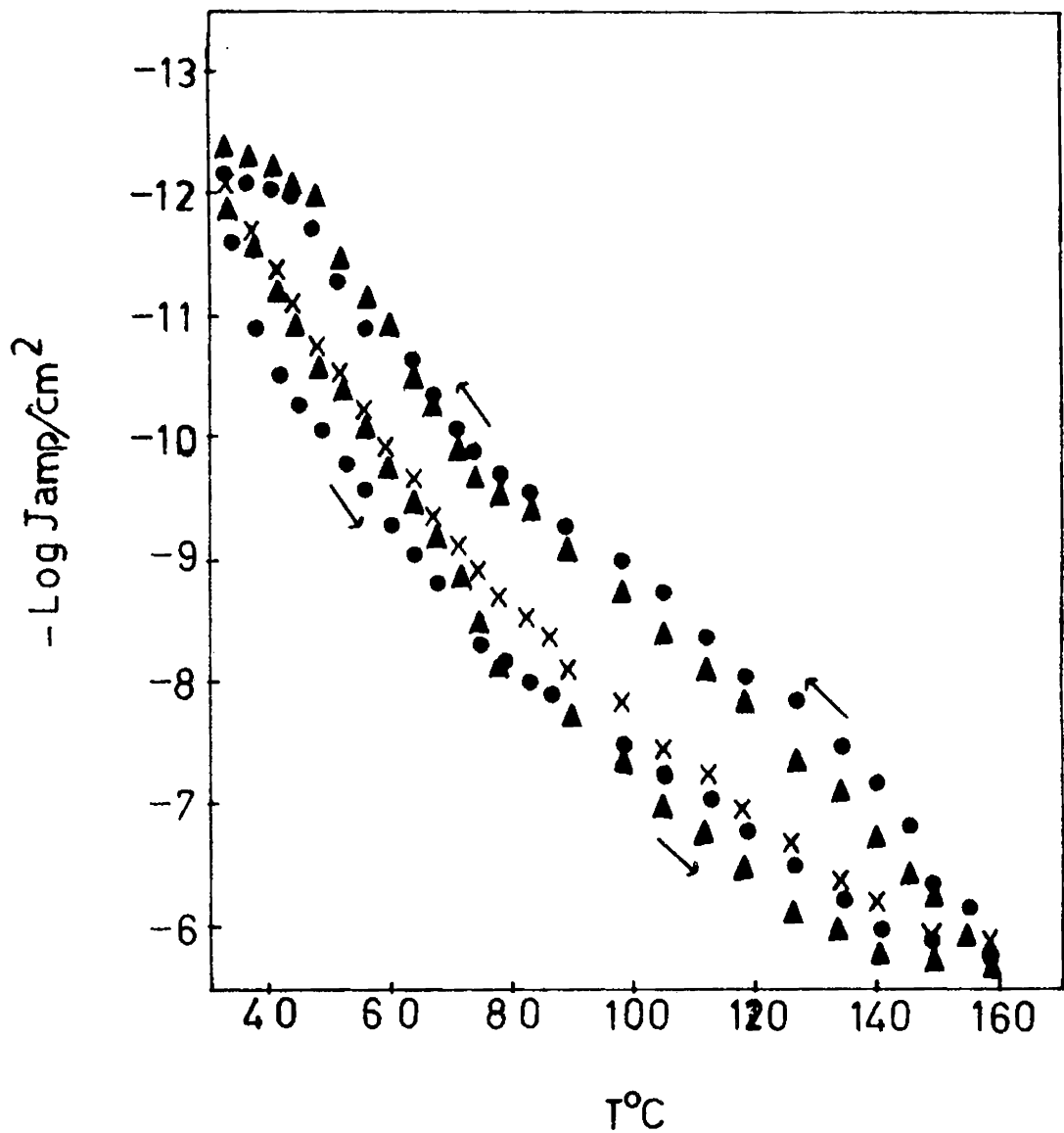
Fig.4.04. The short-circuited current Vs. temperature
for Al-PAN-Al films when the inner electrodes
are thicker. ● and ▲ are the curves on heat-
ing and cooling when the thickness of the inner
electrode is 2950Å, the outer electrode 730Å
and the PAN 1360Å and 1120Å respectively. X is
the curve on heating when the thickness of the
inner electrode is 730Å, the outer electrode
550Å and the PAN 700Å. (-log J implies that the
current flows from the outer electrode to the
inner in the external circuit. The arrow shows
the direction of the closed loop).

102

thicknesses of P·N. The short-circuited current on heating
and cooling forms a closed loop.

When the outer free electrode is thicker than the
inner bound electrode, the current flows from the inner
bound electrode to the outer free electrode at the initial
temperatures and reverses at elevated temperature. In
Fig.4.05, logarithmic short-circuited current is plotted
against temperature for a specimen whose outer free electrode
is thicker. In the heating cycle, the current is increased
exponentially upto $60^{\circ}C$ and then decreased sharply. The
current is reversed at $75^{\circ}C$. In the figure, the short-
circuited current is recorded against temperature when the
electrometer is connected to outer free electrode (A) and
also when the same is connected to the inner bound electrode
(B). In the process of cooling the short-circuited current
decreases exponentially with temperature. Unlike the
heating cycle, in this case, the current reversal is
observed only at the vicinity of the room temperature.
The symmetric variation of curves A and B indicates that
the observed short-circuited current is a bulk process of
the material rather than the surface process. In Fig.4.06
the short-circuited current of Al-PAN-Al with the outer
free electrode thicker for different thicknesses of PAN
is plotted against temperature in the heating and the
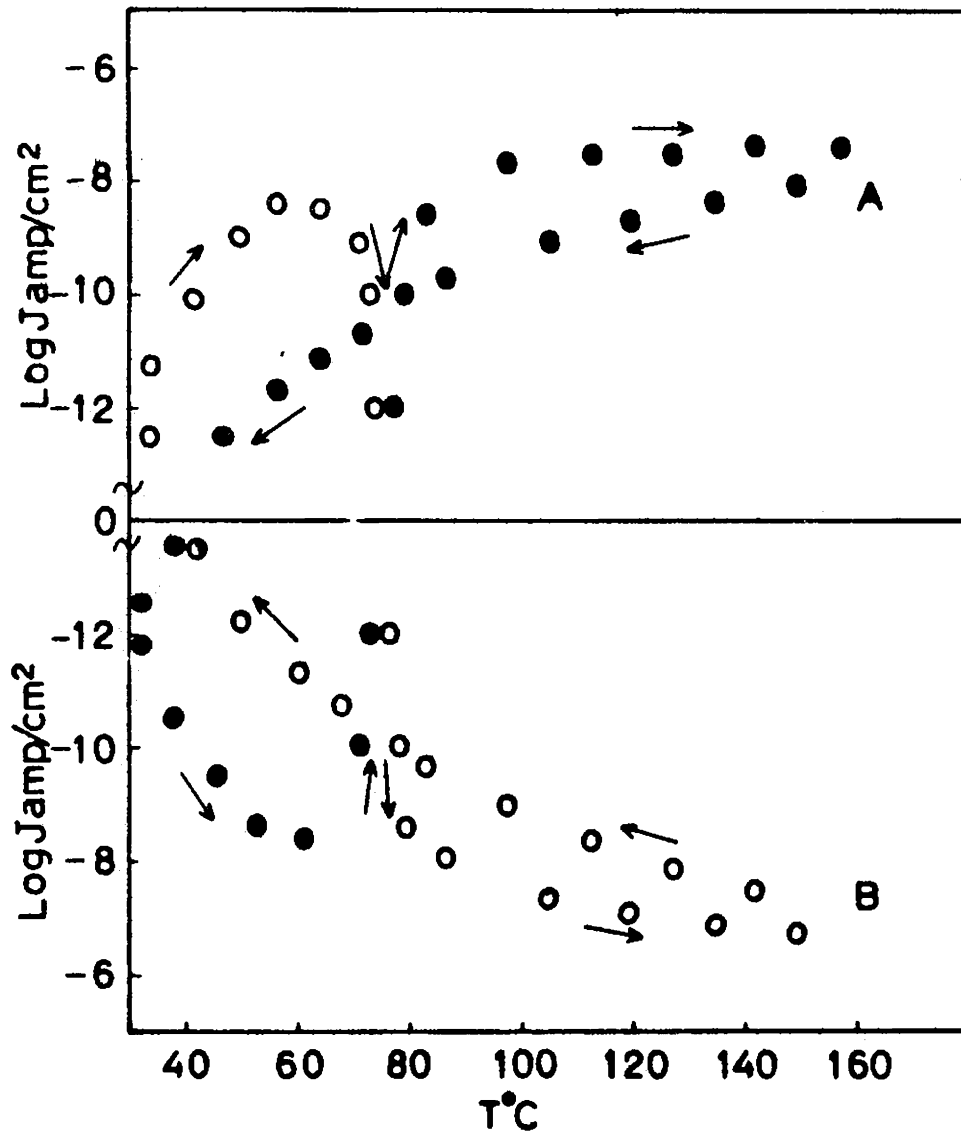
Fig.4.05. Short-circuited current Vs. temperature for
Al-PAN-Al films when the outer free electrode
is thicker. (A) is the current when the electro-
meter is connected to the outer electrode and
(B) the current when the electrometer is
connected to the inner bound electrode. The o
thickness of the inner bound electrode is 650Å
the outer electrode is 2500 Å and the PAN is
1200Å. (-log J implies that the current flows
from the outer electrode to the inner in the
external circuit).
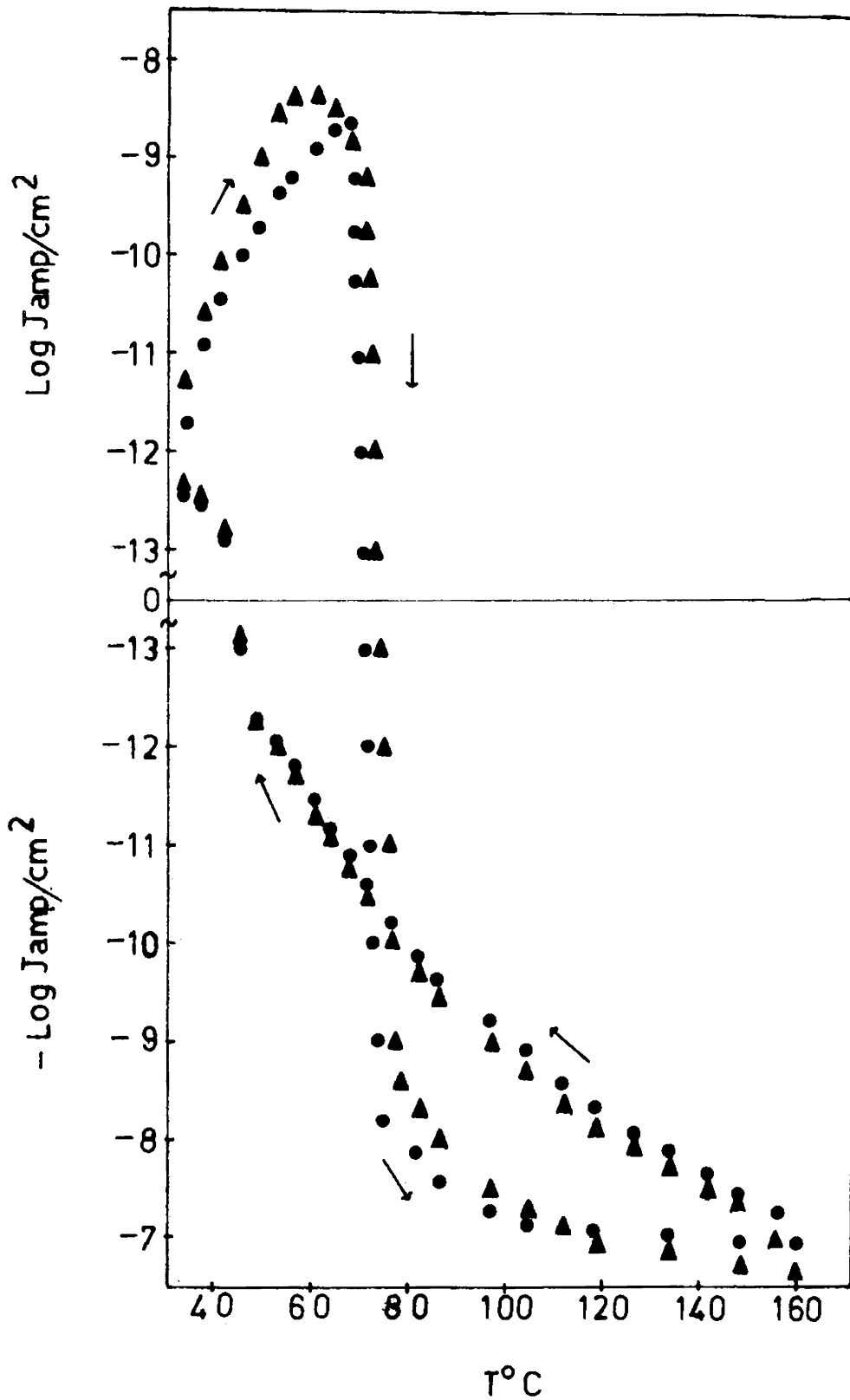
Fig.4.06. The short-circuited current Vs. temperature
for Al-PAN-Al films when the outer electrodes
are thicker. ● and ▲ are the curves on heat-
ing and cooling when the₀thickness of the
inner electrode is   730 Å, the outer electrode
2950Å and the PAN 1420 Å and 1120 Å respectively.
(-log J implies that the current flows from the
outer electrode to the inner in the external
circuit. The arrow shows th direction of the
closed loop).

cooling cycles. It can be seen from the figure that the current variation in the heating and cooling processes form a closed loop.

4.31 Effect of application of field across the specimen

In order to have a better insight into this anomalous process of current reversibility, the potential of the outer free electrode is raised in the positive direction for those samples which do not show a current reversibility on heating. In Fig.4.07, ($\blacktriangle$) the typical results when the potential of the outer electrode is raised to produce a mean field of 3×10^4 V/cm in the P$_A$N is presented. On heating, the current initially increases and reaches a maximum at about 60°C. On further heating, the current drops sharply and at about 70°C the direction of short-circuited current reverses. In the cooling cycle, the current drops exponentially and at about 65°C, the direction of the current again reverses. It reaches a maximum at 60°C and decreases to room temperature current. One of the notable features is that the low temperature current peaks, one on heating and the other on cooling, show a difference in magnitude of two orders. For comparison, the short-circuited current of Al-P$_A$N-Al specimen with thicker outer free electrode is also plotted in the figure
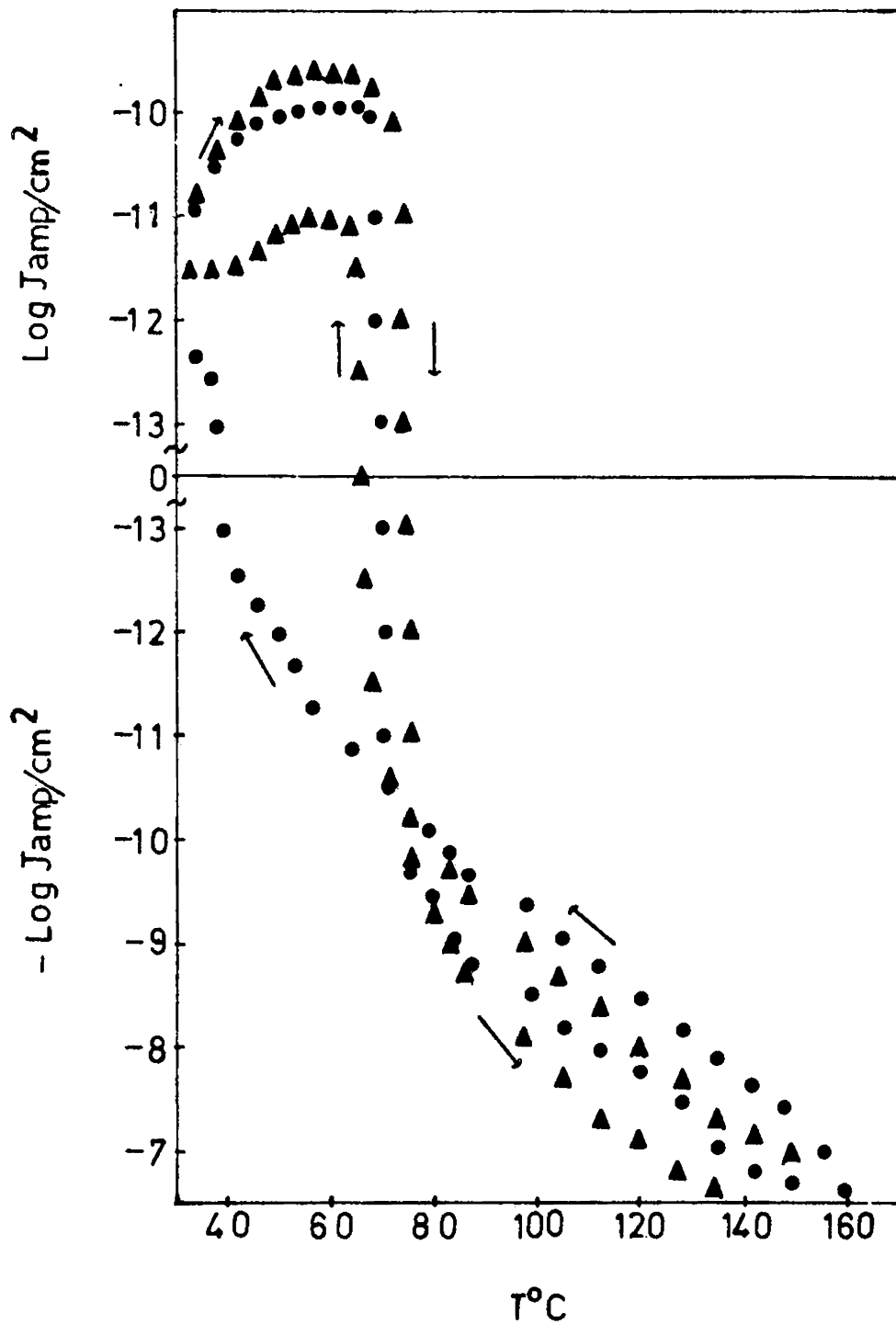
Fig.4.07. ● is the short-circuited current on heating and cooling for Al-PAN-Al film whose the inner electrode is 550Å, the outer electrode 730Å and the PAN 700Å. ▲ is the curve on heating and cooling when the potential of the outer electrode (730Å) is raised in the positive direction to produce a mean field 3 x 10⁴V/cm across the PAN film (1120 ₀Å); the thickness of inner electrode is ⁻⁻⁵0Å.

(Fig.4.07, ●). It can be observed that on heating, the two samples show identical curves while on cooling, the curves are different.

It is important to study the variation of current with temperature at higher fields. By applying higher fields, the current reversibility as shown in Fig.4.07 is not observed till 160°C, but on cooling the current abruptly goes to the negative side and decreases on cooling. A typical plot is shown in Fig.4.08 when the potential of the outer electrode is raised to produce a field of 5×10^4 V/cm across the PAN film. In the figure A-B shows the current variation on heating and B-C gives the current reversal on cooling. On further cooling the current decreases and at D it reverses as shown in figure. At room temperature, it again reaches A. But when the specimen is heated again from the point D, Fig.4.08, B-C-D form a closed cycle and the loop is repeated on heating and cooling from 75°C to 160°C.

4.40 DISCUSSION

The origin of short-circuited current in M-I-M. structures is described elsewhere [6,7]. On the contact of the polymer with a metal, the electrons are usually transferred between the polymer and metal mainly because of
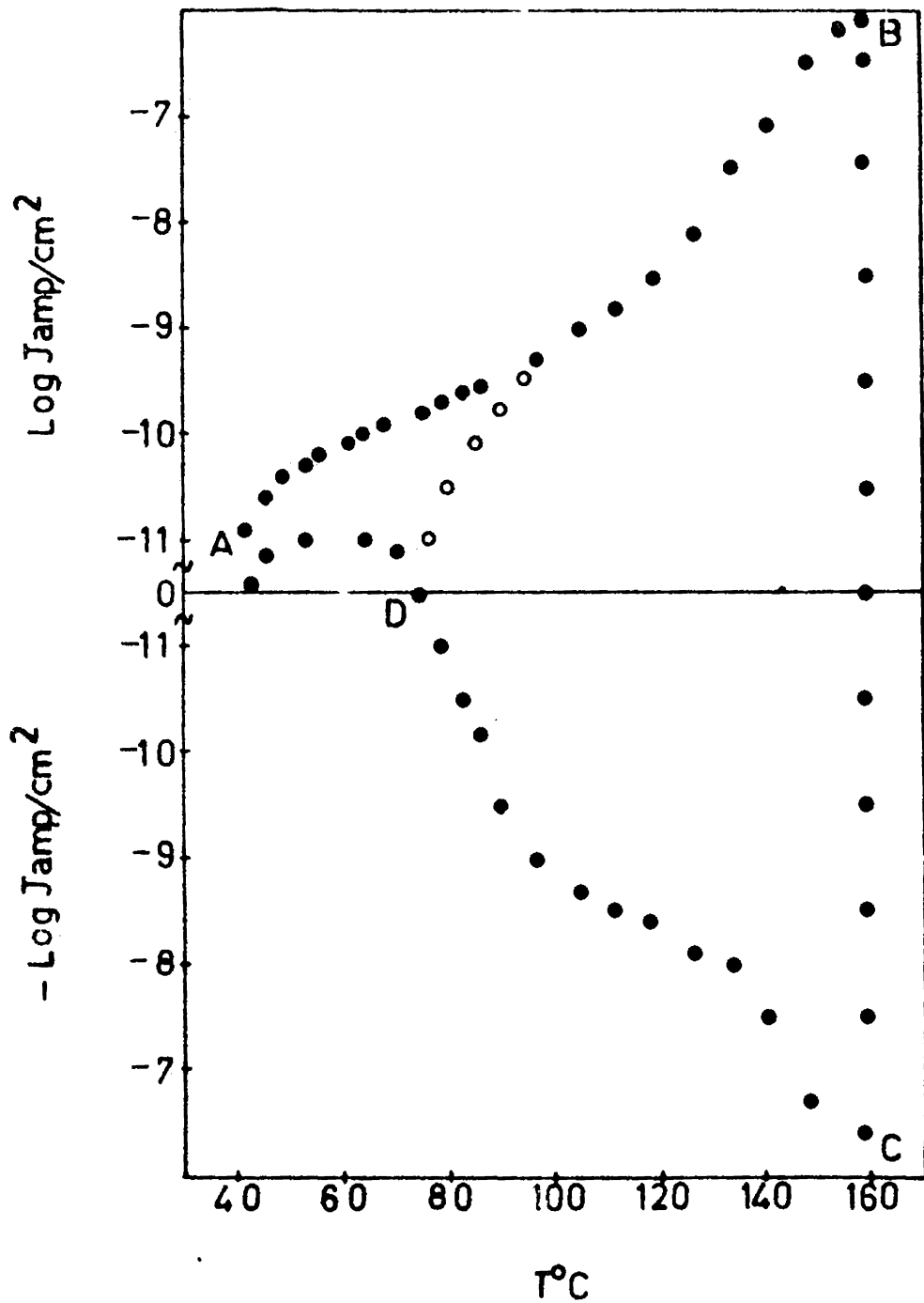
Fig.4.0%. ● is the curve on heating and cooling when the potential of the outer electrode (730 A) is raised in the positive direction to produce a mean field of 5×10^4 V/cm across the PAN (1360Å); the thickness of the inner electrode is 2950Å. O is the curve when the specimen is reheated from 75°C.

the difference in the work functions, which will in turn
bend the conduction band due to the space-charges. If the
work functions are temperature dependent, a transient
current flows in the external circuit which depends on
the rate of change of temperature [6]. Also an electro-
chemical current will be produced [7] when the temperature
of the system is increased. For all the above observations,
the two electrodes are to be of different metals and hence
they may not be applicable to Al-PAN-Al. However, even
with electrodes of the same metal a thermo-electric current
is possible, the magnitude of which in the present investi-
gation will be very small as compared to the observed
current and can also be neglected. It may be inferred
from the behaviour of the thermally stimulated current,
that the unreacted monomer vapours are not contributing
to the observed current. The thermally stimulated depola-
risation current peaks observed by Comstock et al [1] at
95°C and 185°C and attributed to the dipole orientations
and residual charges might have been superposed on the
large space-charge current generated from Al-PAN-Al
specimen.

4.41 Thermally released space-charge induced current

Several processes contribute to the thermally
stimulated current in insulators. Immobilised and

thermally released space-charges produce a thermally

stimulated current in insulators. In polar insulators

the disorder of the dipoles may also contribute a thermally

stimulated current. The possible mechanism that explains

the observed thermally stimulated current is outlined

below by taking into consideration the magnitude and the

direction of the short-circuited current. From the

direction of the current shown in Figs.4.03 and 4.04, the

observed short-circuited current is not due to the surface

charges but associated with the bulk of the polymer film.

Hence whatever changes found in the electrometer connected

to one electrode is observed in the other one as a mirror

image. Hence from the direction of the current, it may be

inferred that the trapped negative charge density is

maximum at the vicinity of the outer electrode. Due to

the irradiation of electrons and ions having the energy

of the order of 1 KeV, shallow trapped holes and electrons

are possibly formed in the specimen enhancing the condu-

ctivity of the system. The space-charge field in the

specimen may orient the polar side group-CN towards the

outer electrode [1]. When the specimen is short-circuited,

charge migration of the space-charges and the disorientation

of dipoles develop a current in the external circuit. At

room temperature, the relaxation time is very large and

trap modulated mobility is very small. As charges move

in the system, they may either get trapped again or recombine with the opposite charges. The blocking of electrons by aluminium electrodes may prevent the motion of the charge carriers from the electrodes to the insulator so that recombination of charges is minimum. As mobility and relaxation time vary exponentially with temperature, the thermally stimulated short-circuited current increases exponentially as shown in Figs.4.03 and 4.04. The steady exponential increase of current with temperature indicates that the relaxation time of the permanent dipoles and space-charges are widely distributed in plasma-polymerised PAN as it has been reported for styrene [15]. The re-appearance of current on repeating the experiment shows that only a part of the charge is untrapped on heating. Thus it is plausible to assume that thermally stimulated short-circuited current mainly arises from the untrapping and conduction of real charges in plasma polymerised PAN. However, the contribution from the disorientation of the dipoles is not to be ignored. As the specimen is cooled, the decrease in current of one to two orders may be an indication to the reversible polarisation of the dipoles at a lower rate explaining the closed loop as shown in the figure.

4.42   The short-circuited current induced by electrodes
       of dissimilar thicknesses

From Figs.4.05 and 4.06 it is observed that the
thickness of the inner bound electrode and outer free
electrode develop an additional contribution to the observed
short-circuited current. For thermally stimulated current
studies the specimens are heated by specially designed
copper blocks mounted symmetrically at the ends of the
substrates. The heating is therefore due to the conduction
along the length of the films. The thickness of aluminium
electrodes and, to a lesser degree, the thickness of the
PAN with much smaller thermal conductivity therefore
control the quantity of heat conducted. Thus, the polymer
film sandwiched by the two electrodes of dissimilar thick-
nesses when heated with copper blocks develop a temperature
gradient across the film with thicker electrode always
at a higher temperature. The average heating and cooling
rate is maintained at $1^{o}C/min$. Since the cooling takes
place by radiation, the temperature gradient across the
film on cooling is relatively very small with inner
electrode always at a higher temperature and the disorder
exhibited by the specimen during thermally stimulated
current studies is not significant. Hence in the sandwich
system a temperature gradient will be developed during the
process of heating and this temperature gradient may

develop an additional component to the short-circuited current [16]. The mobility and detrapping of the electrons are increased in the region of the thicker outer electrode which has a larger concentration of trapped electrons. But the temperature in the region of the inner bound electrode will be less. Hence, mobility of the charge carriers in that region will be small. The activated electrons at the vicinity of the outer free electrode move from the outer free electrode to the inner one giving a current in the external circuit. Also due to the large expansion coefficient of aluminium electrodes, the PAN surface which has a lower expansion coefficient might have been strained on heating. It is reported that as the PAN film is strained, the dipoles formed due to the nitrile side group may rotate inducing a charge on the surface [1]. Thus in Al-PAN-Al as the temperature is increased, the observed current of $C_E(\frac{dT}{dx})$ can be considered to be a function of the temperature gradient and the surface strain. Within the specimen the charges migrate towards the inner bound electrode resulting in a current of magnitude C_D which is an exponential function of temperature. Hence the total electron current C is given by $C = C_D - C_E(\frac{dT}{dx})$. At the initial temperatures, $C_E(\frac{dT}{dx})$ will be predominant and hence the net electron current will be from the outer free electrode to the inner

one in the external circuit producing a peak current

density of 5×10^{-9} ./cm^2 at 65°C. As the temperature

increases C_D predominates and the direction of current

reverses as seen in the Figs.4.05 and 4.06. On the

contrary, when the inner bound electrode is thicker, the

magnitude of $C_E(\frac{dT}{dx})$ will be very small due to low concen-

tration of trapped electrons at the vicinity of the inner

electrode and the resulting current will be approximately

C_D. Hence, as seen before, there is no current maximum

at the initial temperatures. If the positive charges were

trapped in the vicinity of the inner electrode, the direction

of $C_E(\frac{dT}{dx})$ would have been opposite to C_D and the current

would have been reversed when the inner electrode is

thicker. Hence in plasma-polymerised PAN, the negative

charge gradient with a maximum at the outer electrode can

explain the observed thermally stimulated current. It can

also be inferred that there are no positive charges trapped

at the inner bound electrode.

4.43 Vector addition of short-circuited currents due to trapped charges and due to electrodes of nonidentical thicknesses

To test the vector addition of C_D and $C_E(\frac{dT}{dx})$

in the thermogram of the specimen whose outer free electrode

is thicker, a current is generated using external sources

in place of $C_E(\frac{dT}{dx})$ in a sample whose inner bound electrode is thicker. For that, a field of 3×10^4 V/cm is applied on the outer thinner electrode to oppose the current due to the trapped charges. When the potential of the M-I-M structure is raised, an ohmic current $C_{\curvearrowleft}$ and a polarisation current C_p due to the motion of space charges and orientation of dipoles will be developed in the direction of the field [17,18]. For a system with a thinner outer free electrode, $C_E(\frac{dT}{dx})$ will be very small compared to C_D. Hence the total current C towards the direction of the field is given by $C = C_{\curvearrowleft} + C_p - C_D$. As the temperature increases, all the contributions to the observed current increases and at the temperature of 70°C, C_D dominates and the direction of the total current reverses as shown in the Fig.4.07. In the cooling cycle the polarisation current C_p will be zero because the specimen is poled with maximum amount of dipoles and space charges. Hence the total current will be $C = C_{\curvearrowleft} - C_D$. At about 65°C, $C_{\curvearrowleft}$ becomes relatively large and the direction of the current will be towards the field. Hence the low temperature peak in the cooling process is less by two orders than the one in the heating cycle which may be due to the absence of C_p. On comparing Fig. 4.07($\blacktriangle$) and Fig.4.07($\bullet$), it is clear that the current reversibility is due to the additional contribution of short-circuited current which is in the opposite

direction of C_D and in the case of Fig.4.07($\bullet$), it is

explained on the basis of a temperature gradient due to

the electrodes of dissimilar thicknesses and a trapped

charge accumulation at the vicinity of outer electrode.

In the cooling cycle of the specimen with thicker outer

free electrode, only C_D will be predominant at higher

temperatures while at the vicinity of room temperature

the current due to reversible polarisation will be

slightly higher. Hence Fig.4.07 ($\bullet$) shows a current

reversal at the vicinity of room temperature in the cooling

cycle. The decrement of short-circuited current by one to

two orders may be an indication of reversable polarisa-

tion which leads to a short-circuited current in the next

heating cycle.

When higher potential is applied to the specimen

whose outer free electrode is thinner, the thermogram

obtained (Fig.4.08) is different from what is observed

before. When the potential of outer thinner electrode

is raised to produce a field of 5×10^4 V/cm, the current C

will be towards the field (Fig.4.08, A-B). In this case

$C_{\Omega} + C_p$ is field dependent and hence very large. At

higher temperatures, thermally stimulated charges are

formed and move in the field resulting in a sharp increase

in current above 120°C. The current due to the space-charges

as well as reorientation of dipoles is given by Goro
Sawa et al [7] as

$$C_p = \frac{SV}{d} \beta \frac{d\varepsilon}{dT} \quad \text{where} \quad \beta = \frac{dT}{dt} \quad \text{and} \quad \frac{d\varepsilon}{dT} \quad \text{is the change}$$

in dielectric constant with temperature. For plasma
polymerised PAN the quantities in the above expression
are positive on heating while C_p becomes negative on
cooling. Thus on cooling, the direction of the total
current C reverses (Fig.4.08, B-C). On further cooling,
at about 75°C, the ohmic current C_Ω dominates showing
a current reversal as seen in Fig.4.08,(D). It is also
found that the point D shifts on changing the applied
field. When the applied field is of the order of 10^5V/cm,
the C_Ω and C_p are appreciably large and hence the
influence of C_D is unobserved. In such cases the current
reversal is not observed. At low fields the cyclic nature
of the current with temperature may be due to the to and
fro motion of space charges and the reorientation of
dipoles. Since this process is repeatable, it can be
assumed that the recombination rate of space charges is
very small.

4.44 Energy levels of trapped charges

The temperature activation energy is calculated
to be $\sim$ 1.4 eV from the expression $\log J = C - \frac{E}{kT}$ using

the low temperature tail of the short-circuited current [19] shown in Figs.4.03 and 4.04. It is in good agreement with the energy required to create charge carriers in a structure consisting principally of C-C bonds [20]. Hence it is clear that trap levels are situated at ~ 1.4 eV below conduction band. From the absorption spectra of PAN discussed in chapter III, it is found that the absorption band starts from the frequency close to the above energy level (1.7 eV). Hence it is clear that the absorption takes place at the trap centers. It is concluded that negative charges are trapped at the covalent bonds of the carbon atoms most probably in the termination process and released on heating.

4.50 ORIGIN OF SHORT-CIRCUITED CURRENT

The short-circuited current generated from plasma-polymerised unpoled Al-PAN-Al sandwich system may originate from the accumulation of negative trapped charges in the vicinity of the outer electrode and the preferential orientation of dipoles due to the rotation of -CN side groups towards the outer electrode. The electrons are trapped at the tail ends of the polymer chain and they form a negatively charged molecule of charge $e^{(--)}$. From the behaviour of the current, it is inferred that the degree

of polymerisation will be maximum near the inner electrode and minimum near the outer. Hence the electrons may trap at different levels in the process of plasma polymerisation with a maximum of trapped charges at the outer electrode producing a gradient towards the inner. The space charge gradient might have been due to the decrease in the pressure in the vacuum chamber in the process of polymerisation. From the study of the additional current produced due to nonuniform heating as well as the surface strain of the specimen, it is inferred that no positive charges are trapped at the vicinity of inner electrode. Since the activation energy is $\sim$ 1.4 eV, it is concluded that the charges are formed from the covalent bond of the carbon atoms and this supports the formation of electrons from the tail ends of the molecules. These types of sandwich systems can store a large amount of negative charges and can be used as electrets and thermal current sources.

REFERENCES

[1] R.J.Comstock, S.I.Stupp and S.H.Carr, J. Macromol. Sci. Phys., B13, 101 (1977).

[2] R.G.Kepler and R.A.Anderson, J. Appl. Phys. 49, 4490 (1978).

[3] D.K.Das Gupta and J.S.Duffy, J. Appl. Phys., 50, 561 (1979).

[4] S.I.Stupp and S.H.Carr, J. Appl. Phys., 46, 4120 (1975).

[5] Goro Sawa, Shuhei Nakamura, Yoji Nishio and Masayuki Ieda, Japan J. Appl. Phys., 17, 1507 (1978).

[6] Goro Sawa, Duck Chool Lee and Masayuki Ieda, Japan J. Appl. Phys., 15, 1983 (1976).

[7] Goro Sawa, Duck Chool Lee and Masayuki Ieda, Japan J. Appl. Phys., 16, 359 (1977).

[8] H.Burkard and G.Pfister, J. Appl. Phys., 46, 3360 (1974).

[9] R.G.Kepler and R.A.Anderson, J. Appl. Phys., 49, 1232 (1978).

[10] R.G.Kepler, Ann. Rev. Phys. Chem., 29, 497 (1978).

[11] Noriyoshi Chubachi and Toshio Sannomiya, Japan J. Appl. Phys., 16, 2259 (1977).

[12] A.M.Glass and J.H.Mc Fee, J. Appl. Phys., 42, 5219 (1971).

[13] S.I.Stupp and S.H.Carr, Studies in Electrical and Electronic Engineering-2, Charge Storage, Charge Transport and Electrostatics with their Applications, Y.Wada, M.M.Perlman and H.Kokado (Ed.), Elsevier, p.123.

[14] R.J.Shuford, A.F. Wilde, J.J.Ricca and G.R.Thomas, Polymer Eng. Sci., 16, 25 (1976).

[15] Shinichi Takeda, J. Appl. Phys., 47, 5480 (1976).

[16] P.H.Murphy and F.E.Hoecker, J. Appl. Phys., 42, 4094 (1971).

[17] Shireesh D.Phadke, Thin Solid Films, 55, 391 (1978).

[18] Shireesh D.Phadke, K.Sathianandan and R.N.Karekar, Thin Solid Films, 51, L-9 (1978).

[19] M.M.Perman and S.Unger, J. Appl. Phys., 45, 2389 (1974).

[20] Arthur Bradley and John P. Hames, J. Elect. Chem. Soc., 110, 15 (1963).

CHAPTER V

THERMALLY STIMULATED DEPOLARISATION CURRENT IN POLED PLASMA-POLYMERISED POLYACRYLONITRILE

ABSTRACT

Results on the depolarisation and thermally stimulated short-circuited currents obtained from plasma-polymerised polyacrylonitrile are presented in detail by varying the magnitude and direction of the polarisation field. A low temperature thermally stimulated current peak is observed and analysed on the basis of a uniform polarisation associated with the orientation of the dipoles, migration of charges and injection of electrons from the electrode to polymer. The depolarisation kinetic parameters are calculated by initial rise method. It is observed that there is no permanent polarisation below a field of 6.2×10^4 V/cm and at high field polarisation, some local structure is developed which limits the depolarisation current.

5.10 INTRODUCTION

Thermally stimulated depolarisation (TSD) current analyses give detailed information on the mechanism of charge storage in electrets. In poled polymer electrets, usually two peaks are observed, one below (β-transition) and the other above (α-transition) the glass transition temperature [1-3]. The α-transition is due to relaxation of trapped charges while β-transition is associated with movement of side groups around the equilibrium position where large scale confirmational rearrangement on the main chain is frozen. In poled polyacrylonitrile (PAN), two peaks, one at 90°C and the other at 180°C, are reported for normal polarising voltages [1,4]. At higher polarising voltages the peak at 90°C is suppressed and additional peak appears at 150°C to 160°C [1]. The glass transition temperature, though not well defined for PAN, is proposed to be at 140°C [1]. A spurious emission of short-circuited current due to chemical degradation on heating has also been reported for PAN by Stupp and Carr [5]. Large thermally stimulated currents due to compositional inhomogeneity have been observed in PAN and discussed in the previous chapter. The high dipole moment and large thermally stimulated currents of PAN enhance its suitability as an electret. The studies reported so far on PAN are made using chemically processed material. Considering

the increased industrial applications of polar electrets in recent years, a detailed study on the charge storage mechanism of poled PAN formed by plasma-polymerisation is considered to be important and has been undertaken.

5.20 EXPERIMENTAL PROCEDURE

All the measurements are made on plasma-polymerised PAN thin films sandwiched by aluminium electrodes. The polymerisation of acrylonitrile (BDH, Laboratory reagent) is carried out in a glow-discharge chamber. Weighed amount of aluminium is pre- and post-evaporated for the purpose of electrical contacts. The details of preparation of Al-PAN-Al sandwich specimens are discussed in the section 2.24. The sandwich structures thus prepared for short-circuited current measurements are schematically shown in Fig.2.09(a and b). For the present investigations, importance is given to the TSD current of poled PAN and hence identical aluminium electrodes of thickness 1500Å is prepared for all specimens. For the thickness measurement of the polymer films, identical films are prepared at the same time on separate substrates and the thickness is measured by Fizeau fringes.

5.21 Thermally stimulated depolarisation current measurements

Al-PAN-Al specimens thus prepared are transferred to the conductivity chamber and evacuated to 10^{-3} torr. Using copper pressure contacts, connection leads are taken out. As shown in Fig.5.01, the leads are short-circuited through an electrometer amplifier (ECIL, EA-815). The electrometer is normally connected to inner bound electrode while the other end of the electrometer is always earthed. The outer free electrode is connected to a switch (single pole double throw) such that in case (i) the electrode is directly earthed and in case (ii) it is connected to the negative voltage with the positive being earthed. Before making thermally stimulated current measurements, the short-circuited specimens are heated to $160^{\circ}C$ at a rate of $1^{\circ}C/min$. The samples are maintained at that temperature for one hour and then cooled to room temperature at the same rate. This heating and cooling process is done in order to remove the condensed monomer and trapped charges. This is repeated for three or four times until a steady negative current is observed in the electrometer when connected to the inner bound electrode. The short-circuited current of the unpoled specimen is already discussed in the previous chapter. From those studies it is inferred that when the outer free electrode is thicker, an additional contribution of
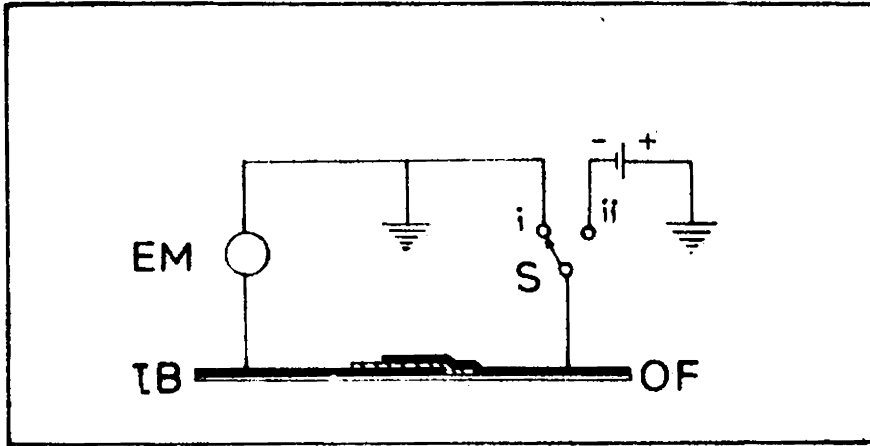
Fi .5.01.
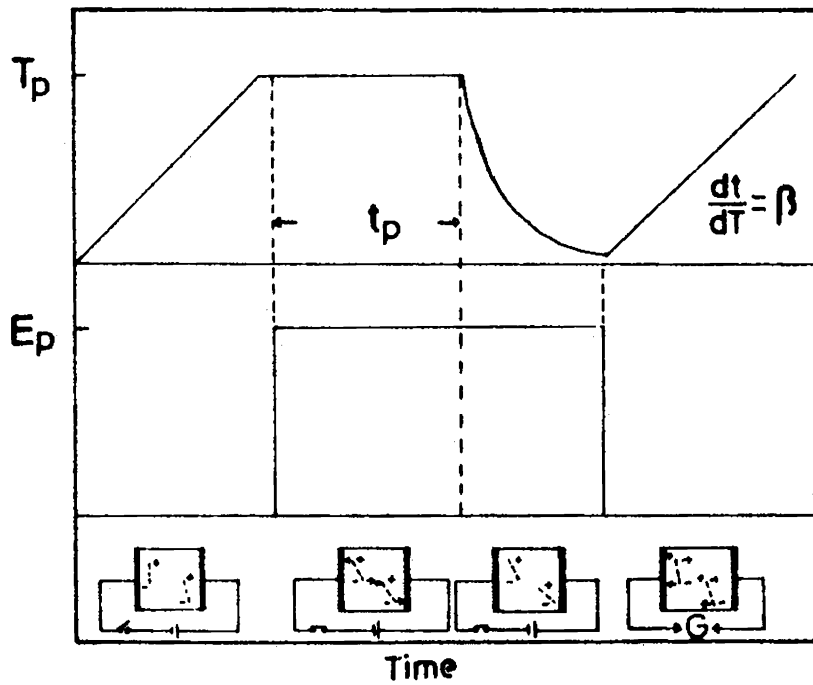
Fig.5.06.

Fig.5.01. The electrical connections for polarisation and
short-circuited current measurements: IB - inner
bound electrode, OF - outer free electrode,
EM - electrometer amplifier and S - single pole
double throw switch with (i) electrode is directly
earthed and (ii) the electrode is connected to the
voltage source.

Fig.5.02. Schematic representation of poling process.

short-circuited current is to be included. Hence to make
the investigation easier, in the present investigations,
both electrodes are prepared with the same thickness so
that the contribution due to dissimilar electrode is
eliminated.

5.22 Experimental method for poling the specimen

As discussed in the introduction, during the
process of poling, the dipoles in the material attain a
preferred orientation and the charges migrate to one side
depending upon the poling voltage V_p. For this purpose,
the specimen is heated to a higher temperature T_p, above
the transition temperature and the poling voltage V_p is
applied across the specimen. The relaxation time of dipoles
are quite small at T_p and they turn towards the applied
voltage. The charges also accumulate to one direction
depending upon the sign of the charges. To assure a complete
poling with voltage V_p, the specimen is maintained for one
hour at T_p, and then cooled to room temperature at the rate
of $1^{\circ}C/min$. When the specimen is cooled to room temperature,
it is short-circuited through the electrometer amplifier.
The connections used for the poling process and for the
short-circuited studies are shown in Fig.5.01. In Fig.5.02,
the variation of temperature with time and the application

of field in the poling process are diagramatically represented. The scheme of the dipolar motion in the sample corresponding to the physical situation is also shown.

5.23 Parameters controlling the depolarisation current

From the initial experiments, it is observed that the depolarisation current mainly depends on the direction and magnitude of the poling voltage. For example, when the poling voltage is applied to the specimen with the positive terminal connected to the outer free electrode and after poling, the depolarisation current is measured with electrometer connected to the inner bound electrode, no well resolved depolarisation characteristics are observed. On the contrary, when the voltage source is connected to the specimen with positive bias given to inner bound electrode and electrometer connected to the same electrode, in the depolarisation current measurements, a well resolved peak is observed. It is also found that depending on the direction of the poling field, the magnitude of the depolarisation peak changes. It is strange to note that a minimum field is necessary for the occurrence of polarisation in the Al-PAN-Al specimen. Hence, a detailed study of the TSD current as a function of the poling voltage is reported here.

For poling the specimen, there are certain experimental limitations. The specimens are permanently destroyed for a temperature above 135°C on poling even with 10 volts. Hence T_p is chosen as 135°C for all polarisation voltages ($V_p < 10$ volts). To study the effect of T_p, a second temperature of 85°C is chosen as an intermediate temperature. In certain cases, depolarisation current is analysed by reversing the direction of the poling field.

5.30 THEORY OF THERMALLY STIMULATED DEPOLARISATION CURRENT

Due to thermally stimulated depolarisation process, the dipoles that are aligned by the poling field will disorient randomly at a rate proportional to the number of dipoles aligned. The depolarisation will therefore decay according to the Debye rate equation

$$\frac{dP(t)}{dt} = -\alpha(T)P(t) \tag{5.01}$$

where $\alpha(T)$ is the relaxation frequency at a temperature T. As the polarisation P is a function of both temperature and time, the current density J(T) and total polarisation P_o can be related [6] by the equation

$$P_o = \frac{1}{\beta} \int_{T_o}^{T_B} J(T)dT \tag{5.02}$$

where β is the rate of heating $\frac{dT}{dt}$ and T_B is the temperature at which $J(T_B) = 0$. T_o is the temperature at which the depolarisation starts. From the above equation, a convenient expression [6-9] for TSD current density can be written as

$$J(T) = P_o \; \alpha(T) \exp(- \tfrac{1}{\beta} \int_{T_o}^{T} \alpha(T) dT) \qquad (5.03)$$

As the glass transition temperature T_g for PAN is proposed to be around $140^{\circ}C$ [1], for temperature below this, the relaxation frequency $\alpha(T)$ can be represented by Arrhenius relaxation function [8].

$$\alpha(T) = \alpha_o \; e^{-A/kT} \qquad (5.04)$$

where A is the activation energy, k is the Boltzmann constant and α_o is the relaxation frequency at absolute zero. Hence for the maximum current $J(T_{max})$

$$\frac{dJ(T_{max})}{dT} = 0$$

Equating the differential of eqn.(5.03) to zero we have

$$\frac{dJ(T)}{dT} = P_o \alpha_o \frac{d}{dT}[\exp(- \tfrac{A}{kT} - \tfrac{1}{\beta} \int_{T_o}^{T} \alpha_o e^{-A/kT} dT)] = 0$$

$$(5.05)$$

Hence

$$\frac{A}{k(T_{max})^2} = \frac{1}{\beta} \alpha_0 exp[\frac{-A}{k(T_{max})}]$$ (5.06)

Then $\alpha(T_{max}) = \frac{\beta A}{k(T_{max})^2}$ (5.07)

where T_{max} is the temperature at which J(T) is amaximum.

At low temperature $\frac{1}{\beta} \int_{T_0}^{T} \alpha(T)dT$ being small, the exponential

can be considered as unity [6]. Differentiating eqn.(5.04) with respect to 1/T, one obtains

$$\frac{d}{d(1/T)}[ln\ J(T)] = \frac{-A}{k}$$ (5.08)

from which the activation energy can be calculated.

In order to obtain the information regarding the mechanism of polarisation in PAN, the orientational aspects of dipoles are to be considered. In PAN, the contribution to the dipole moment is mainly due to the nitrile side group and if one considers the nitrile side group as immersed in a nonpolar medium, the equilibrium polarisation at the

polarising temperature T_p is given by Langevin equation [9,10]

$$P_o = \frac{N p^2 E_p'}{3kT_p}$$ (5.09)

where N is the number of dipoles per unit volume, p is the dipole moment and E_p' is the effective field across the specimen. But when the influence of the local field is also considered, an expression for P_o in a polarisable medium can be written as [11]

$$P_o = \frac{NgE_p'}{(1 - \frac{\gamma\alpha}{a^3})}[\alpha + \frac{1}{(1 - \frac{\gamma\alpha}{a^3})} \cdot \frac{p^2}{3kT_p}]$$ (5.10)

where $g = \dfrac{3\varepsilon_o}{2\varepsilon_o + 1}$, $\gamma = \dfrac{2\varepsilon_o - 1}{(2\varepsilon_o + 1)\varepsilon}$ and $\dfrac{\alpha}{\varepsilon a^3} = \dfrac{n^2 - 1}{n^2 + 1} = \dfrac{4\pi N\alpha}{3\varepsilon}$

ε_o is the dielectric constant of the material, ε the permittivity of free space and α the polarisability. In the case of PAN, since the polarisation is due to the orientational motion by rotation of nitrile side group and because the atomic polarisability α can be taken to the zero in the system, the total polarisation is given by a more simple equation

$$P_o = \frac{Np^2}{3kT_p}(\frac{3\varepsilon_o}{2\varepsilon_o + 1})E_p'$$ (5.11)

Thus, if one knows the dipole moment of the material, the total polarisation P_O can be determined from eqn.(5.11). The total polarisation can also be calculated from eqn.(5.02). In the present work, the theoretically predicted and experimentally observed values for polarisation are compared. Thus the possible mechanism for the charge storage in M-I-M structures can be explained with the additional help of other related studies.

5.40 RESULTS

5.41 Depolarisation currents in poled and unpoled Al-PAN-Al

Fig.5.03 shows the plots of logarithmic short-circuited current vs. temperature for unpoled and poled Al-PAN-Al specimen (thickness of PAN = 3350$\overset{o}{A}$) with the electrometer connected to inner bound electrode. A short-circuited current is always found in unpoled PAN as shown in Fig.5.03(●). This temperature dependent short-circuited current is inherent in the material and it is designated as a spontaneous short-circuited current (I_{sp}).

When the specimen is poled with a negative inner electrode and positive outer electrode, no well resolved depolarisation peaks are observed in the short-circuited
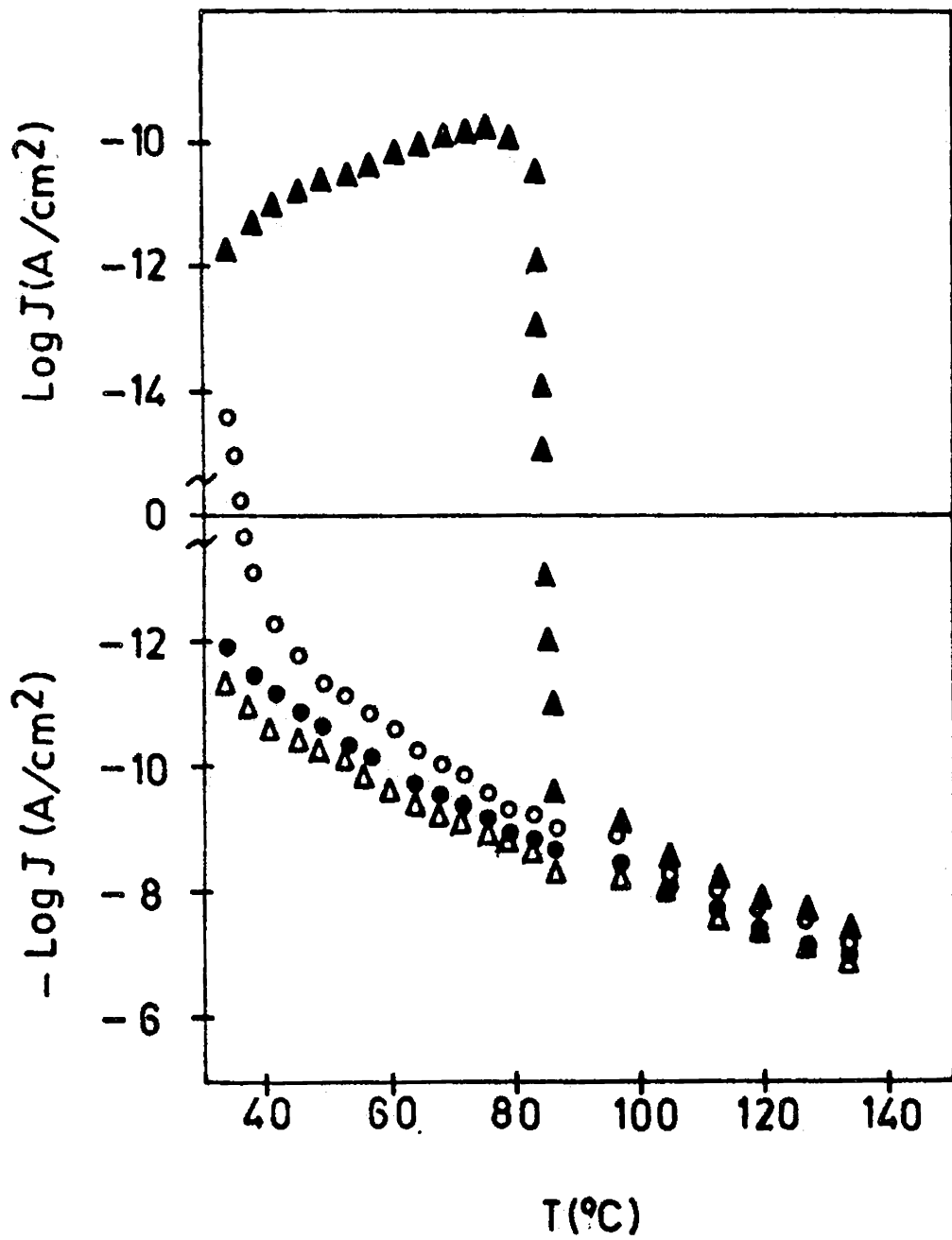
Fig.5.03. Thermally stimulated logarithmic current vs. temperature for Al-PAN-Al films (thickness of PAN = 3350Å), polarised at 135°C, are shown. ● is the curve for unpoled specimen and ▲ and ○ are for films polarised by 10V and 2V respectively with the inner electrode positive. △ is the curve for the specimen polarised by 10V with the outer electrode positive.

current as shown in Fig.5.03($\triangle$) (V_p = 10V and T_p = 135°C).
In this case the spontaneous current (I_{sp}) and depolarisation
current (I_{dp}) are in the same direction. On reversing the
poling voltage, ie., when the specimen is poled with
positive inner electrode and negative outer electrode, a
well resolved peak is observed in the short-circuited
current (Fig.5.03,$\blacktriangle$) (V_p = 10V and T_p = 135°C). Since
this current peak is a field induced one, the main contri-
bution to this peak can only be from the depolarisation
current. It is also found that when the poling voltage
V_p is reduced, the height of the depolarisation peak is
also decreased and finally at a poling voltage of 2V, the
depolarisation current peak completely disappears. In
Fig.5.03(O) the depolarisation current is shown when the
poling voltage V_p is 2V and T_p is 135°C. Below this
voltage, there is no indication of the existence of the
depolarisation current.

5.42   Variation of depolarisation current peaks with
        polarisation voltages

The depolarisation current is analysed by plotting
the discharge current as a function of temperature for
different polarising voltages. Fig.5.04(a,b and c) shows
the depolarisation current spectra for a polarising
temperature T_p = 135°C and polarising voltages V_p = 5V,
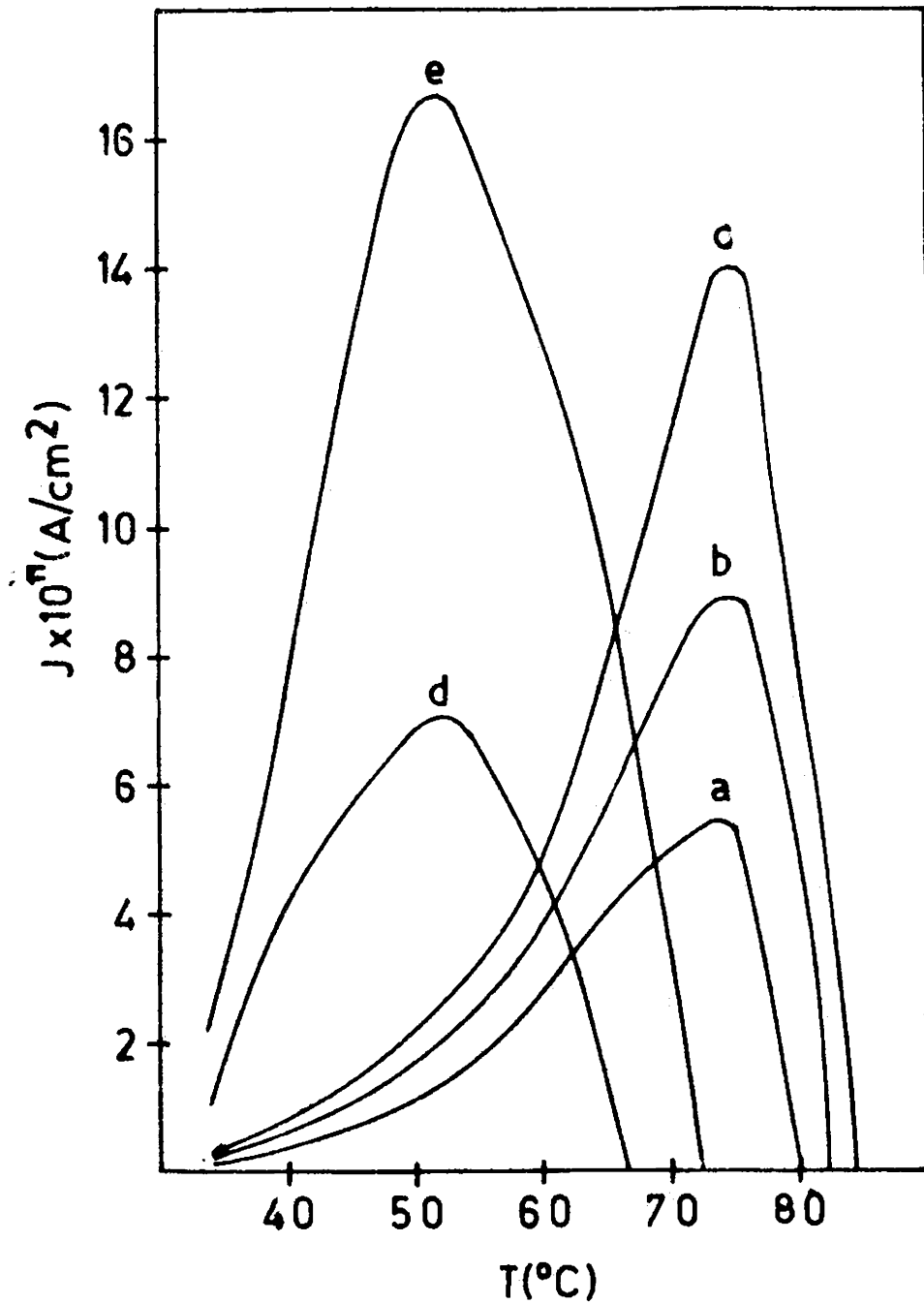
Fig.5.04   Thermally stimulated current vs. temperature
for Al-PAN-Al (thickness of PAN = 3350Å)
polarised by 5V, 7V and 10V applied with the
inner electrode positive are shown as a, b
and c respectively for a polarising tempera-
ture of 135°C. The TSC is shown as d and e
for a polarising temperature of 85°C when
specimen is polarised by 7V with the inner
electrode and the outer electrode respectively
positive.

7V and 10V respectively. The current maximum, J_{max}, is observed at 75°C for all the three curves. The J_{max} of each peak is $5.4 \times 10^{-11} A/cm^2$, $8.8 \times 10^{-11} A/cm^2$ and $1.4 \times 10^{-10} A/cm^2$ respectively.

5.43 Shift in the current peak with poling temperature

It is found that when the poling temperature T_p is decreased, the depolarisation current peak is shifted to lower temperature. It is also found (Fig.5.04,b) that the depolarisation current peak is observed at 75°C, when the poling temperature T_p is 135°C. But when T_p is decreased to 85°C, the TSD peak is shifted to 52°C. Fig.5.04(d) shows such a shift in depolarisation current. It can also be observed that J_{max} is reduced to $6.8 \times 10^{-11} A/cm^2$.

5.44 Variation in current maximum with the direction of poling

Under the same conditions of poling temperature T_p, when the poling voltage is reversed, (ie., when the specimen is poled with positive inner bound electrode and negative outer free electrode and also with the electrometer connected to positive electrode) a well resolved peak is clearly observed. The magnitude of J_{max} is appreciably increased while T_{max} will be still at 52°C. The TSD peaks

in Fig.5.04(d and e) show the increase in the magnitude of J_{max} when the poling voltage is reversed. The J_{max} is found to be $6.8 \times 10^{-11} A/cm^2$ for the peak in Fig.5.04(d) and increases to $1.65 \times 10^{-10} A/cm^2$ for the other peak in Fig.5.04(e).

5.50 MECHANISM OF DEPOLARISATION CURRENT

It has already been reported that the thermally stimulated short-circuited current generated from unpoled PAN is due to chemical degradation [5] and compositional inhomogeneity which has been already discussed in the previous chapter. However, for the poled specimen, the total depolarisation current will be the vector sum of the spontaneous current (I_{sp}) and depolarisation current (I_{dp}). When the specimen is poled with the negative inner electrode and positive outer electrode, no well resolved peak is observed for short-circuited current and may be due to the fact that the (I_{sp}) and (I_{dp}) are in the same direction. But when the V_p is reversed but with the electrometer connected to the inner electrode, a well resolved peak is observed in the depolarisation current. Since the short-circuited current peak is a field induced one, the main contribution to the peak can only be from the depolarisation current (I_{dp}). From Fig.5.03 ($\triangle$ and $\blacktriangle$), it can also be inferred that (I_{sp}) and (I_{dp}) are of the same order of magnitude but with (I_{dp})

larger than (I_{sp}) during the initial stages of heating.
Hence, parametric variations in the poling process should
show characteristic variation of the depolarisation peak
in the Fig.5.03($\blacktriangle$) and this in turn can offer new inform-
ation regarding the poling mechanism. The disappearance of
TSD peak below the $V_p = 2V$ may be due to two reasons
(i) the existence of an internal built in field within the
specimen which opposes the applied field and (ii) the
magnitude of (I_{dp}) is less than the (I_{sp}) at all temperatures
resulting in a current in the direction of (I_{sp}). Stupp
and Carr [5] have already reported that thermally generated
charges will be formed in PAN due to chemical degradation
of the material. On poling the sandwich structure, the
charges will migrate over a microscopic distance. Also
the accumulated charges will develop an internal built-in
field within the specimen which in turn restricts the
orientation of dipoles. Hence there should be a threshold
field below which the polarisation due to the orientation
of dipoles is not observed. Also for higher fields, the
magnitude of the orientation is lesser than what is expected
theoretically. In the case of depolarisation, the dipoles
and the migrated charges will normally retrace to their
original position. But some amount will be discharged in
the direction of (I_{sp}). It may also reduce the effect of
depolarisation current due to dipoles when the poling

voltage is below the threshold voltage. In such cases, the magnitude of (I_{sp}) is higher than the magnitude of (I_{dp}) at any temperature. Among the two mechanisms, it is very difficult to identify which is predominant. But it is hoped that from the analysis of depolarisation current, certain information about the mechanism of charge storage can be obtained.

5.51 Depolarisation current analysis

The TSD peaks can be analysed by calculating the total polarisation P_o, the relaxation frequency at T_{max} ie., $\alpha(T_{max})$ and the activation energy A. As the depolarisation current satisfies the equation (5.03), the activation energy can be calculated by the initial rise method. In Fig.5.05, the logarithmic current of the initial portion of the peak is plotted against the reciprocal of the temperature in absolute unit for all the peaks and found to be a straight line. From the slope of the straight lines and using eqn.(5.08) the activation energy is calculated. From the activation energy, the relaxation frequency $\dot{\alpha}(T_{max})$ can be calculated with the knowledge of other parameters in eqn.(5.07). The area bound by each peak is calculated from graphical measurements and by using proper unit conversions, $\int_{T_o}^{T_B} J(T)dT$ can be obtained. The total
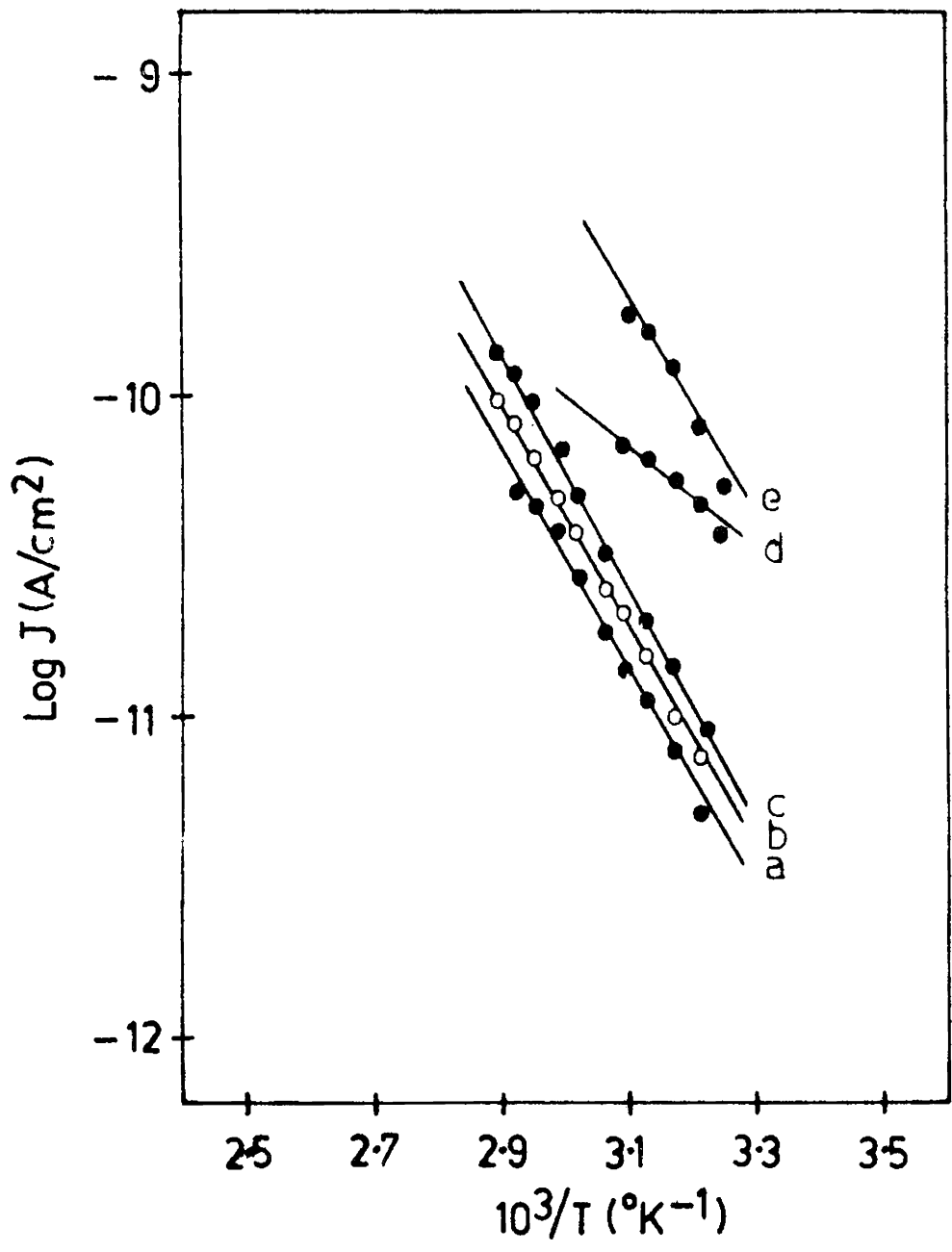
Fig.5.05. Plots of log J vs. 1/T obtained from the
initial rise of TSD curve, a, b, c, d and
e of the Fig.5.04.

polarisation P_o is straightaway calculated from eqn.(5.03).
The depolarisation kinetic data, namely the calculated
values of activation energy A, the relaxation time
$\tau_{max} = \frac{1}{\alpha(T_{max})}$ and total polarisation P_o for all the
curves Fig.5.04(a,b,c,d and e) are presented in Table 5.01.
From the table, the general nature of the peak can be
understood.

5.52 The variation of J_{max} and P_o with E_p

When J_{max} and P_o are plotted against V_p for the
curves in Fig.5.04 (a,b and c), it is found that the
variation is linear (Fig.5.06, I and II). The linearity
of J_{max} and P_o with V_p (or E_p) satisfy the eqn.(5.03 and
5.11). This suggests that the polarisation is uniform and
is due to the dipolar orientation or migration of charges
over microscopic distances [9]. A TSD peak observed in
PAN [1,4] at $90^{\circ}C$ (T = $130^{\circ}C$) has been interpreted as the
β-transition and is due to the relaxation of the nitrile
side group. The peak at $75^{\circ}C$ has an average calculated
activation energy of 0.81 eV. Usually TSD peaks formed
due to the reorientation of dipoles in high molecular
weight polymers have an activation energy of the order
of 0.4 eV [12]. A high value of activation energy of
0.81 eV shows that the TSD peak is not only due to the
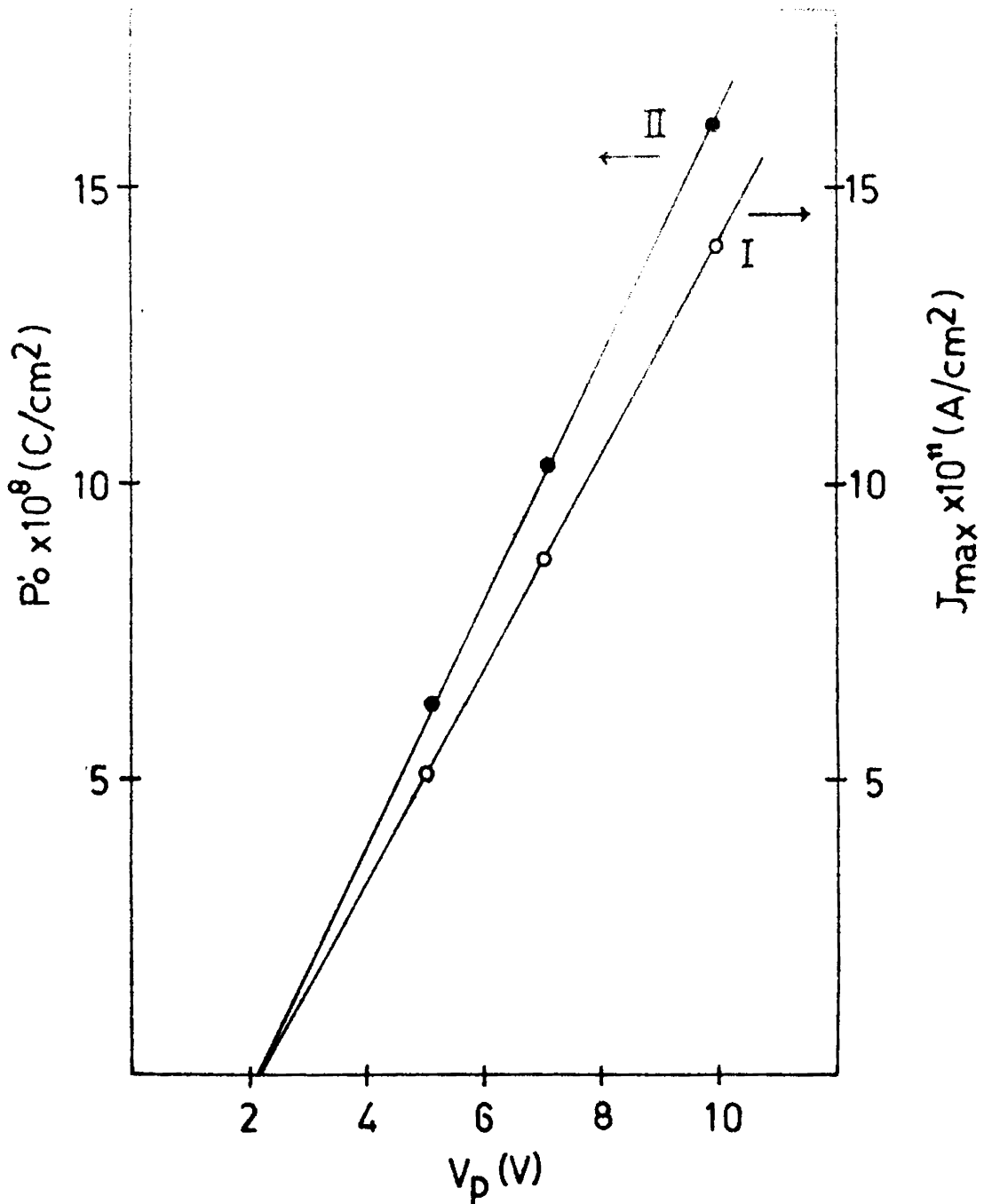
Fig.5.06. I - The variation of J_{max} and II - the variation of polarisation P_o vs. The applied polarising voltage with the inner electrode positive are shown for Al-PAN-Al (T_p = 135°C, thickness = 3350Å).

Table 5.01 Depolarisation kinetics data calculated for TSD peak of PAN films of thickness 3350Å.

Curve	T_p (°K)	$E_p \times 10^{-5}$ (V cm^{-1})	$E_p' \times 10^{-5}$* (V cm^{-1})	$J_{max} \times 10^{11}$ (A cm^{-2})	T_{max} (°K)	A (eV)	$\tau_{max} \times 10^{-2}$	P_o (μC cm^{-2})
a	408	1.50	0.88	5.4	348	0.79	7.92	0.063
b	408	2.09	1.47	8.8	348	0.84	7.46	0.103
c	408	3.00	2.38	14.0	348	0.81	7.73	0.160
d	358	2.09	1.47	6.8	325	0.48	11.50	0.087
e	358	2.09	2.71	16.5	325	0.71	7.70	0.230

* $E_p' = E_p + 0.62 \times 10^5$

reorientation of aligned dipoles but also due to some other
mechanism. But since the maximum current corresponding to the
peak and the charge associated with it increase linearly with
E_p, it can be inferred that the additional contribution may
be associated with the migration of charges through a micro-
scopic distance. In PAN, the dipoles are due to -CN side
group and the charges are formed due to thermal degradation
and these two together develop a depolarisation current
peak in Al-PAN-Al structures.

It is interesting to note that in Fig.5.06, (I and
II) J_{max} as well as P_o coincide on the Y-axis when the poling
voltage is ∿ 2.1V. The absence of a well resolved peak
in Fig.5.01, which is already discussed earlier, supports
the above observation. These two observations indicate that
a threshold voltage is necessary to pole the Al-PAN-Al
specimen. Thus the existence of an internal built-in field
and an additional contribution to (I_{sp}) create a reduction
in the depolarisation current. Hence the effective pola-
risation field can be taken as $E'_p = E_p \pm 6.2 \times 10^4$ V/cm
where 6.2×10^4 V/cm is the virtual drop in the poling field.

5.53 Effect of T_p on the discharge current

On comparing the TSD peaks Fig.5.04(b and d) it
is found that T_{max} is shifted to a lower temperature when
T_p is reduced from 135°C to 85°C. Such a shift in TSD peak

has been reported earlier [3]. As the T_p is lowered, the activation energy is also reduced to 0.48 eV. This indicates that the dipolar orientation and charge migration still occur even with reduced polarisation temperature. Hence, there exists dipoles or charges having relaxation frequencies which will fit with T_p and t_p and they can actively take part in the process of polarisation. As reported earlier [2] depending on the order of polymerisation, the relaxation time of the dipoles will vary widely. In the present case, since T_{max} is shifted with T_p, it can be concluded that in plasma-polymerised PAN, the order of polymerisation is widely distributed. In PAN, when the order of polymerisation is increased, the size of the molecule is also increased. Hence, in the poling process, the energy required for dipole alignment will be normally increased. When the order of polymerisation is low, the dipoles will reach a stable position with applied voltage even at lower temperatures. The reduction of T_{max} when T_p is reduced, indicates the occurrence of dipoles of lower relaxation time. The thermally generated charges formed in the system is generally of widely distributed relaxation time. Hence it can be inferred that the dipoles in the polymer as well as the thermally generated charges are of widely distributed relaxation time. If dipoles are of distributed relaxation time, the order of polymerisation in PAN is also widely distributed.

5.54   Effect of poling direction on polarisation

It is found that the total polarisation associated with the specimen poled at $85^{\circ}C$ is 0.087 μC cm^{-2}. But the total polarisation P_o of the peak (Fig.5.04,c) is calculated to be 0.228 μC cm^{-2}. This means that when the direction of poling field is reversed, the charge stored in the polymer is increased appreciably. This indicates that along with the orientation of dipoles, the injection of homo-charges through contact electrodes also contribute to the total polarisation. The amount of injected homo-charges are heavily controlled by the work-function of inner and outer surfaces of the polymer. When the work-function is different, the contact potential barrier will be different. Hence when the direction of the poling field is reversed, the contribution of the injected charges will vary which will in effect change the total polarisation.

It has been already discussed that in plasma-polymerised PAN, the order of polymerisation is different due to compositional inhomogeneity. In that case, the order of polymerisation is maximum at the vicinity of inner bound electrode. If the electrons are trapped at the tail ends of the polymer molecule, the density of electrons will be maximum at the vicinity of outer bound electrode. On poling with a negative outer free electrode,

further negative charges may not be injected from that electrode. The injection of positive charges at the inner bound electrode may be negligibly small. In such a case, the orientation of dipoles along the direction of the field and the microscopic displacement of the charges may form a major contribution to the total polarisation P_O. Hence this will give a TSD peak Fig.5.04(d). On reversing the poling field, the negative charges may be injected through the inner bound electrode. In this case also, the possibility of injection of the positive charges will be feeble. The positive charges if injected at the outer electrode will be neutralised by the trapped charges. The possibility of positive charge injection cannot be completely ruled out. The observed characteristics can be explained by the above described model.

Thus the additional contribution of the injected charges may promote the resulting polarisation when the specimen is poled with the positive outer free electrode. The model with the trapped charges and hence a difference in contact potential at the two surfaces explains the observed increase in polarisation on reversing the poling field. The trapped charges may also develop an internal field in the specimen which is one of the supporting reasons for the observation in Fig.5.03,( ) and 5.06.

5.55 Origin of polarisation

From the linear variation of J_{max} and P_o with

poling voltage (Fig.5.06), it is clear that upto a poling

field of 2.38×10^5 V cm^{-1} (the maximum poling field applied

in the present investigation), the polarisation is uniform.

As reported by Pillai [9] uniform polarisation is due to

dipolar orientation and/or charge migration over microscopic

distances. If it is assumed that the polarisation is due

to dipoles only, the upper bound to polarisation arising

from the preferentially oriented nitrile side group in

PAN [10] is $14.8 \mu C$ cm^{-2}. Assuming the density of plasma-

polymerised PAN to be 1.18 gm cm^{-3}, the number of monomer

units per unit volume is calculated to be $1.34 \times 10^{22} cm^{-3}$.

The acrylonitrile molecule contains only one -CN side group

and this side group is responsible for the dipole moment

in the polymer. Hence the number of dipoles contained in

unit volume of the material is also $1.34 \times 10^{22} cm^{-3}$. From the

upper bound to polarisation, the dipole moment is calculated

as $1.1 \times 10^{-27} C$ cm (3.4D). From the peaks in Fig.5.04(a,b and c),

if the corresponding values of E_p' and T_p are substituted in

eqn.5.11, one may expect a total polarisation of $0.125 \mu C$ cm^{-2},

$0.208 \mu C$ cm^{-2} and $0.337 \mu C$ cm^{-2} respectively ($\varepsilon_o = 1 + \chi = 33$

where χ is taken as 32 for PAN [4] at $130^\circ C$). But the

total polarisation P_o calculated experimentally (Table 5.01)
is lower than the theoretically predicted value. This
suggests that the nitrile side-groups have only a slight
preferred orientation in the direction of polarisation.
The use of birefringence [4] and infrared dichroism studies
[13] have confirmed this low level of nitrile side group
orientation. It is well established that the amount of
dipolar orientation developed is relatively small and
therefore contributes a very small (less than 1%) portion
to the total electrical polarisation [10]. Testing of the
theoretical prediction in PAN reveals that some local
structure must be developed by the polarised state. For
strongly polarised specimens, the original structure will
be regained only at very high temperatures [10]. Hence in
the TSD studies of PAN, only a part of the polarisation is
released at normal ranges of temperature. This causes a
reduction of depolarisation current contributed by dipoles
when compared with the theoretically predicted values.
Also, since the thermally stimulated spontaneous current
(I_{sp}) opposes the depolarisation current the peaks are
suppressed uniformly and hence the characteristic nature
of uniform depolarisation is shown. Due to these reasons,
it is concluded that the depolarisation current originates
from the dipole orientation and displacement of charges
through microscopic distances. But it is also concluded

that the injected charges can also contribute additionally
to the total polarisation if the interface potential barrier
permits the charges to pass through.

5.60 DEPOLARISATION CURRENT IN PAN

In plasma-polymerised Al-PAN-Al, a low temperature
current peak is observed on poling the specimen whereas such
a peak is absent for the unpoled specimen. The linear
increase in P_o and J_{max} with V_p shows that the polarisation
is uniform upto a field of 2.38×10^5 V cm^{-1} and this linearity
is in agreement with the theory. It is concluded that the
origin of polarisation is mainly due to the orientation of
the dipoles associated with -CN side group and migration of
charges through microscopic distances. An additional
contribution due to the injection of charges may occur.
From a comparison of the experimentally calculated total
polarisation with that of the theoretically predicted, it
is concluded that some local structure must be developed
by the polarised state when high field polarisation occurred.
It is revealed that the electrons are trapped at the vicinity
of the outer electrode due to compositional inhomogeneity
resulting in a field of $\sim 6.2 \times 10^4$ V/cm across the specimen.
The polarisation current characteristics below this field
has been discussed in the previous chapter and it is clear

that polarisation current on heating and cooling flow in different directions. Hence there is no permanent polarisation at low fields ($<6.2 \times 10^4$ V/cm). The activation energy, relaxation time at peak temperatures and total polarisation are calculated and presented.

REFERENCES

[1] S.I.Stupp and S.H.Carr, J. Appl. Phys., 46, 4120 (1975).

[2] P.C.Mahendru, K.Jain and N.Kumar, Thin Solid Films, 70, 7 (1980).

[3] S.K.Shrivastava, J.D.Ranade and A.P.Shrivastava, Thin Solid Films, 67, 201 (1980).

[4] R.J.Comstock, S.I.Stupp and S.H.Carr, J. Macromol. Sci. Phys., B 13(1), 101 (1977).

[5] S.I.Stupp and S.H.Carr, J. Polym. Sci. Polym. Phys., 15, 485 (1977).

[6] J.Van Turnhout, Electrets, Topics in Applied Physics, G.M.Sessler (Ed.), Springer-Verlag, New York, V.33, 106-126 (1980).

[7] Cesare Bucci and Roberts Fiechi, Phys. Rev., 148, 816 (1966).

[8] G.Pfister and M.A.Abkowitz, J. Appl. Phys., 45, 1001 (1974).

[9] P.K.C.Pillai and M.Mollah, J. Macromol. Sci. Phys., B 17(1), 69 (1980).

[10] S.I.Stupp and S.H.Carr, Studies in Electrical and Electronic Engineering-2, Elsevier, 123-127.

[11] N.E.Hill, Dielectric and Molecular Behaviour, Van Nostrand Reinhold, London, 18-23 (1969).

[12] Y.Takahashi, J. Phys. Soc. Jpn., 16, 1024 (1961).

[13] S.I.Stupp and S.H.Carr, J. Polym. Sci., Polym. Phys., 16, 13 (1978).

CHAPTER VI

DIELECTRIC PROPERTIES AND ELECTRICAL CONDUCTION OF PLASMA-POLYMERISED POLYACRYLONITRILE

ABSTRACT

Extensive studies have been made on the dielectric behaviour of plasma-polymerised PAN. From the variation of temperature coefficient of dielectric constant, it is concluded that the dipoles are associated with widely distributed relaxation times. The frequency response of dielectric constant and loss factor are studied in detail and the structure combination of Al-PAN-Al sandwich is analysed. From the conductivity studies, it is concluded that the mechanism of conduction process obeys Poole-Frenkel effect and the Poole-Frenkel coefficient is calculated to be $\sim 3.4 \times 10^{-15}$ esu.

6.10   INTRODUCTION

In the previous chapter it is reported that plasma-polymerised P.N forms highly polymeric electret with good charge storage capability. Since this polymer is a good polar insulator, it is necessary to study the dielectric properties. The dielectric properties of chemically processed bulk P.N [1] and P.N formed by silent electric discharge [2] have been already reported. It has been reported [3,4] that the dielectric properties of plasma-polymerised polymers are different from that of chemically processed ones. It is also reported [4] that the temperature coefficient of dielectric constant (ε) of a normal polystyrene film is negative, while it is positive for plasma-polymerised styrene. Hence in the present investigation importance is given to the variation of the temperature coefficient of ε of plasma-polymerised P.N with temperature which will give the nature of the relaxation of dipoles in the polymer unit. Also, the variation of ε and dielectric loss are studied at various frequencies. The structure combination of Al-Ferrocene-Al [5] is analysed with the help of standard characteristics of non-Debye capacitor [6]. Hence to understand the performance as a capacitor, the frequency response of dielectric constant and loss factor of Al-P.N-Al capacitor are studied and the structure combination is analysed.

For insulator films, it is well known that the current obeys Ohm's law at low fields. The high field conduction, for example, is due to space charge limited currents [7,8], Schottky emission [9], or Poole-Frenkel effect [10]. It has been reported that the high field conduction mechanism in plasma-polymerised styrene is due to Poole-Frenkel effect [10] whereas that in solution grown PAN thin film is Schottky emission [9]. A detailed study of the high field conduction mechanism of glow-discharged PAN has been made by Hirai and Nakada [2] and they concluded that the main mechanism is Poole-Frenkel conduction. Hence in the present work, only a few typical samples are studied and the results are compared with published work [2].

6.20 EXPERIMENTAL PROCEDURE

The PAN is prepared directly from acrylonitrile vapour. The Al-PAN-Al sandwich structures are made as discussed earlier. Thus parallel plate capacitors of effective area of 1 cm^2 are prepared (Fig.2.09 a and b). For all the samples the aluminium electrodes are of 1500Å thickness.

6.21 Capacitance measurement of Al-PAN-Al

Al-PAN-Al samples thus prepared are transferred to the conductivity chamber and evacuated to 10^{-3} torr. Using copper pressure contacts, the connection leads are taken out.

First, the two electrodes are shorted externally and the specimen is heated to $150^{\circ}C$ to remove moisture and stray charges. It is then cooled to room temperature and the capacitance is measured using a Universal bridge (Radart-5104). To measure the capacitance of the specimens at different temperatures, the built-in oscillator (1 KHz) of the universal bridge is used. In the present investigations all the specimens are heated only to $\sim 110^{\circ}C$ because from the initial experiments, it is found that no additional information is possible at higher temperatures.

The variation of capacitance and loss factor with frequency are studied using the same Universal bridge. An external audio frequency generator (Systronics-type 1011) is connected to the bridge and the measurements are made by varying the frequency. Since the working frequency range of the Universal bridge is 20Hz to 30KHz, all the experiments are limited to this frequency range.

6.22 Measurements of current-voltage characteristics

The pre-heated specimen in the evacuated conductivity chamber is connected to a DC power supply and the electrometer amplifier (ECIL-EA-815) as shown in Fig.6.01. The DC voltage is continuously varied using a potential divider system. The voltage across the specimen is measured
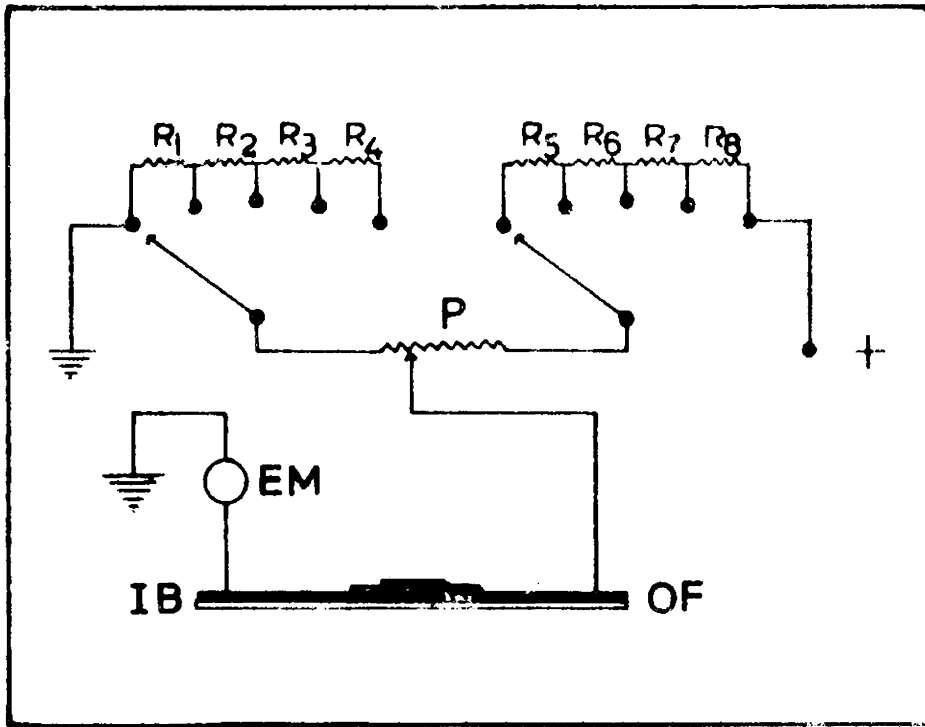
Fig.6.01. Connection for conductivity measurements:
IB - inner bound electrode, OF - outer free
electrode, EM - electrometer, P - potentio-
meter (1 Meg ohm) and R_x - resistances (1 Meg ohm).

using a VTVM (Unitec-VV015). The current through the specimen
is accurately measured in the electrometer. The maximum field
given across the specimen is about 1.5×10^6 V/cm above which
the specimen is damaged or shorted at room temperature.


6.30 RESULTS

6.31 Variation of capacitance with temperature

The capacitance of Al-PAN-Al sandwich specimen
is increased when the temperature of the system is raised.
The variation of the capacitance of different specimens on
increasing the temperature is shown in Fig.6.02. The capa-
citance is recorded only upto $105^{\circ}C$ above which no additional
notable features are observed. From a large number of
samples, only three samples of thicknesses t = 3900$\overset{o}{A}$, 3170$\overset{o}{A}$
and 1820$\overset{o}{A}$ are presented in the figure.

From the value of the capacitance the dielectric
constant can be calculated from the expression

$$C = \frac{\varepsilon A}{4\pi t} \text{ esu} \qquad (6.01)$$

If capacitance C is in Farads, effective area A in cm^2 and
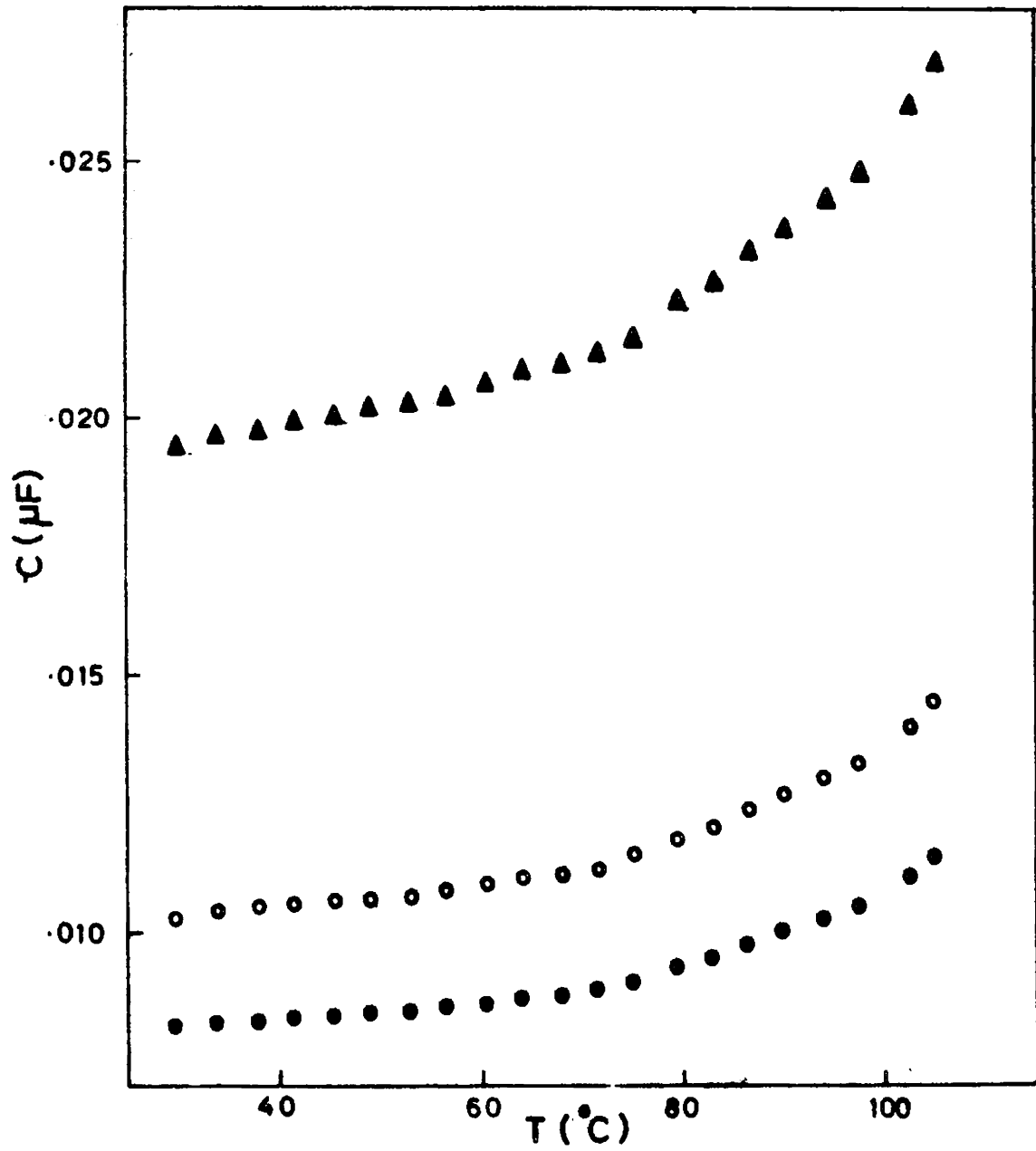
Fig.6.02. Capacitance (C) Vs. temperature (T) plot for
Al-PAN-Al. Thicknesses of PAN: (▲) = 1820Å,
(○) = 3170Å and (●) = 3900Å.

thickness t in cm, then

$$\varepsilon = \frac{4\pi Ct \times 9 \times 10^{11}}{A} \; \text{esu}$$

$$= \frac{Ct}{8.85 \times 10^{-14} A} \; \text{esu} \qquad\qquad (6.02)$$

In Fig.6.03, the dielectric constant of each specimen is plotted against temperature. In the figure it is found that for all samples, the dielectric constant increases linearly with temperature upto $70^\circ C$ and afterwards sharply. Another important feature is that when the thickness of the specimen increases, the dielectric constant (ε) decreases whereas theoretically the ε remains constant for all the thicknesses of the dielectric. In Fig.6.04, the ε is plotted against the thickness of the PAN. The variation of ε with thickness is nonlinear. At lower thicknesses, the variation of ε with thickness is higher and when it goes to the higher thickness region, the trend is to attain a constant value for ε .

To explain the nature of the variation of ε with temperature, the temperature coefficient of ε is plotted against the temperature. Since the temperature coefficient of ε is proportional to $\frac{d\varepsilon}{dT}$, the nature of variation of the
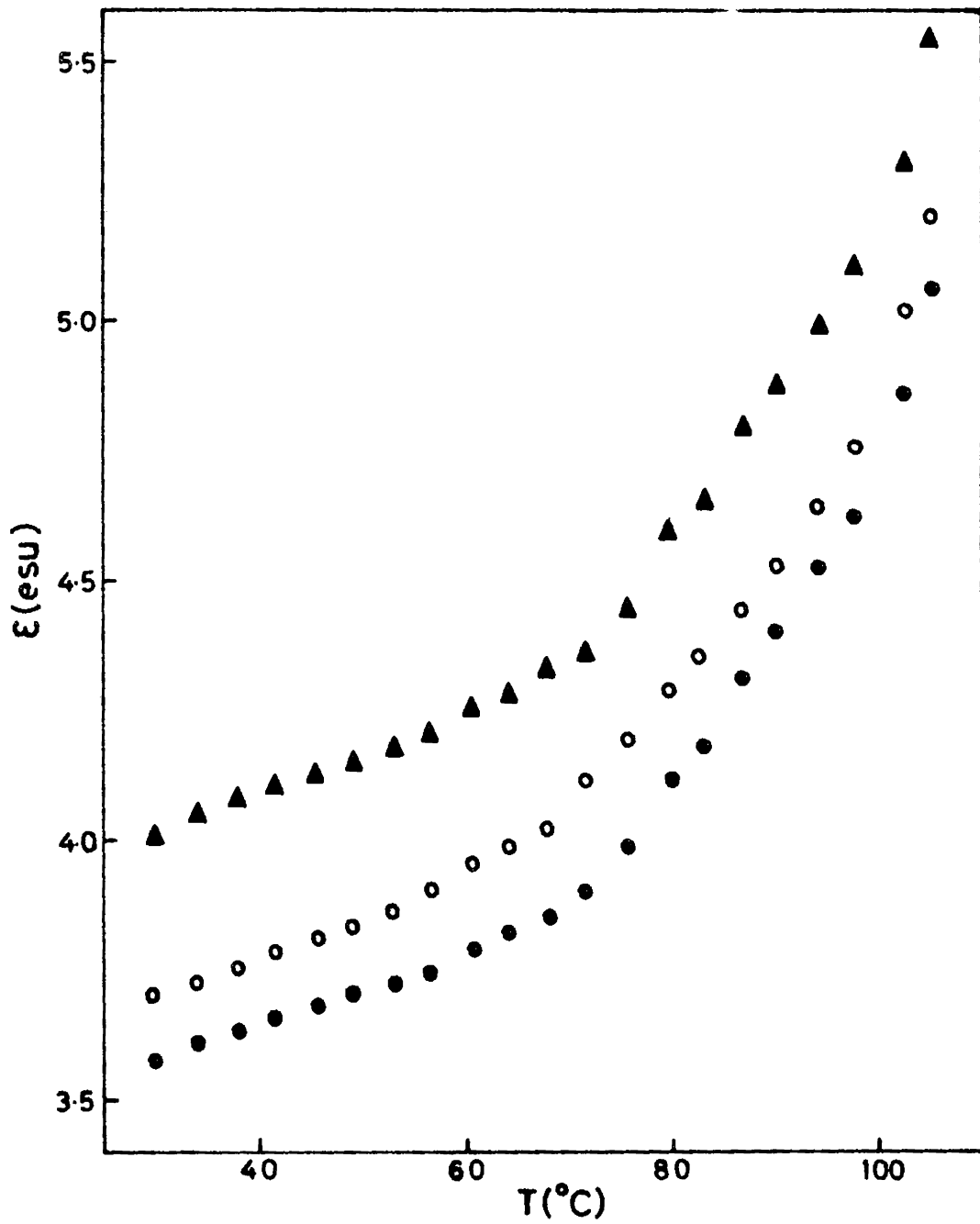
Fig.6.03. Dielectric constant (ε) Vs. temperature (T) plot
for PAN. Thicknesses of PAN: (▲) = 1820Å,
(o) = 3170Å and (●) = 3900Å.

Fig. 6.04. Dielectric constant (ε) Vs. thickness for PARI.

$\frac{d\epsilon}{dT} \times 10^2$

5

4

3

2

1

40   60   80   100

T(°C)
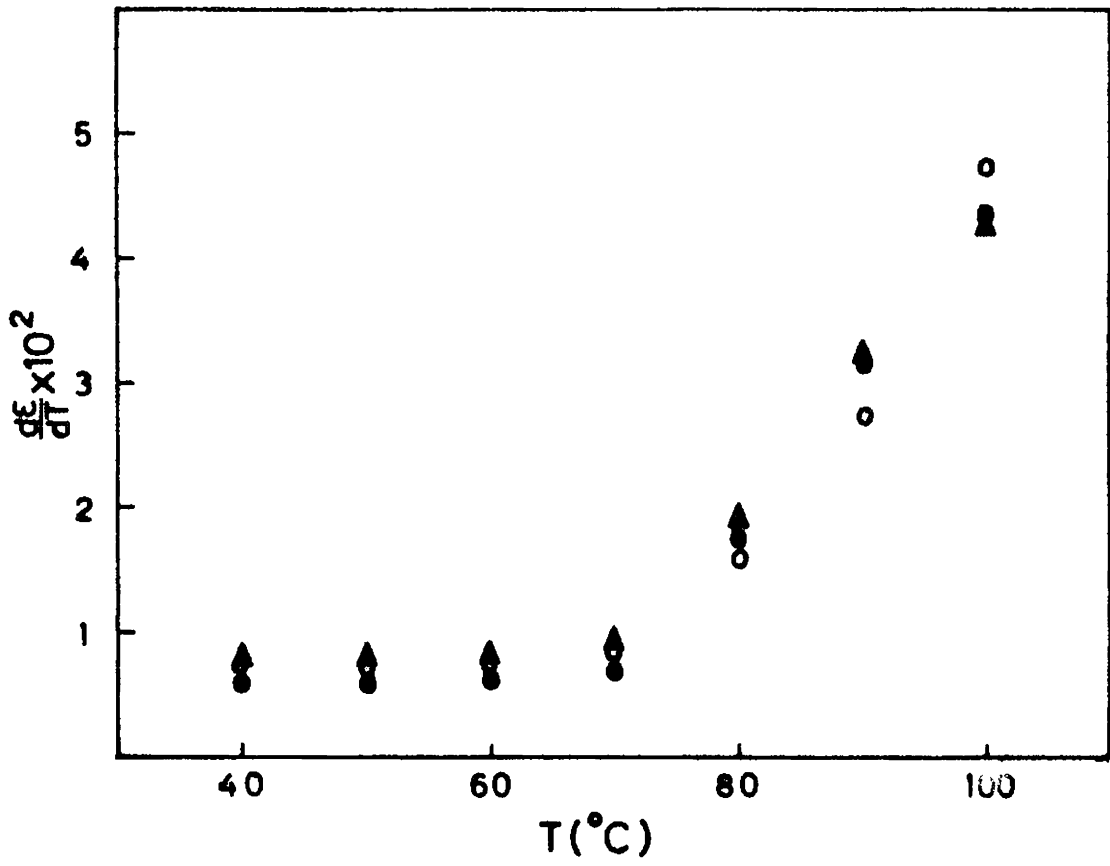
Fig.6.05 $\frac{d\epsilon}{dT}$ Vs. temperature plot for PAN. The thicknesses
of PAN: (▲) = 1820Å, (O) = 3170Å and
(●) = 3900Å.

temperature coefficient of ε with temperature can be studied from $\frac{d\varepsilon}{dT}$ vs. T plot. The $\frac{d\varepsilon}{dT}$ for different temperatures is calculated from Fig.6.03 by taking the slope at different temperatures and $\frac{d\varepsilon}{dT}$ is plotted against the respective temperatures as shown in Fig.6.05. From the figure, it is clear that the temperature coefficient of ε is positive at all the temperatures. It is found that $\frac{d\varepsilon}{dT}$ is invariant upto $70^\circ C$ and then increases nonlinearly. There is only a negligible variation of the magnitude of $\frac{d\varepsilon}{dT}$ with thickness of the sample but the variation of $\frac{d\varepsilon}{dT}$ with temperature is identical for all the samples.

6.32 Variation of dielectric constant with frequency

The usefulness of a capacitor is always decided by the frequency response of the capacitor. Also from the frequency response of the capacitor, the equivalent circuit of the capacitor can be analysed. In Fig.6.06, the capacitance of Al-PAN-Al is plotted against logarithmic frequency for two samples (t = 3170Å and 1820Å) within a frequency range of 20Hz to 10KHz, showing very little variation of capacitance. But above 10KHz, the capacitance gradually decreases by 10 to 15 percent for all the samples. The variation is identical for all the specimens. In Fig.6.07, the ε of PAN is plotted against logarithmic frequency. As mentioned in the last part, the ε decreases
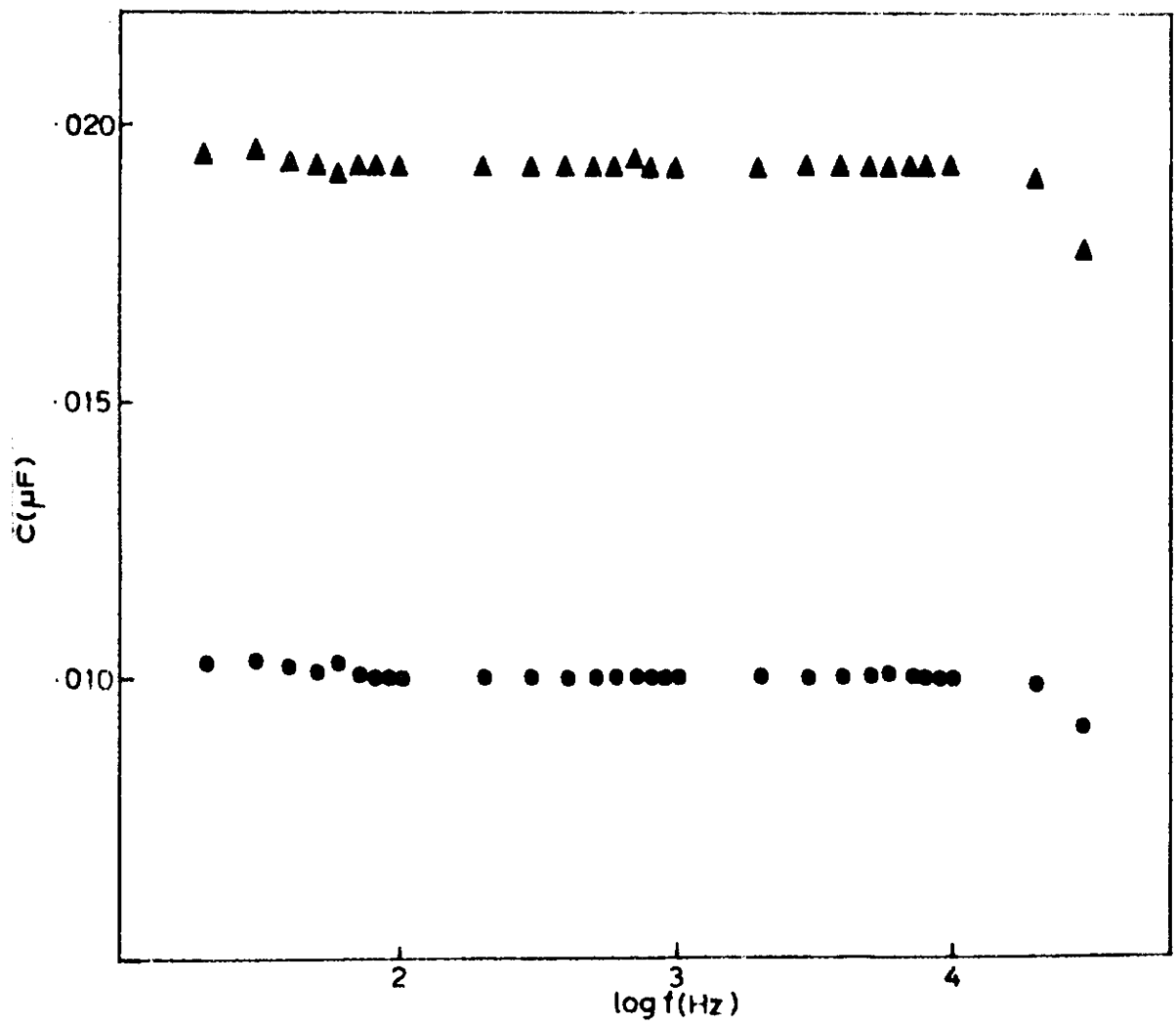
Fig.6.06. Capacitance ( ) vs. logarithmic frequency (log f) plot for PAn.
In thickness. PAn (▲) 1920Å and (●) 1370Å.
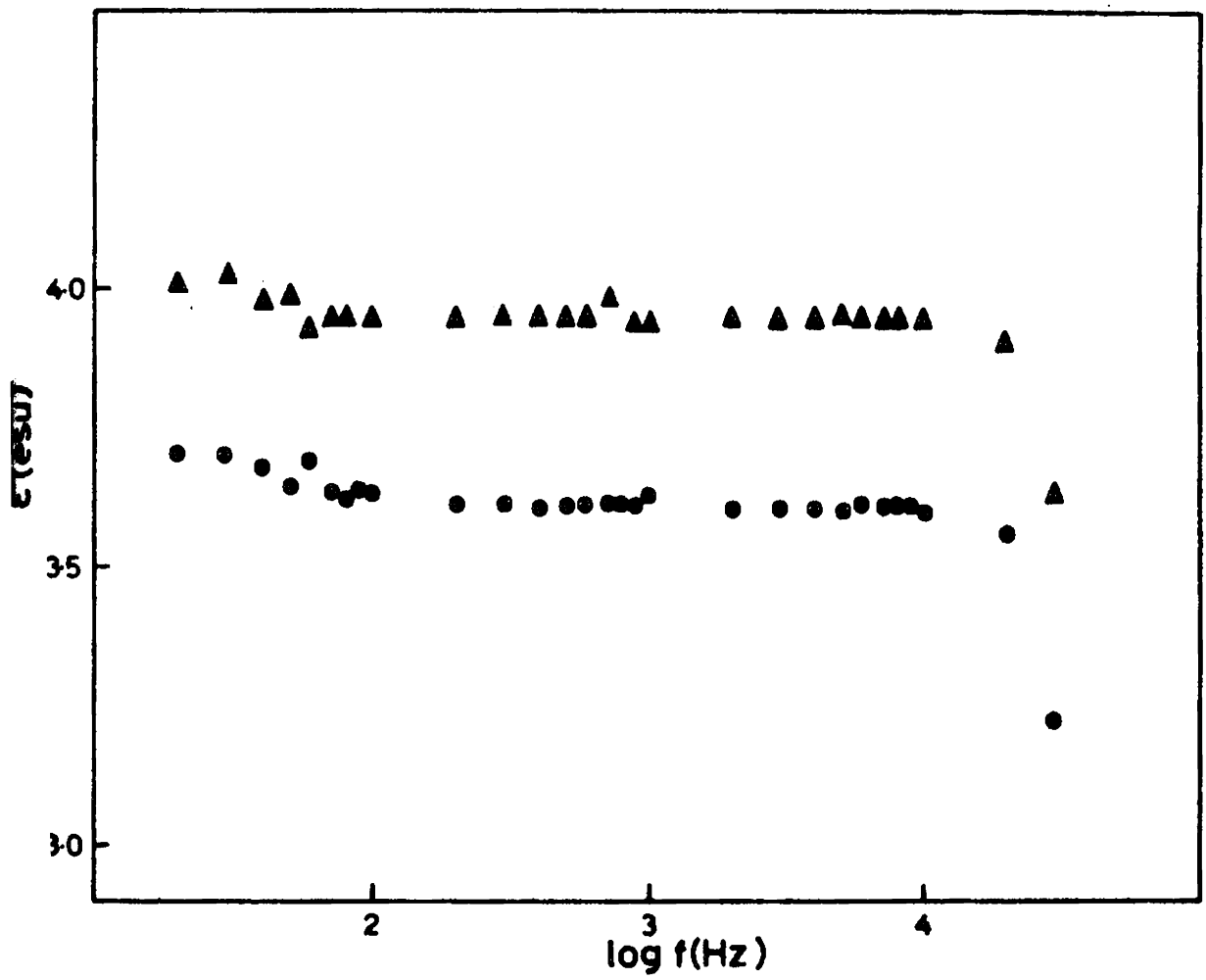
Fig.6.07. The dielectric constant ($\mathcal{E}'$) Vs. logarithmic frequency (log f) plot for PAN. Thicknesses of PAN: (▲) = 1820 Å and (●) = 3170 Å.
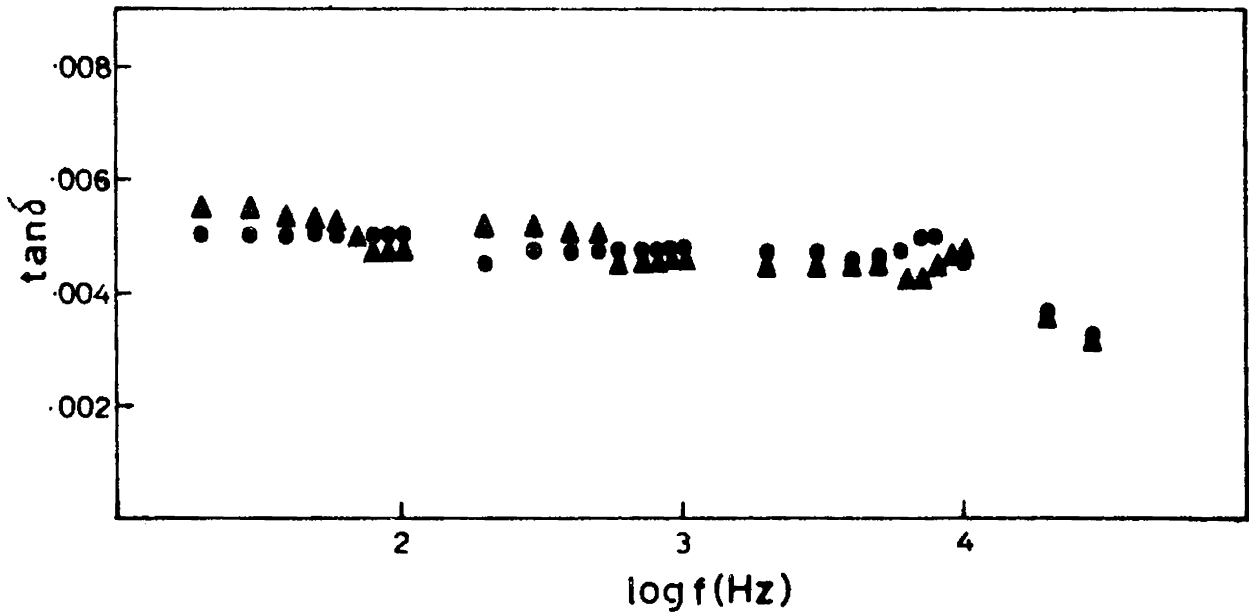
Fig.6.08. The loss factor tanδ Vs. logarithmic frequency plot
for PAN. Thicknesses of PAN: (▲) 1820Å and (●) 3170Å.
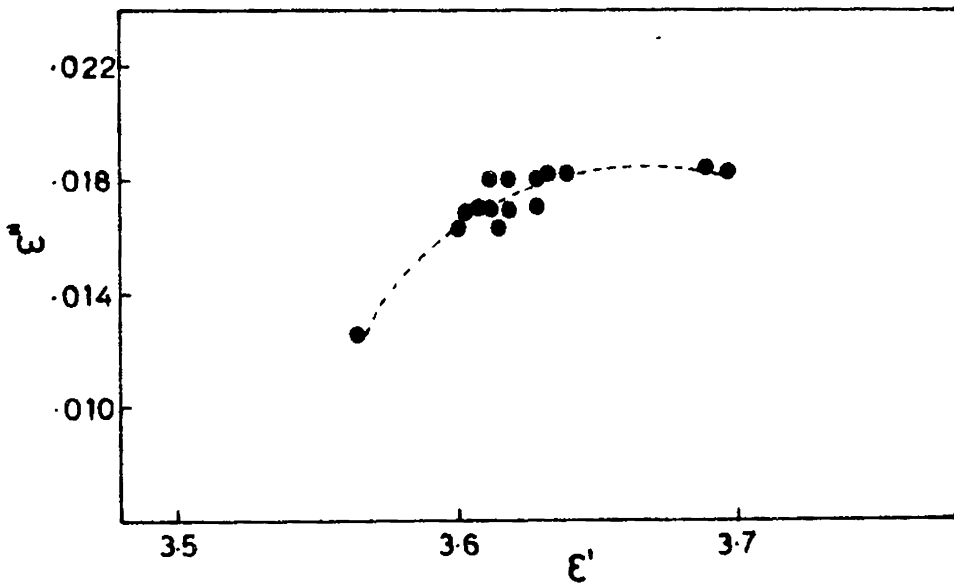
Fig.6.09. The imaginary part of dielectric constant (ε'')
is plotted against the real part of dielectric
constant (ε') for PAN of thickness 3170Å.

when thickness of P.N increases. Upto 10KHz, there is no
notable variation in ε with frequency, but above 10KHz,
the ε drops appreciably for all the samples.

6.33 Variation of loss factor with frequency

To obtain information on the relaxation of dipoles,
the study of variation of loss factor (tan δ) with frequency
is essential. In Fig.6.08, tan δ is plotted against the
logarithmic frequency. For different specimens, tan δ is
nearly of the same magnitude. Eventhough different samples
show small changes of tan δ with frequency, these changes
are appreciably small and are within experimental errors.
All the changes of tan δ are negligibly small upto 10KHz
while a sharp drop is observed above 10KHz.

6.40 DISCUSSION

The glow-discharged polystyrene thin films have
many different electrical and physical properties (ie.
relative dielectric constant, dielectric loss, flexibility
and solubility) in comparison with ordinary polystyrene [11].
The general dependence of dielectric constant with tempera-
ture and dependence of ε and tan δ with frequency for the
plasma-polymerised P.N is quite similar to other plasma-
polymerised polymers [4,6] at first sight. But the special
features of the dielectric properties of plasma-polymerised
P.N need special attention.

6.41 Temperature coefficient of dielectric constant

It has been reported [3,4] that temperature coefficient of ϵ of normal polystyrene thin films are different from those prepared by glow-discharge polymerisation. In the former case, temperature coefficient of ϵ is negative. Differentiating the Clausius-Mossotti formula with respect to temperature, one obtains

$$\frac{d\epsilon}{dT} = \frac{(\epsilon - 1)(\epsilon + 2)}{3}(- \frac{1}{V} \frac{dV}{dT}) \qquad (6.03)$$

Hence, the expansion of volume with increase in temperature leads to a negative temperature coefficient of ϵ. For the latter case, the widely distributed relaxation time is the main reason for the positive temperature coefficient.

It is well established that the dipoles in PAN are associated with the -CN side-group. From the Fig.6.05, it is found that $\frac{d\epsilon}{dT}$ is positive for all temperatures studied. Hence the temperature coefficient of ϵ is also positive. In the case of plasma-polymerised PAN also the process is associated with dipoles of widely distributed relaxation time. When the temperature is raised while measuring ϵ, the dipole orientation occurs, because the relaxation time depends upon the temperature as

$\tau = \tau_0 \exp A/kT$. Hence the number of dipoles which can

orient increases with temperature and the temperature
coefficient of ε is positive. In the figure, upto 70°C
$\frac{d\varepsilon}{dT}$ is constant. This may indicate that the number of
dipoles which can associate with ε increases linearly
in the polymer. In chapter V, from TSD studies it is
concluded that in plasma-polymerised PAN, the dipoles are
widely distributed. The dielectric measurements also support
the existence of dipoles with widely distributed relaxation
time.

A nonlinear increase in $\frac{d\varepsilon}{dT}$ above 70°C shows that
some other mechanism is also associated with the value of ε.
It is reported that the thermally generated charges will be
formed on heating PAN due to chemical degradation [12].
These charges may also contribute to the observed ε.
In chapter III, a nonlinear increase in short-circuited
current is observed on heating Al-PAN-Al sandwich structures.
These thermally generated charges increase sharply with
temperature. Hence it can be concluded that above 70°C,
the major contribution to ε is thermally generated charges
while below 70°C the permanent dipoles in PAN is associated
with the ε.

6.42 Variation of dielectric constant with thickness

From Fig.6.04, it is clearly found that the
of PAN is decreased with increase in the thickness of the

polymer. This would clearly indicate that the effective

dipole moment of PAN is decreased. The film thickness of

the sample is increased with deposition time. Therefore,

depending upon the thickness, the structure of the film is

slightly altered during the deposition. In the process of

plasma-polymerisation, the electrons/ions formed due to

high voltage discharge, collide on the surface of the polymer

film. Due to the bombardment of these charges, the structure

of the polymer will be changed. There is a possibility of

high degree of cross-linking in the polymer due to high

energy bombardment of charges. The decrease in ε due to

the increase in thickness is due to larger cross-linking.

For very thick films ($>4000\overset{o}{A}$) a constant value of ε is

obtained indicating that no further structural changes are

taking place due to ion bombardment. At the initial stages

of polymerisation, the rate of structural changes is very

high and hence the decrease in ε is very sharp with

thickness as shown in the figure.

6.43 The analysis of Al-PAN-Al capacitor

From the Figs.6.06, 6.07 and 6.08, it is clear

that the frequency response of the Al-PAN-Al capacitor is

flat upto 10KHz. But above 10KHz, ε and $\tan\delta$ decreases

by 10 to 15 percent for all the specimens. Since same amount

of decrease is found in all the specimens at all conditions,

it is suspected that this drop is due to the inaccuracy of the instrument at the extreme frequency limit. Hence it is not meaningful to explain the drop of ε and $\tan \delta$ in the range 10KHz to 30KHz before understanding the variation at higher frequencies.

To analyse the capacitor, usually Cole-Cole plot is initially made. In Cole-Cole plot, the real part of the dielectric constant ε' is plotted along X-axis while imaginary part ε'' along Y-axis. For that, the ε' and ε'' are calculated from the observed dielectric constant $|\varepsilon^*|$.

$$\varepsilon^* = \varepsilon' - i\varepsilon'' \tag{6.04}$$

$$|\varepsilon^*|^2 = \varepsilon'^2 + \varepsilon''^2 \tag{6.05}$$

we have $\dfrac{\varepsilon''}{\varepsilon'} = \tan \delta$ $\qquad\qquad$ (6.06)

Hence $|\varepsilon^*|^2 = \varepsilon'^2 (1 + \tan \delta)$ $\qquad$ (6.07)

Since $\tan \delta$ is found to be $\ll 1$ then $|\varepsilon^*| \cong \varepsilon'$, ε'' can be calculated from Eqn.(6.06).

In Fig.6.09, the imaginary part of dielectric constant ε'' is plotted against the real part of the dielectric constant ε' for the full range of frequency

(Cole-Cole plot). It can be seen from the figure that the Cole-Cole plot does not lead to any semicircular arc or even a segment of an arc over the frequency range. One of the possible reasons is that the dielectric material may not be similar to that assumed in the Debye analysis. This means that the capacitor Al-PAN-Al do not follow Debye assumptions. Another possibility is that the frequency range may not be sufficient to form the arc.

Recently Jonscher [13] has reported a different method of analysing the dielectric data and the above said method is applicable to a wide range of solid dielectric materials like inorganic, organic, polymeric, ionic and electronic which show deviations and irregularities in the commonly expected Cole-Cole plot. For explaining this, Jonscher had assumed a non-Debye material i.e., a material which shows a frequency independent ratio of energy stored to energy lost per cycle and necessarily show the frequency dependence as ω^{n-1} for both the real and imaginary parts of the dielectric constant, ε^*.

It is customary, however, to represent the dielectric data as a plot of ε' and ε'' in complex-conjugate ε^* plane (Cole-Cole plot). Jonscher has proposed that when the experimentally available data do not agree with Cole-Cole plot, the representation of the data in terms of complex

admittance (Y) and complex impedance (Z), may help in interpreting the obtained data. The quantities Y and Z are defined as

$$Y(\omega) \;=\; Ki\omega\, \varepsilon'(\omega) \;=\; G_p(\omega) + i\omega C_p(\omega) \qquad (6.08)$$

$$Z(\omega) \;=\; \frac{1}{Y(\omega)} \;=\; R_s(\omega) - \frac{i}{\omega C_s(\omega)} \qquad (6.09)$$

By equation 6.04, $\varepsilon^*(\omega) \;=\; \varepsilon'(\omega) - j\,\varepsilon''(\omega)$.

Here   Y = Complex admittance

Z = Complex impedance

ε^* = Complex permittivity

ω = Angular frequency = $2\pi f$

G_p = Effective parallel conductance

C_p = Effective parallel capacitance

R_s = Effective series resistance

C_s = Effective series resistance

K = Geometric constant = $\dfrac{\text{Area}}{\text{Thickness}}$ of parallel

plate capacitor under consideration.

In the case of the inhomogeneous material, considered as consisting of a relatively conducting bulk layer in series with a relatively insulating barrier layer, Z^* representation favours while for the inhomogeneous

material assumed to have a parallel leakage conductance
with a perfect capacitance together with a negligible
series resistance, Y representation may be a more suitable
one. With the above consideration Jonscher has given a
possible nature of plots in each plane for different combi-
nations of ideal resistance R with non-Debye capacitance.

To compare our experimental results with the
predicted results of Jonscher [6], the data obtained for
PAN is to be expressed in terms of G_p, C_p, R_s and C_s.
The values are calculated with the help of the following
expressions.

$$R_s = \frac{\varepsilon''}{K\omega(\varepsilon'^2 + \varepsilon''^2)}$$ (6.10)

$$\frac{1}{\omega C_s} = \frac{\varepsilon'}{K\omega(\varepsilon'^2 + \varepsilon''^2)}$$ (6.11)

$$G_p = K\omega\varepsilon''$$ (6.12)

$$\omega C_p = K\omega\varepsilon'$$ (6.13)

The dielectric data obtained from the experiment
are now presented in terms of Y - plot (ωC_p against G_p)
in Fig.6.10 and Z^* - plot($\frac{1}{\omega C_s}$ against R_s) in Fig.6.11. Since
all the specimens give identical results, only one typical
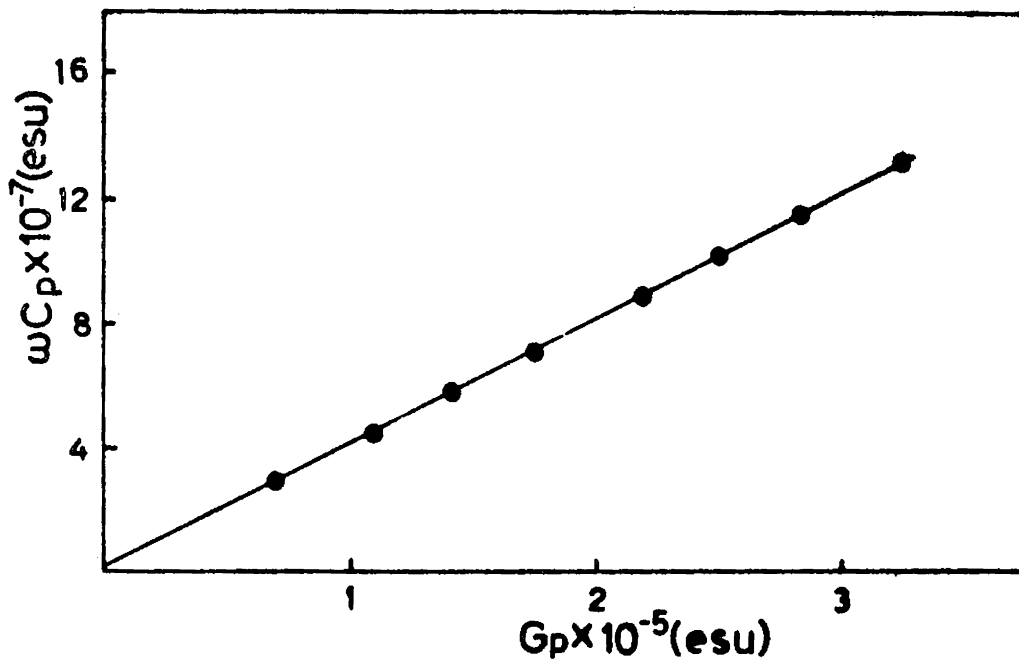
Fig.6.10. The ωC_p is plotted against G_p for PAN of thickness 3170Å.
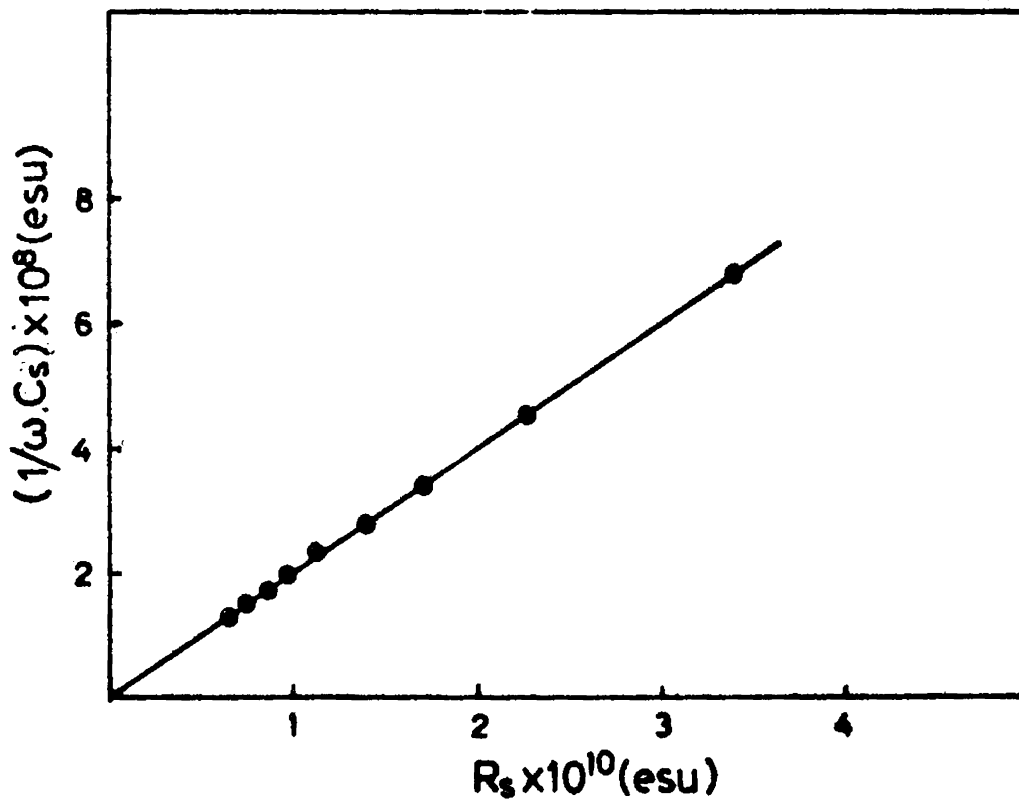
Fig.6.11. $\frac{1}{\omega C_s}$ is plotted against R_s for PAN of thickness 3170Å.

plot is presented. From Fig.6.10 and Fig.6.11, it can be seen that for all specimens a linear relationship is established as expected. In comparison with the relationship observed earlier [6], it can be shown that Y and Z^* curves are similar to those expected for a Jonscher capacitor without any parallel or series combination of ideal resistance in the circuit.

Further, the frequency dependence of $|Y|$ and $|Z|$ in the empirical relation is given by

$$\omega C_p = a G_p = A \omega^n \qquad (6.14)$$

$$\frac{1}{\omega C_s} = a R_s = \frac{a}{A(a^2 + 1)} \omega^{-n} \qquad (6.15)$$

where a and A are constants.

The plots of ωC_p, G_p, $\frac{1}{\omega C_s}$ and R_s against ω on log-log scale enable one to determine the value of n. Typical plots of $\log \omega C_p$ vs. log f, $\log G_p$ vs. log f, $\log \frac{1}{\omega C_s}$ vs. log f and $\log R_s$ vs. log f are shown in Fig.6.12. From the figure, it is found that all the plots give a linear relationship with the frequency. The slope of all the straight lines are calculated and found to be unity with proper signs. This indicates that there will not exist
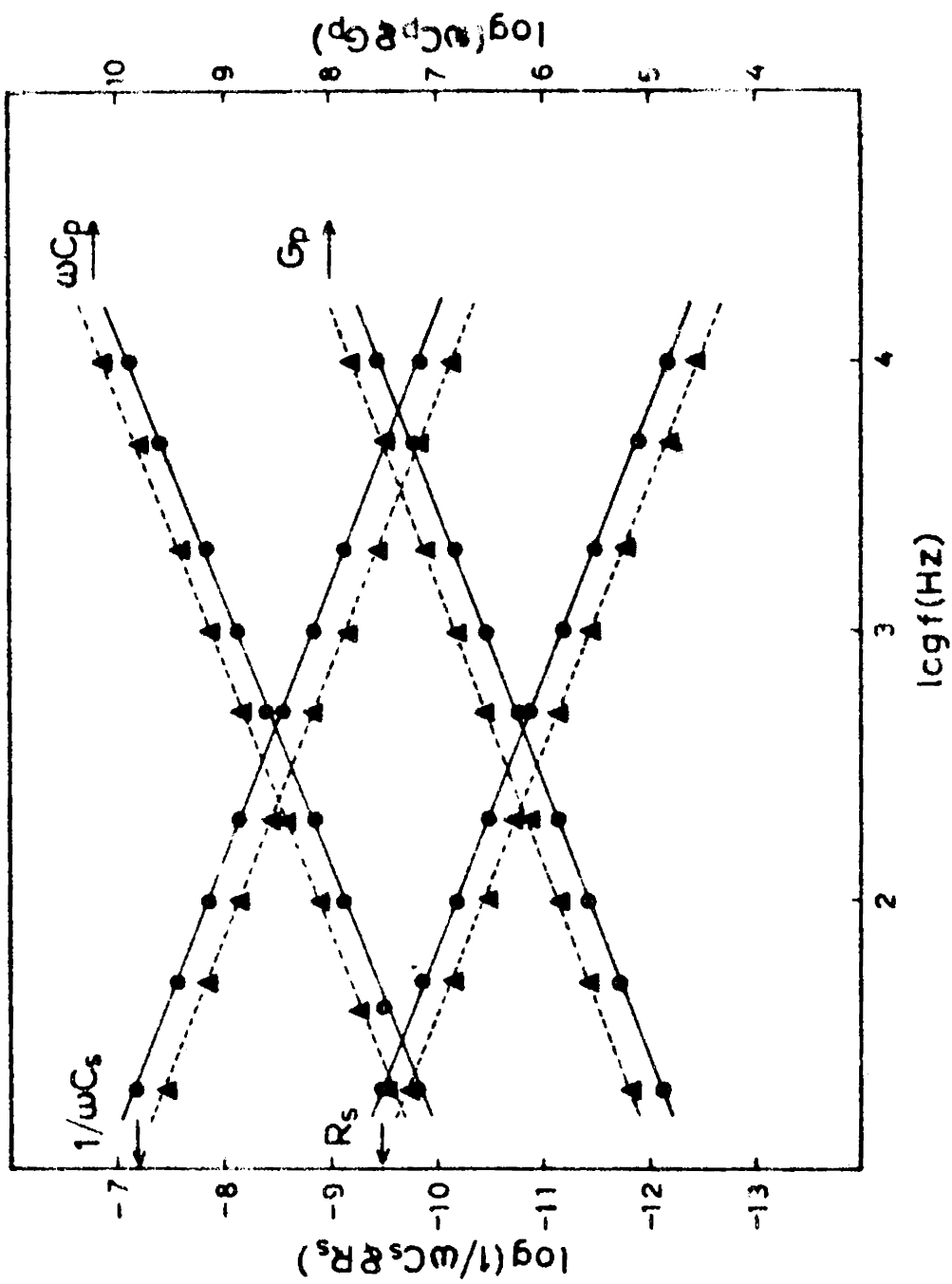
Fig.6.12. log ωC_p, log G_p, log $\frac{1}{\omega C_s}$ and log R_s are plotted against log f for PAN. Thicknesses of PAN: (▲) = 1620Å and (●) = 3.70μm.

any additional frequency dependent circuit element except
the test capacitor. From the information gathered from
Fig.6.10, Fig.6.11 and Fig.6.12, it can be concluded that,
for the audio frequency range, the Al-PAN-Al exists as a
non-Debye capacitor (Jonscher capacitor) without any
parallel or series resonance components virtually connected
to it.

6.50   DIELECTRIC BEHAVIOUR OF Al-PAN-Al

Eventhough the present data are not sufficient
to provide any clear information regarding the resonance
circuit components of Al-PAN-Al and dipole relaxation of
the material, the existing information have given certain
conclusions. It is clear that the frequency range of 20Hz
to 30KHz is not sufficient to analyse the relaxation
mechanism of polymer films. From the temperature dependence
of the dielectric constant, it is clear that the temperature
coefficient of ϵ is positive and is due to widely distri-
buted relaxation time. Above $70^{\circ}C$, the contribution of
thermally generated charges is predominant and hence a non-
linear increase in ϵ with temperature is observed. The
dielectric constant ϵ decreases with increase in thickness
of the film and concluded to be due to structural change in
the polymer (particularly an increase in degree of cross-
linking).

For the audio frequency range (ie., 20Hz to 30KHz) the variation of dielectric constant is negligibly small. Also for this range the loss tangent is very small and remains the same for all the frequency ranges. From the analysis it is found that no additional resonance circuit components has to be included with Al-PAN-Al capacitor.

6.60 CONDUCTION IN Al-PAN-Al

In Fig.6.13, the relation between the conductivity and the applied voltage is presented. The conductivity of Al-PAN-Al is approximately a constant upto a voltage of 18.5V (5.5×10^5 V/cm) and then increases nonlinearly. At this region, only log σ vs. $V^{\frac{1}{2}}$ plot gives a linear relation. In the present experiment, the maximum voltage given across the specimen is $\sim$ 36V. Above this, the specimen shows eratic observation and is even completely destroyed.

From the literature [2], it is found that for plasma-polymerised PAN, the high field conduction is due to Poole-Frenkel effect. This means that the charge carriers may be released by ionised impurity centres in the dielectric. In the present case also, from current voltage characteristic, it can be inferred that the high field conduction is associated with Poole-Frenkel effect. Hence, Fig.6.13
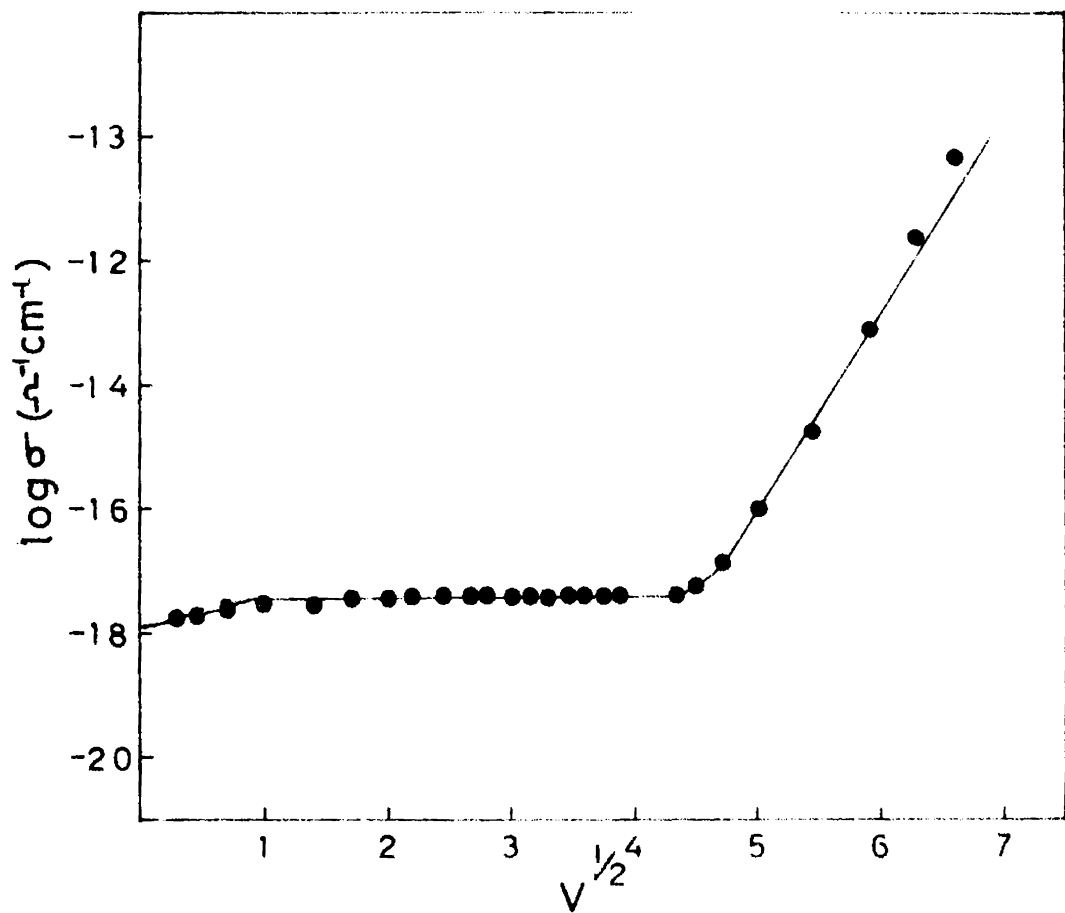
Fig. 6.13. The log σ [plotted] against the [square root of applied] voltage $(V)^{1/2}$ for Al-PAN-Al specimen with thickness of PAN 335 Å.

obeys the following expression

$$\sigma = \sigma_o \exp[-(\emptyset - \beta_{PF} E^{\frac{1}{2}})/kT] \qquad (6.16)$$

where σ_o is the constant conductivity at high fields
and $\emptyset$ is the impurity energy level. The Poole-Frenkel
coefficient β_{PF} is given by

$$\beta_{PF} = [\frac{e^3}{\epsilon}]^{\frac{1}{2}} \qquad (6.17)$$

From the slope of the straight line part of
Fig.6.13, β_{PF} is calculated to be 3.44×10^{-15} esu. According
to Eqn.(6.17), the value of β_{PF} is 5.5×10^{-15} esu by assuming
the dielectric constant, $\epsilon = 3.6$ (from Fig.6.4) and the
electron charge $e \cong 4.8 \times 10^{-10}$ esu. The reasonable agreement
of the observed non-ohmic characteristics with calculated
values proves that the mechanism of conduction in plasma-
polymerised Al-PAN-Al is Poole-Frenkel. The ohmic
conductivity σ_o is obtained from the figure as
8.2×10^{-18} mho/cm.

Extensive studies are made on the mechanism
of conductivity in plasma-polymerised PAN [2] prepared by
silent discharge and arrived at the same model for condu-
ction mechanism. The experimentally derived β_{PF} is

9.1×10^{-15} csu which is also of the same order of magnitude as the calculated values. It may, therefore, be safely concluded that Poole-Frenkel conduction is an appropriate mechanism for conduction through plasma-polymerised PAN.

REFERENCES

[1] Vera V.Daniel, Dielectric Relaxation, Academic Press, London and New York, 186 (1967).

[2] Tadaaki Hirai and Osamu Nakada, Jap. J. Appl. Phys., 7, 2, 112 (1968).

[3] S.Takeda and M.Naito, Proc. 7th Intern. Vac. Congr. 3rd Intern. Conf. Solid Surface, (Vienna 1977) 2007.

[4] S.Takeda, J. Appl. Phys., 47, 5480 (1976).

[5] Shireesh D.Phadke, Thin Solid Films, 48, 319 (1978).

[6] Shireesh D.Phadke, Ph.D. Thesis, University of Poona (1978).

[7] N.M.Bashara and C.T.Doty, J. Appl. Phys., 35, 3498 (1964).

[8] Shireesh D.Phadke, Thin Solid Films, 55, 391 (1978).

[9] J.Chutia and K.Barua, Phys. Stat. Sol., (a) 55, K13 (1979).

[10] Keiichi Ando and Minoru Kusabiraki, Memoirs of the Faculty of Engineering, Osaka City University, 19, 95 (1978).

[11] M.Stuart, Proc. IEEE 112, 1614 (1965).

[12] S.I.Stupp and S.H.Carr, J. Polym. Sci. Polym. Phys., 15, 485 (1977).

[13] A.K.Jonscher, Coll. and Polym. Sci., 253, 231 (1975).

CHAPTER VII

SUMMARY AND CONCLUSIONS

ABSTRACT

All the conclusions relating to the various studies on PAN such as short-circuited current of poled and unpoled specimens, dielectric properties and mechanism of conduction are summarised in this chapter.

166

7.10 SUMMARY AND CONCLUSIONS

It has been established that plasma-polymerisation
process is a useful method for preparing insulating and
dielectric polymers from monomer vapours. The process is
relatively economical particularly because of the efficiency
of polymerisation and the optimisation of the rate of flow
of the monomer. From the growth rate of polyacrylonitrile
thin films prepared by plasma-polymerisation method it has
been found that the rate of growth is proportional to the
square of the current in the plasma tube. It is also
concluded that the accelerated ions collide with monomer
molecules and due to the energy transfer the monomer radicals
are generated. In the polymerisation process, these radicals
combine together to form the polymer chain. A special
chamber has been designed to produce good, pin-hole-free
and uniform polymer thin films. Using this set up, a
brownish yellow coloured polymer is prepared while the
chemically processed PAN is transparent. From different
parametric studies at elevated temperatures, it is established
that the observed properties are associated with PAN. The
polymer dissolves in ethyl alcohol, acetone and dimethyl
formamide showing a low order of polymerisation and low
degree of cross-linking.

From the infrared studies, it is concluded that PAN is a long planar zig-zag chain molecule. It is further concluded that the forming process of plasma-polymerisation is not a controlled process resulting in the formation of amorphous polymer and it was not possible to identify the steric configuration. From the analysis of the emission spectrum of the monomer plasma and also from the structure of the resulting polymer, it is concluded that radical polymerisation is the most suitable mechanism for the formation of PAN by this method. For the termination reaction, it was not possible to confirm the mechanism from the present experimental data, but hydrogen addition and charge trapping have been put forward as the most probable processes. The additional bands of CO in the plasma spectrum and also in the infrared spectrum show the existence of the CO group as an impurity which is perhaps the characteristic of the gas phase discharge method of polymerisation. The visible ultraviolet absorption band of the polymer film shows band broadening suggesting the formation of long chain macromolecules.

A short-circuited current is generated from plasma-polymerised unpoled Al-PAN-Al thin films on heating. The current originates from the accumulation of negative trapped charges in the vicinity of the outer electrode. The preferential orientation of the dipoles due to rotation of -CN side group towards the outer electrode also contribute to the

short-circuited current. It is concluded that the charge

trapping is associated with the compositional inhomogeneity

in PAN films during the polymerisation process. The electrodes

of dissimilar thicknesses also produce an additional contri-

bution to the short-circuited current due to the nonuniform

heating and surface strain. Since the activation energy

is $\sim$ 1.4 eV, it is concluded that the charges are formed

from the covalent bonds of the carbon atoms and thus in turn

suggests the trapping of charges at the tail end of the

molecules. From the initial part of the optical absorption

band of the polymer films, it is found that a trap level

exists at $\sim$ 1.7 eV below the conduction band and is in

agreement with the temperature activation energy. From the

thermally stimulated current data, it is concluded that a

preferred orientation of the dipoles is not possible at low

fields ($\sim$ 5×10^4 V/cm).

In poled Al-PAN-Al, a low temperature peak is

observed in depolarisation current studies. It is concluded

that the origin of the polarisation is mainly due to the

orientation of dipoles associated with -CN side groups and

migration of charges through microscopic distances. A

partial contribution has also to be considered due to the

injection of charges. The theoretically predicted total

polarisation is found to be greater than the experimentally

predicted one. This shows that the preferred orientation of

dipoles are restricted in PAN. Some local structure develops in PAN on high field polarisation preventing the dipoles from returning to their original position on depolarisation. From the polarisation studies, it is concluded that the electrons are trapped at the vicinity of the outer electrode due to compositional inhomogeneity. As a result an internal field of $\sim$ 6.2x10^{4}V/cm is developed across the specimen.

For sufficiently large thicknesses ($>$4000Å), the dielectric constant of plasma-polymerised PAN is found to be $\sim$ 3.4 esu. But at lower thicknesses the dielectric constant is larger. The decrease in the value of the di-electric constant with the increase in the thickness of the film may be attributed to the structural changes due to ion bombardment during the formation of the films. From the dielectric studies it is concluded that the dipolar relaxa-tion is widely distributed. The thermally generated trapped charges also contribute to the dielectric constant at high temperatures. From the frequency response of Al-PAN-Al capacitors in the range 20Hz to 30KHz, it is found that there are no changes in dielectric constant and loss factor. From the Jonscher analysis it is concluded that in the audio frequency range, Al-PAN-Al behaves as an ideal capacitor without any resonance components associated with it.

From the conductivity studies it is found that upto a field of 5×10^5V/cm, plasma-polymerised PAN obeys Ohms law and shows a conductivity of $\sim 3\times10^{-18}\Omega^{-1}$ cm^{-1} at room temperature. Above this field the conduction mechanism is due to Poole-Frenkel effect. The Poole-Frenkel coefficient β_{PF} is calculated to be 3.4×10^{-15}esu and is in good agreement with the theoretical values.

It is well known that PAN is a very good polar electret. Above experimental data also shows that PAN can store large amount of charges. The dipole orientation is constrained by the formation of local structure on high field polarisation. Hence stored energy will not be completely released on depolarisation process. But thermally released charges contribute a large depolarisation current. One of the notable features of PAN is that it has a very large dipole moment (3.4D) associated with the -CN side group and as such piezoelectric and pyroelectric effects are expected. Hence further work has to be done in this direction especially on stretched polymer so as to get information regarding these properties.